

A Pain in the Neck:

Articular Process Joint Osteochondrosis
and Intervertebral Disc Degeneration in
Warmblood Horses

Wilhelmina Bergmann



**A Pain in the Neck:
Articular Process Joint
Osteochondrosis and
Intervertebral Disc Degeneration
in Warmblood Horses**

Wilhelmina Bergmann

**A Pain in the Neck:
Articular Process Joint Osteochondrosis and Intervertebral Disc
Degeneration in Warmblood Horses**

Wilhelmina Bergmann

PhD thesis, Utrecht University, Faculty of Veterinary Medicine, The
Netherlands

ISBN: 978-94-6473-179-8

Cover: Wilhelmina Bergmann and Irene Schaafsma

Layout: Wilhelmina Bergmann

Print: Ipskamp printing

© 2023 Wilhelmina Bergmann

A Pain in the Neck: Articular Process Joint Osteochondrosis and Intervertebral Disc Degeneration in Warmblood Horses

**Nekpijn: osteochondrose van wervelgewrichten en
tussenwervelschijfdegeneratie bij wambloedpaarden**
(met een samenvatting in het Nederlands)

Proefschrift

ter verkrijging van de graad van doctor aan de
Universiteit Utrecht
op gezag van de
rector magnificus, prof. dr. H.R.B.M. Kummeling,
ingevolge het besluit van het college voor promoties
in het openbaar te verdedigen op

Donderdag 14 september 2023 des middags te 12.15 uur

door

Wilhelmina Bergmann

geboren op 22 maart 1978
te Utrecht

Promotor:

Prof. dr. A. Gröne

Copromotor:

Dr. G.C.M. Grinwis

Beoordelingscommissie:

Prof. dr. J.B. Helms

Prof. dr. D. Salvatori

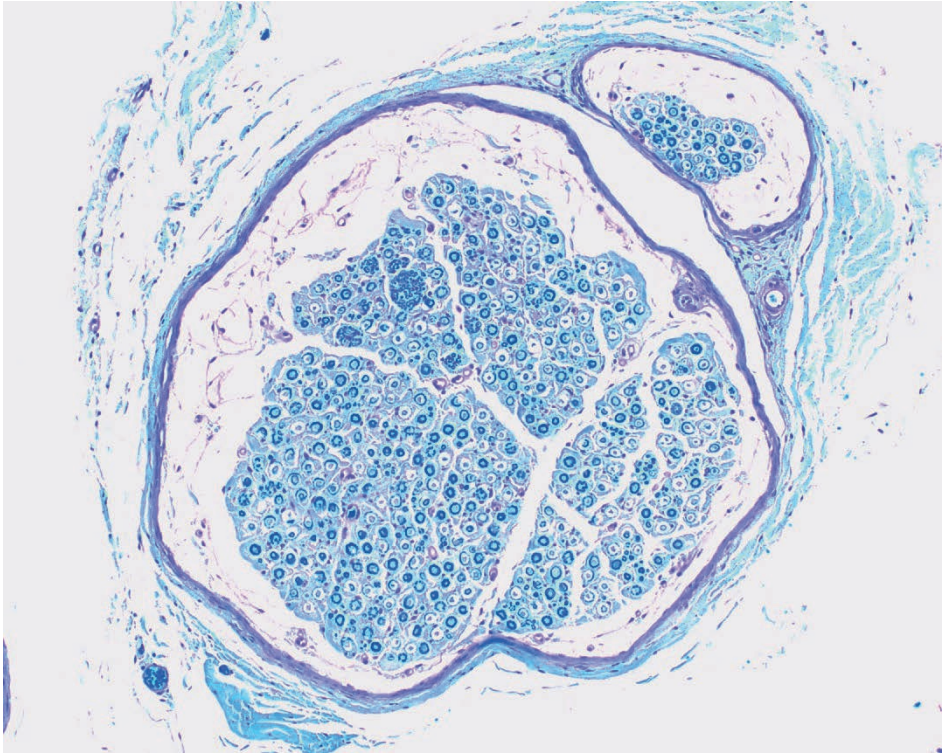
Prof. dr. H. Brommer

Prof. dr. B.P. Meij

Prof. dr. C. Delesalle

Table of Contents

Chapter 1	General introduction, aims and outline of this thesis	7
Chapter 2	Cervical articular process joint osteochondrosis in warmblood foals	27
Chapter 3	Shapes of cervical articular process joints and association with histological evidence of osteochondrosis in warmblood foals: a post-mortem study	51
Chapter 4	Intervertebral disc degeneration in warmblood horses: morphology, grading, and distribution of lesions	85
Chapter 5	Intervertebral disc degeneration in warmblood horses: histological and biochemical characterization	113
Chapter 6	General discussion	155
Addendum		
	Nederlandse samenvatting	174
	Dankwoord	179
	Curriculum vitae	182



General introduction,
aims and outline of this
thesis

1

Cervical vertebral compressive myelopathy

Cervical vertebral compressive myelopathy (CVM) is the most common non-macro traumatic, non-infectious cause for cervical nervous signs in the horse, affecting 15.3 % of all neurological cases (N=4,319) in a French study.³¹ It is a multifactorial syndrome of which the pathogenesis is largely still unclear.^{27, 40, 57} The studies included in this thesis are intended to gain more knowledge on the possible role of the intervertebral disc (IVD) and to broaden the understanding about the role of the articular process joint (APJ) in the pathogenesis of this syndrome.

CVM is most common in young horses, male horses, thoroughbreds, warmblood horses, quarter horses and Tennessee walking horses.^{31, 33, 35, 47} Nervous signs are the result of narrowing of the vertebral canal with subsequent compression of the spinal cord and spinal nerves.^{19, 37, 40, 57} Compression can be present intermittently or statically.

In intermitted CVM, compression only occurs during movement of the neck, predominantly during flexion.^{40, 57} This form of CVM is most commonly seen at the third to fourth cervical vertebrae (C3-C4), C4-C5 and in horses 8-18 months of age (Figure 1).^{37, 47, 51} Particularly in young, male thoroughbreds, this form of compression is often caused by malformation and malarticulation, suggesting a developmental or nutritional aetiopathogenesis.^{31, 35, 58} These malformations include a funnel shaped vertebral canal⁵⁸ and APJ malformations⁵⁷ which can lead to malalignment and instability resulting in secondary changes of the adjacent vertebrae and osteoarthritis (OA) of the APJs.^{10, 57} Also osteochondrosis (OC) can cause intermitted stenosis.^{39, 57}

In the static form of CVM, compression is always present regardless of movement, although extension of the neck can exacerbate this form of compression.⁴⁰ Static CVM is most commonly present at C5-C6 and C6-C7 and is most often seen in horses 1-4 years of age but also in older horses (Figure 1).^{33, 51} Especially in male horses, warmblood horses and Tennessee walking horses of 4 years and older, nervous signs due to static compression are often the results of OA of the APJs characterized by osteophytes, synovial cysts and thickening of the joint capsule (Figures 2a and b).^{33, 35, 40, 58} In these horses, manipulation of the head and neck position may additionally appear painful.^{19, 35, 40, 58}

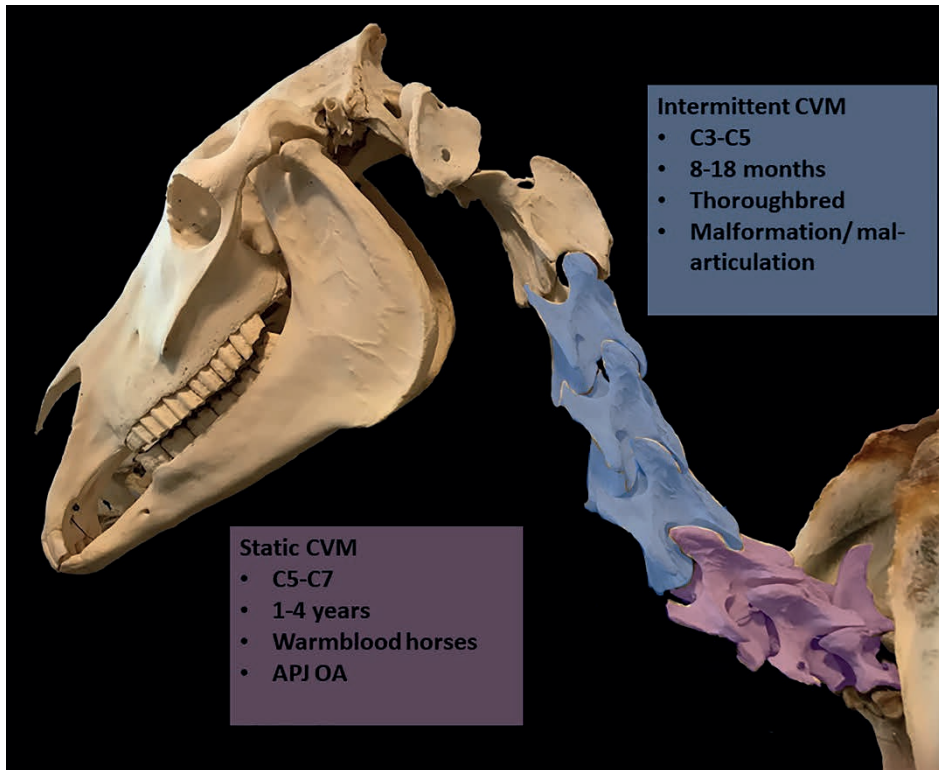


Figure 1. Head and cervical part of the vertebrae of a horse. In blue the predilection site and the most common characteristics for intermittent cervical vertebral stenotic myelopathy (CVM) are indicated. In purple the predilection site and most common characteristics of static CVM are given. C = cervical vertebra; APJ OA = articular process joint osteoarthritis.

However, static CVM can also be the result of APJ osteochondrosis dissecans (OCD), osteosclerosis of the cervical vertebral lamina, osteomyelitis and ligamentum flavum hypertrophy.^{47, 57} OC is often suggested as cause for OA of the APJ^{40, 47} however it has also been suggested that development of CVM in older horses is the result of progression of subclinical malformation and mal-articulation and chronic microtrauma.³³ Yet, skeletal pathology, including OA and OC of the APJs, are also seen in clinically normal horses. Therefore horses with CVM are more likely to have additionally a generalised narrow spinal canal.^{15, 27, 51, 55, 58}

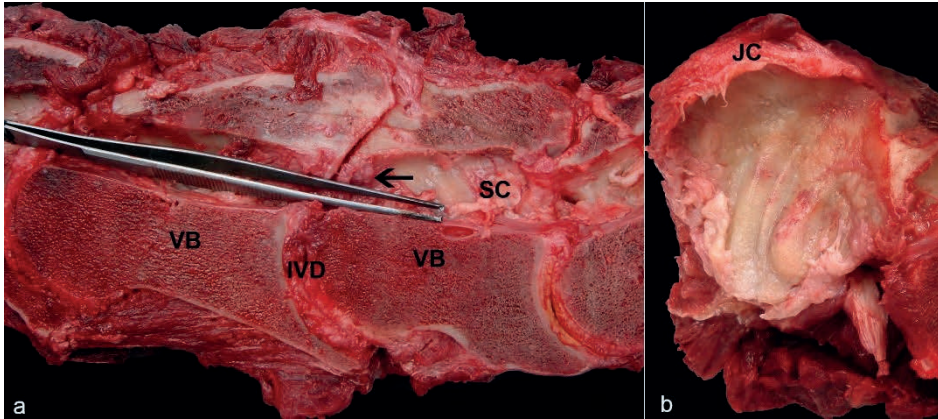


Figure 2. Vertebral column of a 10 years old Royal Dutch Sport Horse with static cervical vertebral compressive myelopathy.

(a) Sagittal cut of the cervical vertebral column at C6C7. The spinal canal (SC) at the height of the C6C7 articular process joints is severely narrowed due to proliferation of bone (arrow) originating from both, degenerated, articular process joint facets. VB = vertebral body; IVD = intervertebral disc.

(b) C6 facet of the right C6C7 articular process joint. The facet is severely enlarged by new bone formation and the surface of the facet is composed of severely irregular bone. The cartilage is lost. The joint capsule (JC) is severely thickened.

Nervous signs caused by CVM are typically insidious and progressive⁵⁸ and are the result of damage to the upper motor neurons and the proprioceptive white matter tracts of both the fore and hind limbs.^{40, 52} Therefore typical signs reflect a dysfunction of muscle tone regulation and voluntary movement such as spastic paresis, hypermetria, ataxia and neurogenic muscular atrophy. Also cervical hyperaesthesia is a common finding, especially in horses with presence of articular process osteophytes. The nervous signs are more pronounced in the hind legs due to the more superficial location of the corresponding tracts in the lateral funiculi of the spinal cord.^{34, 40, 47, 52, 58} Typically the clinical signs are symmetrical, however asymmetrical clinical signs can occur and are often the result of asymmetrically enlarged APJs.⁵²

CVM is diagnosed by a combination of a physical and neurologic examination, where appropriate analysis of cerebrospinal fluid to rule out infectious causes, diagnostic imaging including contrast,

trans-cranial magnetic stimulation, trans-cranial electrical stimulation and electromyography.^{37, 40, 47, 51, 57} However the gold standard remains postmortem pathological evaluation, especially histological examination, of the spinal cord and spinal nerves.^{33, 37, 51, 58}

Macroscopically, the spinal cord can be distorted and flattened at the site of compression and if there is astrocytic sclerosis it can be firm too.^{47, 52, 57}

In histology, white matter changes are randomly visible in all funiculi at the site of compression. These changes comprise presence of spheroids, dilated myelin sheets and digestion chambers, compatible with Wallerian degeneration (Figure 3a). In more chronic cases interstitial astrocytosis and even fibrosis may be seen (Figure 3b). Also degeneration, necrosis and loss of motor neurons (Figure 3c) may be present and in the corresponding nerve roots Wallerian degeneration might be observed.

Cranial from the site of compression, Wallerian degeneration is visible in the ascending tracts in the dorsal funiculus and the superficially placed spinocerebellar tracts in the lateral funiculi of the spinal cord.

Caudal to the site of compression, Wallerian degeneration is present in the descending pathways deep in the lateral funiculi and in the ventral funiculus.⁵²

The site of the lesions within the spinal cord may also point to the possible cause of the compression. For example, Wallerian degeneration localized in the spinal nerves or dorso-lateral funiculi are indicative for compression due to lesions of the APJs^{37, 58}, whereas lesions in the dorsal funiculus are suggestive of a thickened ligamentum flavum or dorsal lamina.⁴⁷

Histological changes consistent with chronic compression neuropathy are not well described in literature. They were however seen in the spinal nerves of the CVM-affected horses used in the different studies of this thesis. These changes are the result of myelin sheath damage. This can result in thickening of the nerves due to epineural and perineural fibrosis and presence of larger and increased numbers of Renaut bodies (Figure 4a). Furthermore, onion bulb formation (overlapping Schwann cells surrounding a demyelinated axon) (Figure 4b), thinning of myelin, remyelinating fibers with cluster formation and fibers with excessively thick myelin sheaths can be seen (Figures 4b and C).¹⁸

Finally, mild denervation muscular atrophy can be demonstrated histologically, characterized by scattered single or small groups of angular atrophied muscle fibers (Figure 5).

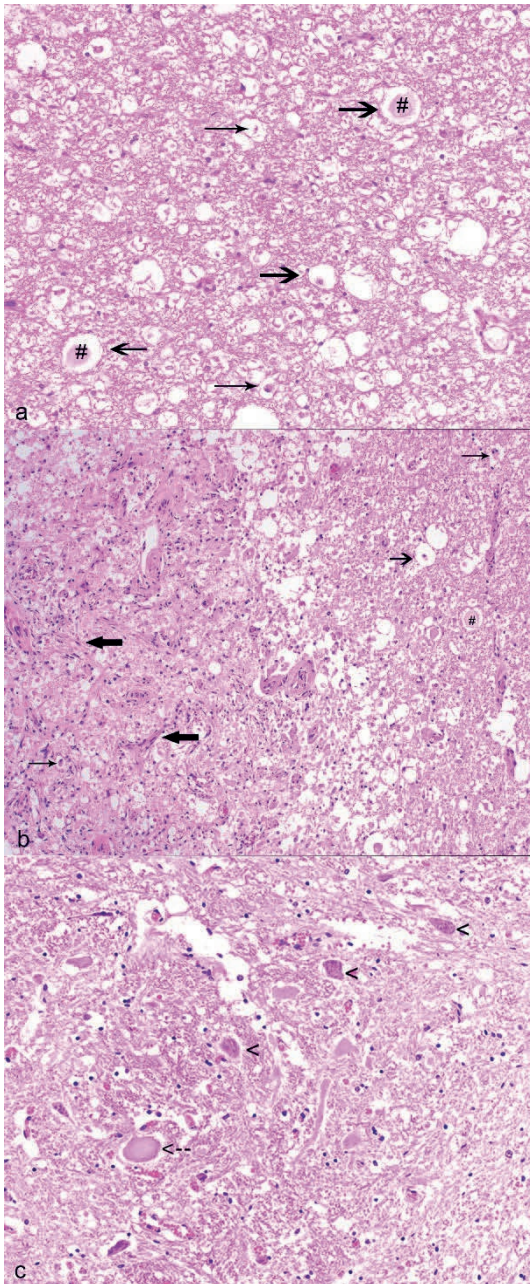


Figure 3. Histological changes in the spinal cord of horses with cervical vertebral compressive myelopathy.

(a) White matter of the spinal cord of a 2 years old Groningen horse. Multifocal dilated myelin sheaths (arrow) with swollen axons (#, spheroids) or macrophages (thin arrow, digestion chambers) are visible, consistent with Wallerian degeneration. Haematoxylin eosin (HE).

(b) White matter of the spinal cord at C6C7 of the same 10 years old Royal Dutch Sport Horse as depicted in Figure 1. On the right site of the picture Wallerian degeneration as seen in Figure 2a is present. On the left site of the picture is additionally fibrosis visible (thick arrow). HE.

(c) Grey matter changes of the spinal cord of the same horse and at the same level as in Figure 2a. Arrowhead= normal neurons, stippled arrow = degenerated neuron with central chromatolysis. HE.

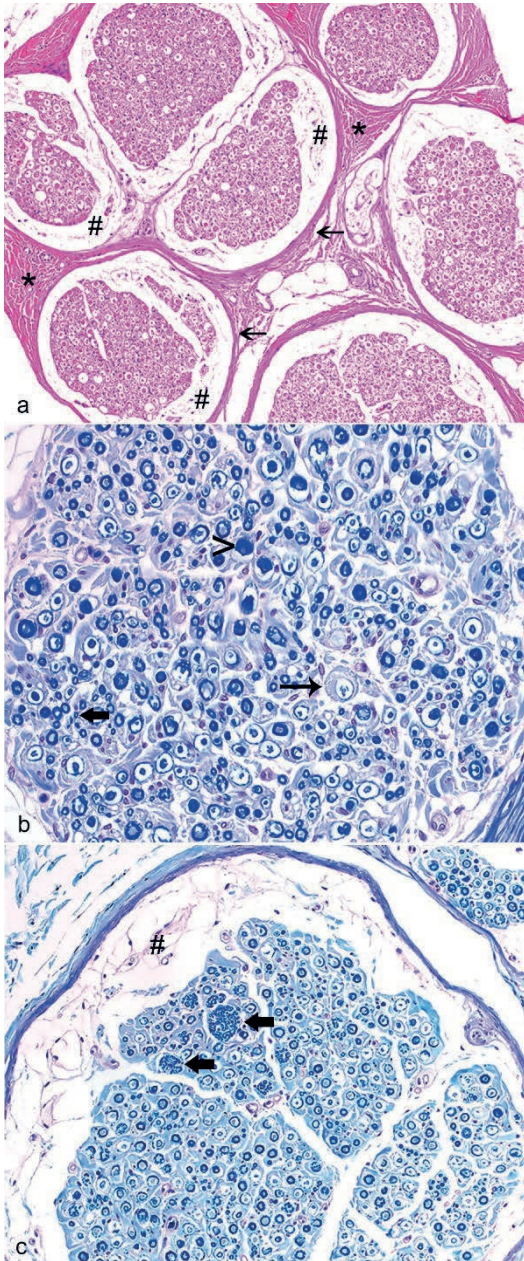


Figure 4. Changes compatible with chronic nerve compression in horses with cervical vertebral compressive myelopathy.

(a) Left spinal nerve C7 of the same 10 years old Royal Dutch Sport Horse as depicted in Figures 2 and 3. Around and multifocal within the nerve fascicles Renaut bodies (#) are visible. Also between the fascicles is a moderate proliferation of the perineurium (arrow) and epineurium (*) visible. Hematoxylin eosin (HE).

(b) Left spinal nerve C5 of a 5 years old Royal Dutch Sport Horse. Remyelination is characterized by onion bulb formation (thin arrow), excessive thick myelin sheaths (arrow head), and scattered small fibers (thick arrow). Luxol fast blue/picrosirius hematoxylin stain (LFB/HE).

(c) Depicted is the same nerve as in Figure 3b. Surrounding the nerve are Renaut bodies visible (#). Within the nerve are clusters of small regenerating fibers present (thick arrow). LFB/HE

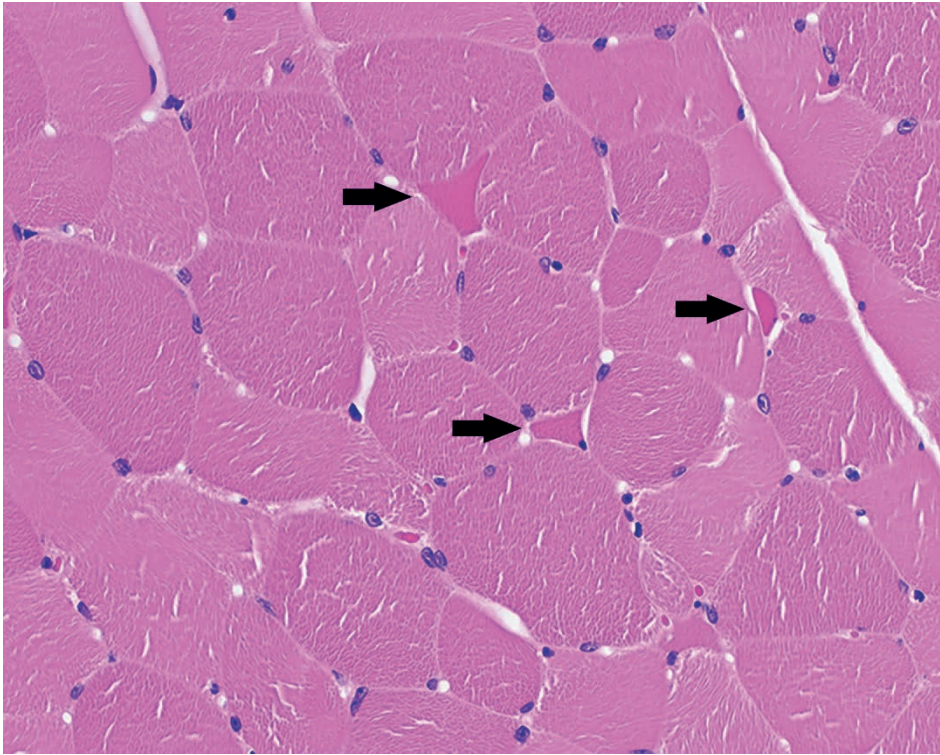


Figure 5. Denervation atrophy. Histological picture of the *Musculus trapezius* of a 1 year old Royal Dutch Sport Horse with cervical vertebral compressive myelopathy. The arrows point to scattered, single, small, angular nerves fibers, characteristic of mild denervation atrophy.

In dogs and humans, analogous syndromes to CVM are known as cervical spondylomyelopathy (dogs) and degenerative cervical myelopathy (human). Canine cervical spondylomyelopathy can be divided in 2 syndromes: disc-associated spondylomyelopathy and osseous-associated spondylomyelopathy.

Disc-associated spondylomyelopathy is most common in large breed dogs, especially older Dobermann pinchers. In this syndrome, neurological signs are the result of intervertebral disc protrusion, most frequently occurring in the caudal part of the neck (C5-C7). Concomitant ligamentum flavum hypertrophy and APJ degeneration is common and it is thought that these are the result of biomechanical changes.¹⁰

In osseous-associated cervical spondylomyelopathy, compression of the spinal cord and spinal nerves results from osseous proliferation of the dorsal lamina and the APJs in the caudal part of the neck (C5-C7). This syndrome is most common in young, male dogs of giant and large breeds (especially great Danes) and is associated with secondary soft tissue proliferation. Although affected dogs often have IVD degeneration (IVDD), a correlation between IVDD and APJ changes could not be found.⁹

In humans, the pathogenesis of degenerative cervical myelopathy starts with degeneration of the IVD, resulting in bulging of the disc into the spinal canal, with ultimately collapse of the disc. Both, disc degeneration, which renders the tissue stiffer, and disc collapse lead to changing biomechanics causing uncovertebral joint- and APJ OA, with formation of osteophytes, and thickening of the ligamentum flavum, contributing to the spinal cord compression. Likewise, ossification of the posterior longitudinal ligament can directly compress the spinal cord and can, due to stiffening, cause abnormal biomechanics with subsequent secondary degeneration of adjacent structures. Similar to horses, human individuals with a congenital small spinal canal (congenital cervical spinal stenosis) are predisposed to develop degenerative cervical myelopathy.^{30, 45}

Experimentally, the correlation of IVDD and APJ OA has been confirmed in sheep. After surgically inducing lumbar disc degeneration, OA of same level and adjacent APJs developed within one to two months.³⁸

The correlation between IVDD and APJ degeneration is well accepted in different species and therefore, it is likely that this correlation is also present in horses, meaning that IVDD could be important in the development of CVM. However there is not much known about equine IVDD and IVDD is thought to be clinically less relevant in horses, although systematic research is lacking.^{8, 29, 39, 48, 56}

Osteochondrosis

OC has been suggested as a likely primary cause for APJ OA as seen in static CVM.^{40, 47} OC of the epiphyseal growth cartilage is characterized by focal disturbance in endochondral ossification, secondary to failure of the blood supply.^{42, 43, 44} The failure of the blood supply is due to cartilage canal vessel necrosis.^{42, 43, 44} The cause for the vascular necrosis is not yet known, however it is known that it occurs during the incorporation of the

blood vessels into the advancing ossification front during growth. As a result, an area of chondronecrosis occurs (OC latens; Figure 6a). When the lesion progresses, the ossification front can also become affected resulting in delayed ossification (OC manifesta Figure 6b).^{41, 42, 44} The superficial cartilage above the necrotic, weakened cartilage, can subsequently fracture due to physiological and traumatic biomechanical forces, giving rise to hinged cartilage flaps or loose cartilage and bone fragments in the joint (OCD; Figure 6c).^{41, 63} Yet, spontaneous regression of all 3 stages is common.¹⁷ OC occurs at specific predilection sites. These predilection sites are inherent to site specific traits of the joints affected.⁶³ In pigs specific joint- and leg shapes have been correlated with the occurrence of grossly visible OC. It is thought that this is the result of shape-associated increased biomechanical forces.^{16 22} Selective breeding against these shapes has decreased the prevalence of OC in pigs.²¹

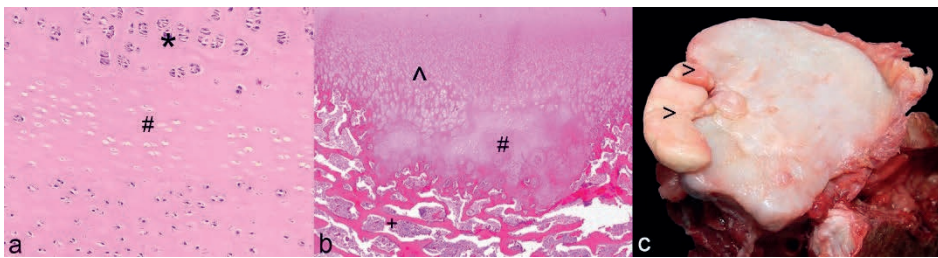


Figure 6. Different stages of osteochondrosis

(a). Articular process joint of a 3 days old Royal Dutch Sport Horse. Osteochondrosis latens. Epiphyseal cartilage with focal extensive chondronecrosis (#). In the periphery proliferation of chondrocytes (chondrones, *). Heamatoxylin eosin (HE).

(b). Articular process joint of a 1 days old Royal Dutch Sport Horse. Osteochondrosis manifesta. Persistent necrotic epiphyseal cartilage (#). + trabecular bone; ^ vital epiphyseal cartilage (HE).

(c). Facet of an articular process joint of a 3 years old Royal Dutch Sport Horse. Osteochondrosis dissecans. Severely irregular cartilage with 2 loose joint mice (>).

Scope of the thesis

The goal of this thesis is to investigate OC, IVDD and APJ OA and their association with factors known to be of importance in CVM.

Hypotheses of this thesis

The research within the scope of this thesis is based on the following hypotheses:

- 1** In warmblood horses, APJ OC is more common, with more severe lesions, in the caudal cervical vertebral column, the predilection site for CVM.
- 2** Certain APJ facet shapes have a higher likelihood to develop OC and these shapes are more common in the caudal part of the cervical vertebral column.
- 3** Equine IVDs are composed of a nucleus pulposus and annulus fibrosis.
- 4** In warmblood horses, IVDD is most common in the caudal part of the cervical vertebral column.
- 5** The gross, histological and biochemical changes of IVDD in warmblood horses are similar to those of dogs and humans.
- 6** The biochemical changes of the degenerated equine IVD have been correlated with loss of function in the IVDs in other species and other equine tissues, suggesting that also in the horse these changes are associated with loss of function.

To explore the likelihood of OC as the main cause of APJ OA in the caudal cervical neck of warmblood horse, the presence of a predilection site of OC within the neck is evaluated in **chapter 2**. If OC is indeed the main cause for APJ OA, overlapping predilection sites of both conditions are to be expected. During sampling of the foal APJs for the study of **chapter 2**, it was noted that a considerable variation in shape was present. As the pathogenesis of OC in pigs is the same as in horses ¹⁴, and in pigs an association between

joint- and leg shape with grossly visible OC has been established^{16, 21, 22}, it was decided to categorize the different shapes of the APJs, to evaluate the distribution of shapes within the cervical and cranial thoracic vertebral column and to evaluate their correlation with OC in **chapter 3**.

Intervertebral disc degeneration

Mammalian IVDs are composed of a collagen-rich, lamellar, outer annulus fibrosus (AF), a central, proteoglycan-rich nucleus pulposus (NP) and a cartilaginous endplate bordering the bony vertebrae.⁶⁰ The IVD serves to transmit compressive forces and provide limited mobility.¹

Surprisingly, there is no consensus about the anatomy and composition of the equine IVD, with some authors claiming that the equine IVD lacks a NP^{8, 56} and other stating there is a NP which is either fibrous^{39, 48} or fibrocartilaginous.^{29, 62} Therefore in **chapter 4** the gross and histological anatomy of the normal equine IVD will be described.

The two most commonly researched species concerning IVDD are the dog and humans. In both species, spontaneous IVDD and development of associated clinical disease is common.^{4, 25} In these species, degeneration starts in the NP and is characterized by cellular and biochemical changes. The initial notochordal cells are replaced by chondrocyte-like cells.^{5, 7, 11, 24} The most characteristic biochemical change is a decrease in the amount of proteoglycans with subsequent dehydration of the intercellular matrix.^{1, 2, 6} A second important biochemical change is an increase in the total amount of collagen and collagen type 1, and a decrease in the amount of collagen type 2, creating a fibrotic phenotype.^{1, 3, 5, 7, 61} In the AF, degeneration is characterized by replacement of fibroblast by chondrocyte-like cells with subsequent disorganization of the lamellae.^{5, 7, 11, 49} Biochemically, there is also in the AF an increase in total amount of collagen.⁷

Grossly, these cellular and biochemical changes result in the NP changing from a bulging gel-like structure to a consolidated, "fibrous" nucleus. In the AF, there is replacement of the discrete fibrous lamellae by a mucinous matrix with focal disruptions. Consequently, the demarcation between the NP and AF becomes less clear.

These degenerative alterations cause the IVD to obtain changed biomechanical characteristics which leads to instability of the spinal unit that

can result in osteophytes developing at the vertebral margins and cause OA of the adjacent synovial joints ^{4, 10, 12, 20, 26, 28, 36, 46, 53, 54}

To objectively investigate whether IVDD is of clinical importance in the horse, a validated and biologically credible grading scheme is necessary. Therefore the second aim of **chapter 4** is to describe the gross changes of the degenerated equine IVD and subsequently, to develop such a macroscopic grading scheme for IVDD in the horse. The predilection site for static CVM caused by APJ OA, as most commonly seen in warmblood horses, is the caudal cervical spine. ^{33, 40, 58} If IVDD is implicated in the development of APJ OA, this would also be most prevalent in the caudal cervical region. Therefore the third objective of **chapter 4** is to determine whether there is a predilection site for IVDD in the warmblood horse.

To evaluate if IVDD in the horse is likely resulting in biomechanical modifications as seen in other species ^{4, 53}, the histological and biochemical properties of healthy and degenerated discs are studied in **chapter 5**.

Histological scoring is considered the gold standard for determining presence of IVDD in dogs and humans. ^{5, 11, 49} As it is expected that in the horse equivalent histological changes are present, the second objective of **chapter 5** is to develop a histological scorings scheme specifically for the horse.

Finally in **chapter 6** the overall obtained results will be discussed and suggestions for future research to answer still open and new questions will be given.

References

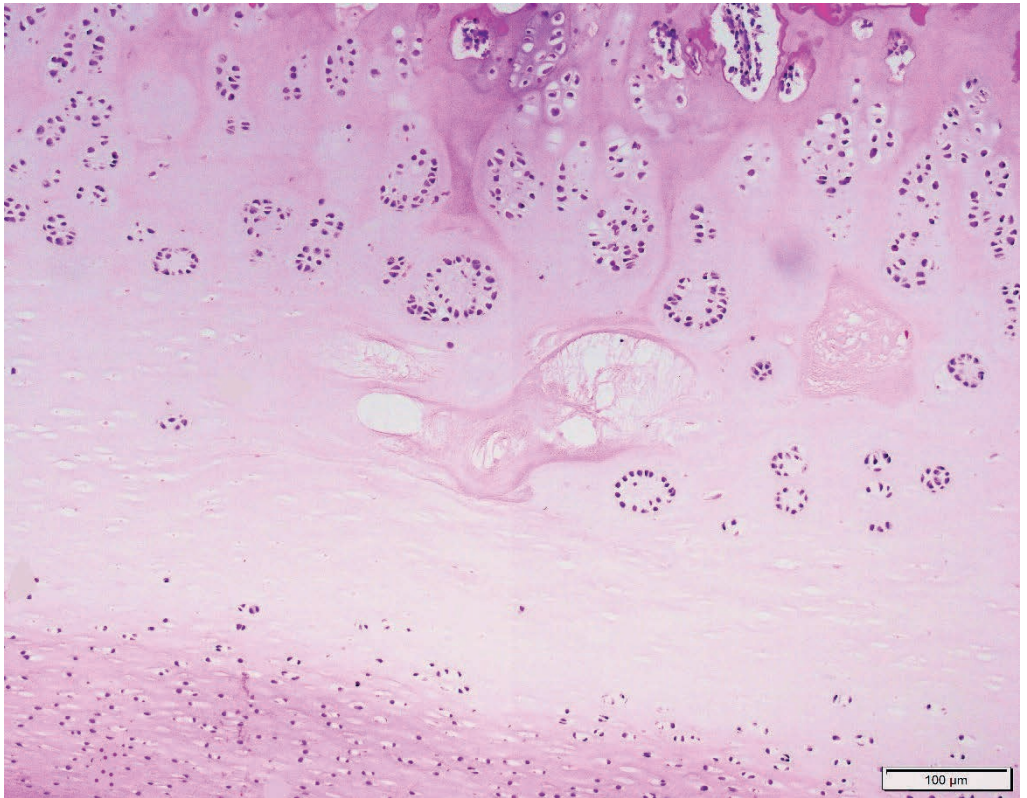
1. Adams MA, Roughley PJ. What is intervertebral disc degeneration, and what causes it? *Spine*. 2006;31(18):2151-2161.
2. Antoniou J, Steffen T, Nelson F, et al. The human lumbar intervertebral disc: evidence for changes in the biosynthesis and denaturation of the extracellular matrix with growth, maturation, ageing, and degeneration. *J Clin Invest*. 1996;98(4):996-1003.
3. Bach FC, Tellegen AR, Beukers M, et al. Biologic canine and human intervertebral disc repair by notochordal cell-derived matrix: from bench towards bedside. *Oncotarget*. 2018;9(41):26507-26526.
4. Bergknut N, Grinwis G, Pickee E, et al. Reliability of macroscopic grading of intervertebral disk degeneration in dogs by use of the Thompson system and comparison with low-field magnetic resonance imaging findings. *Am J Vet Res*. 2011;72(7):899-904.
5. Bergknut N, Meij BP, Hagman R, et al. Intervertebral disc disease in dogs - Part 1: A new histological grading scheme for classification of intervertebral disc degeneration in dogs. *Vet J*. 2013;195(2):156-163.
6. Bergknut N, Rutges JPHJ, Kranenburg H-C, et al. The dog as an animal model for intervertebral disc degeneration? *Spine*. 2012;37(5):351-358.
7. Bergknut N, Smolders LA, Grinwis GC, et al. Intervertebral disc degeneration in the dog. Part 1: Anatomy and physiology of the intervertebral disc and characteristics of intervertebral disc degeneration. *Vet J*. 2013;195(3):282-291.
8. Bollwein A, Hänichen T. Age-related changes in the intervertebral disks of the cervical vertebrae of the horse. *Tierarztl Prax*. 1989;17(1):73-76.
9. Bonelli MA, da Costa, L. B. S. B. C., da Costa RC. Association of neurologic signs with high-field MRI findings in 100 dogs with osseous-associated cervical spondylomyelopathy. *Vet Radiol Ultrasound*. 2021;62(6):678-686.
10. Bonelli MA, da Costa, L. B. S. B. C., da Costa RC. Magnetic resonance imaging and neurological findings in dogs with disc-associated cervical spondylomyelopathy: a case series. *BMC Vet Res*. 2021;17(1):145-5.
11. Boos N, Weissbach S, Rohrbach H, et al. Classification of age-related changes in lumbar intervertebral discs: 2002 Volvo award in basic science. *Spine*. 2002;27(23):2631-2644.
12. Butler D, Trafimow JH, Andersson GB, et al. Discs degenerate before facets. *Spine* . 1990;15(2):111-113.

13. Cai XY, Sang D, Yuchi CX, et al. Using finite element analysis to determine effects of the motion loading method on facet joint forces after cervical disc degeneration. *Comput Biol Med.* 2020;116:103519.
14. Carlson CS, Cullins LD, Meuten DJ. Osteochondrosis of the articular-epiphyseal cartilage complex in young horses: evidence for a defect in cartilage canal blood supply. *Vet Pathol.* 1995;32(6):641-647.
15. Claridge HAH, Piercy RJ, Parry A, et al. The 3D anatomy of the cervical articular process joints in the horse and their topographical relationship to the spinal cord. *Equine Vet J.* 2010;42(8):726-731.
16. de Koning DB, van Grevenhof EM, Laurensen BF, et al. Associations of conformation and locomotive characteristics in growing gilts with osteochondrosis at slaughter. *J Anim Sci.* 2015;93(1):93-106.
17. Dik KJ, Enzerink E, van Weeren PR. Radiographic development of osteochondral abnormalities, in the hock and stifle of Dutch Warmblood foals, from age 1 to 11 months. *Equine Vet J Suppl.* 1999;(31):9-15.
18. Duncan ID, Schneider RK, Hammang JP. Subclinical entrapment neuropathy of the equine suprascapular nerve. *Acta Neuropathol.* 1987;74(1):53-61.
19. Dyson SJ. Lesions of the equine neck resulting in lameness or poor performance. *Vet Clin North Am Equine Pract.* 2011;27(3):417-437.
20. Gotfried Y, Bradford DS, Oegema TR, Jr. Facet joint changes after chemonucleolysis-induced disc space narrowing. *Spine.* 1986;11(9):944-950.
21. Grondalen T. Osteochondrosis and arthrosis in Norwegian slaughter-pigs in 1980 compared to 1970. *Nord Vet Med.* 1981;33(9-11):417-422.
22. Grondalen T. Osteochondrosis and arthrosis in pigs. VII. Relationship to joint shape and exterior conformation. *Acta Vet Scand Suppl.* 1974;46(0):1-32.
23. Hall MC. *Luschka's Joint.* Charles. C. Thomas Publisher; 1965.
24. Hansen T, Smolders LA, Tryfonidou MA, et al. The myth of fibroid degeneration in the canine intervertebral disc: A histopathological comparison of intervertebral disc degeneration in chondrodystrophic and nonchondrodystrophic dogs. *Vet Pathol.* 2017;54(6):945-952.
25. Ikegawa S. The genetics of common degenerative skeletal disorders: Osteoarthritis and degenerative disc disease. *Annu Rev Genomics Hum Genet.* 2013;14:245-256.

26. Iorio JA, Jakoi AM, Singla A. Biomechanics of degenerative spinal disorders. *Asian Spine J.* 2016;10(2):377-384.
27. Janes JG, Garrett KS, McQuerry KJ, et al. Cervical vertebral lesions in equine stenotic myelopathy. *Vet Pathol.* 2015;52(5):919-927.
28. Jaumard NV, Welch WC, Winkelstein BA. Spinal facet joint biomechanics and mechanotransduction in normal, injury and degenerative conditions. *J Biomech Eng.* 2011;133(7):071010.
29. Jeffcott LB, Dalin G. Natural rigidity of the horse's backbone. *Equine Vet J.* 1980;12(3):101-108.
30. Lannon M, Kachur E. Degenerative cervical myelopathy: clinical presentation, assessment, and natural history. *J Clin Med.* 2021;10(16):10.3390/jcm10163626.
31. Laugier C, Tapprest J, Foucher N, et al. A necropsy survey of neurologic diseases in 4,319 horses examined in Normandy (France) from 1986 to 2006. *J Equine Vet Sci.* 2009;29(7):561-568.
32. Lee SH, Son DW, Lee JS, et al. Relationship between endplate defects, modic change, facet joint degeneration, and disc degeneration of cervical spine. *Neurospine.* 2020;17(2):443-452.
33. Levine JM, Adam E, MacKay RJ, et al. Confirmed and presumptive cervical vertebral compressive myelopathy in older horses: a retrospective study (1992-2004). *J Vet Intern Med.* 2007;21(4):812-819.
34. Levine JM, Ngheim PP, Levine GJ, et al. Associations of sex, breed, and age with cervical vertebral compressive myelopathy in horses: 811 cases (1974-2007). *J Am Vet Med Assoc.* 2008;233(9):1453-1458.
35. Levine JM, Scrivani PV, Divers TJ, et al. Multicenter case-control study of signalment, diagnostic features, and outcome associated with cervical vertebral malformation-malarticulation in horses. *J Am Vet Med Assoc.* 2010;237(7):812-822.
36. Li J, Muehleman C, Abe Y, et al. Prevalence of facet joint degeneration in association with intervertebral joint degeneration in a sample of organ donors. *J Orthop Res.* 2011;29(8):1267-1274.
37. Moore BR, Holbrook TC, Stefanacci JD, et al. Contrast-enhanced computed tomography and myelography in six horses with cervical stenotic myelopathy. *Equine Vet J.* 1992;24(3):197-202.
38. Moore RJ, Crotti TN, Osti OL, et al. Osteoarthritis of the facet joints resulting from anular rim lesions in sheep lumbar discs. *Spine.* 1999;24(6):519-525.

39. Nixon AJ, Stashak TS, Ingram JT, Norrdin RW, Park RD. cervical intervertebral disk protrusion in a horse. *Vet Surg*. 1984;154-158.
40. Nout YS, Reed SM. Cervical vertebral stenotic myelopathy. *Equine Vet Educ*. 2003;15(4):212-223.
41. Olstad K, Hendrickson EH, Carlson CS, et al. Transection of vessels in epiphyseal cartilage canals leads to osteochondrosis and osteochondrosis dissecans in the femoro-patellar joint of foals; A potential model of juvenile osteochondritis dissecans. *Osteoarthr Cartil*. 2013;21(5):730-738.
42. Olstad K, Ytrehus B, Ekman S, et al. Early lesions of articular osteochondrosis in the distal femur of foals. *Vet Pathol*. 2011;48(6):1165-1175.
43. Olstad K, Ytrehus B, Ekman S, et al. Epiphyseal cartilage canal blood supply to the metatarsophalangeal joint of foals. *Equine Vet J*. 2009;41(9):865-871.
44. Olstad K, Ytrehus B, Ekman S, et al. Epiphyseal cartilage canal blood supply to the tarsus of foals and relationship to osteochondrosis. *Equine Vet J*. 2008;40(1):30-39.
45. Onofrei LV, Henrie AM. Cervical and thoracic spondylotic myelopathies. *Semin Neurol*. 2021;41(3):239-246.
46. Panjabi MM, Krag MH, Chung TQ. Effects of disc injury on mechanical behavior of the human spine. *Spine*. 1984;9(7):707-713.
47. Powers BE, Stashak TS, Nixon AJ, et al. Pathology of the vertebral column of horses with cervical static stenosis. *Vet Pathol*. 1986;23(4):392-399.
48. Rooney JR. The horse's back: biomechanics of lameness. *Vet Clin N A, Equine Pract*. 1982;4(2):17-27.
49. Rutges JPHJ, Duit RA, Kummer JA, et al. A validated new histological classification for intervertebral disc degeneration. *Osteoarthr Cartil*. 2013;21(12):2039-2047.
50. Sang D, Du CF, Wu B, et al. The effect of cervical intervertebral disc degeneration on the motion path of instantaneous center of rotation at degenerated and adjacent segments: a finite element analysis. *Comput Biol Med*. 2021;134:104426.
51. Stewart RH, Reed SM, Weisbrode SE. Frequency and severity of osteochondrosis in horses with cervical stenotic myelopathy. *Am J Vet Res*. 1991;52(6):873-879.
52. Summers BA, Cummings JF, de Lahunta A. *Veterinary Neuropathology*. Mosby; 1995.

53. Thompson JP, Pearce RH, Schechter MT, et al. Preliminary evaluation of a scheme for grading the gross morphology of the human intervertebral disc. *Spine*. 1990;15(5):411-415.
54. Thompson RE, Pearcy MJ, Downing KJ, et al. Disc lesions and the mechanics of the intervertebral joint complex. *Spine*. 2000;25(23):3026-3035.
55. Tomizawa N, Nishimura R, Sasaki N, et al. Morphological analysis of cervical vertebrae in ataxic foals. *J Vet Med Sci*. 1994;56(6):1081-1085.
56. Townsend HG, Leach DH. Relationship between intervertebral joint morphology and mobility in the equine thoracolumbar spine. *Equine Vet J*. 1984;16(5):461-465.
57. Trostle SS, Dubielzig RR, Beck KA. Examination of frozen cross sections of cervical spinal intersegments in nine horses with cervical vertebral malformation: lesions associated with spinal cord compression. *J Vet Diagn Invest*. 1993;5(3):423-431.
58. van Biervliet J, Mayhew J, de Lahunta A. Cervical vertebral compressive myelopathy: diagnosis. *Clin Tech Equine Pract*. 2006;5(1):54-59.
59. Walraevens J, Liu B, Meersschaert J, et al. Qualitative and quantitative assessment of degeneration of cervical intervertebral discs and facet joints. *Eur Spine J*. 2009;18(3):358-369.
60. Wintrich T, Scaal M, Böhmer C, et al. Palaeontological evidence reveals convergent evolution of intervertebral joint types in amniotes. *Sci Rep*. 2020;10(1):14106.
61. Yee A, Lam MP, Tam V, et al. Fibrotic-like changes in degenerate human intervertebral discs revealed by quantitative proteomic analysis. *Osteoarthr Cartil*. 2016;24(3):503-513.
62. Yovich JV, Powers BE, Stashak TS. Morphologic features of the cervical intervertebral disks and adjacent vertebral bodies of horses. *Am J Vet Res*. 1985;46(11):2372-2377.
63. Ytrehus B, Carlson CS, Ekman S. Etiology and pathogenesis of osteochondrosis. *Vet Pathol*. 2007;44(4):429-448.



Cervical articular process joint osteochondrosis in warmblood foals

2

Published in: Equine Veterinary Journal.
2020;52:664–669

W. Bergmann
M. de Mik-van Mourik
S. Veraa
J. van den Broek
I. D. Wijnberg
W. Back
A. Gröne

Abstract

Background: In warmblood horses degenerative joint disease is involved in cervical malformation and malarticulation (CVM). The degree of contribution of articular process joint (APJ) osteochondrosis (OC) is not clear.

Objectives: a) to explore the presence of predilection sites for APJ OC in cervical and cranial thoracic vertebral columns of warmblood foals and b) to examine correlation of such a site with the predilection site of CVM.

Study Design: Case series.

Methods: Seven hundred APJ facets of C2 to T2 of 29 foals (11 months gestation to 12 months (median age 7 days; range 365 days; 95% confidence interval (95% CI) 2- 47 days)) were examined for OC and prevalence between joints, and the predilection site for CVM and the cranial cervical vertebral column were evaluated.

Results: About 20.6 % of facets revealed OC. There was no predilection site. Prevalence decreased with age up to 1 year (odds ratio (OR) 0.997; (95% CI 0.975-0.998 but not up to 5 months. Severity increased with age in all age ranges (up to 1 year OR 1.023; 95% CI 1.005-1.049; > 1- 5 months, OR 1.203;95% CI 1.014e+00-1.921; up to 1 month, OR 1.114; 95% CI 1.041-1.228). Highest prevalence was in cranial facets of the cervical and cervical thoracic joints and in caudal facets of the thoracic joint up to 1 year and up to 1 month (OR 0.364; 95% CI 0.170-0.745, OR 0.434; 95% CI:0.235 -0.782, OR 7.665; 95% CI: 1.615-66.553 and OR 0.400; 95% CI 0.170-0.880, OR 0.351; 95% CI 0.172-0.700, OR 5.317; 95% CI 1.098-44.344 respectively).

Main limitations: Two thirds of the foals were less than 1 month of age.

Conclusions: APJ OC in warmblood foals is common and is not more prevalent at CVM predilection sites suggesting that abnormalities of endochondral ossification may not be major contributors to CVM.

Introduction

Cervical malformation and malarticulation (CVM) is a common cause for neck pain, pelvic and/ or thoracic limb paresis and ataxia caused by compression of the spinal cord and/or nerve roots.^{8, 9, 10, 12, 14, 16, 17} The pathogenesis for this condition is presumed to be multifactorial.^{9, 10, 14}

Compression of the spinal cord or nerves may be present in a static or dynamic form although there is overlap. The caudal part of the cervical vertebral column from cervical vertebra (C)5 to thoracic vertebra (T)1 is most frequently involved in the static form of spinal cord compression and is most commonly seen in older horses, especially warmblood horses of 4 years and older.^{8, 12, 16, 17} This form is most often caused by osteoarthritic changes of the articular process joints (APJs), with resulting enlargement of the joints, hypertrophy of the ligamentum flavum and the joint capsule, and formation of synovial cysts.^{8, 10, 14} The presence of APJ osteochondrosis (OC) has been described in cases of CVM^{12, 13, 14, 17} and it has been suggested that degenerative changes of the APJs in horses with CVM is secondary to primary OC.^{12, 13}

This study has two aims. First to investigate whether the different cervical and cranial thoracic vertebral APJs or certain regions within this part of the vertebral column of warmblood foals have predilection sites for OC. Second, to determine the extent of agreement between predilection sites of OC and the predilection site for CVM as seen in adult warmblood horses. It is hypothesized that APJ OC is more common with more severe lesions in the caudal cervical region, the predilection site for CVM in warmblood horses.

Materials and Methods

Horses

A total of 31 warmblood foals, that were privately owned by 25 different owners, were examined. The foals either died unexpectedly or were humanly subjected to euthanasia for reasons unrelated to the current study between July 2012 to August 2013 and April 2017 to July 2018 and subsequently referred for necropsy to the Division of Pathology of Utrecht

University (Supplementary Table S1). One of the foals (at term, foal 1; Table S1) was removed from the uterus of its dam during the necropsy of this mare. Foals were excluded from this study if disorders were present that could affect the morphology of the APJs (e.g. fractures, osteomyelitis, arthritis)

Two foals (foal 7 and foal 10; Table S1) had a septicaemia with resultant microscopically visible vascular changes in the facet cartilage. As these changes can lead to OC-like lesions these foals were removed from further investigation.²¹ The remaining 29 foals were of different ages, varying from 11 months gestation to 12 months post-partum (median age 7 days; range 365 days; 95% confidence interval (95% CI) 2-47 days), breed (28 Royal Dutch Sport horses, 1 Zangersheide horse) and sex (11 females, 18 males; Table S1). For the flowchart concerning the eligibility of the available foals see Figure S1.

Data collection

Necropsy was performed on all foals with the owner's informed consent to investigate the cause of death or the cause for the clinical signs (Table S1). After necropsy, the cervical and cranial part of the thoracic vertebral column were removed and the neck was dissected with subsequent gross evaluation of the APJs. For histological evaluation slices of approximately 3 mm thickness were cut perpendicular to the facet. The area was selected based on possible OC-related gross changes. A slice was taken from the middle of the facet when no gross changes were visible. In 17 foals (foals 1, 2, 5, 13, 14, 15, 17, 18, 19, 20, 21, 22, 23, 27, 29, 30 and 31) the facets of the cervical vertebrae C3, C5, C6, C7, the thoracic vertebra T1 and the cranial facet of T2 were examined (22 facets each). In 11 foals (foals 3, 4, 6, 8, 9, 12, 16, 24, 25, 26 and 28) the caudal facets of C2 and the facets of C4 were additionally assessed (28 facets each). In foal 11 the facets of C2, C3 and C4 were not collected, whereas those of C5, C6, C7, T1 and the cranial facets of T2 were (a total of 18 facets). The bone slices were fixed in 4% buffered formaldehyde and decalcified in 10% ethylenediaminetetraacetic acid (EDTA) before routine processing and staining with haematoxylin and eosin and subsequent light microscopic evaluation for osteochondral lesions. Although lesions suggestive for OC (focal thickening of cartilage, soft and red

cartilage²² can be identified during gross evaluation, histology was considered the 'gold standard' for confirmation and for diagnosing initial lesions (OC latens), which cannot be diagnosed grossly.^{11, 22}

Each affected facet was designated to one of the subtypes of OC (latens, manifesta or dissecans) to classify the severity of the lesions. OC latens is characterised by focal epiphysial cartilage necrosis, OC manifesta is accompanied by the involvement of endochondral ossification and OC dissecans is accompanied by fissure formation through articular cartilage.²² The presence of only OC latens was classified as mild, presence of at least one area with OC manifesta was classified as being moderate and presence of at least one area with OC dissecans was classified as severe OC. Other joints were not evaluated for the presence of OC.

Sites of interest

The focus of this study was on the APJs of the caudal cervical vertebral column from the caudal APJs of cervical vertebra 5 up to the cranial APJs on the first thoracic vertebra (region C5CA-T1CR) with a total of 236 facets. The facets of caudal APJs on the second cervical vertebra up to the facets of the cranial APJs on the fifth cervical vertebra (region C2CA-C5CR) with a total of 348 facets were added as control (Figure 1). Furthermore a possible predilection site was investigated for the different individual joints C2C3, C3C4, C4C5, C5C6, C6C7, C7T1 and T1T2. In total, 700 facets were assessed. Facet locations are abbreviated by vertebra (C2, C3, C4, C5, C6, C7, T1, T2), left or right side (L or R) and cranial or caudal position on the vertebra (CR or CA).

Data analysis

Facets without histological signs of OC were given a score 0, while facets with lesions consistent with OC were given a 1, thus producing binary data. The outcomes were analysed using a logistic regression model with foal as a random effect and the fixed effects of age, sex, joint, region of the vertebral column, position (cranial/caudal) of the facet on the vertebra and site (left/right) of the facet on the vertebra (Figure 1).

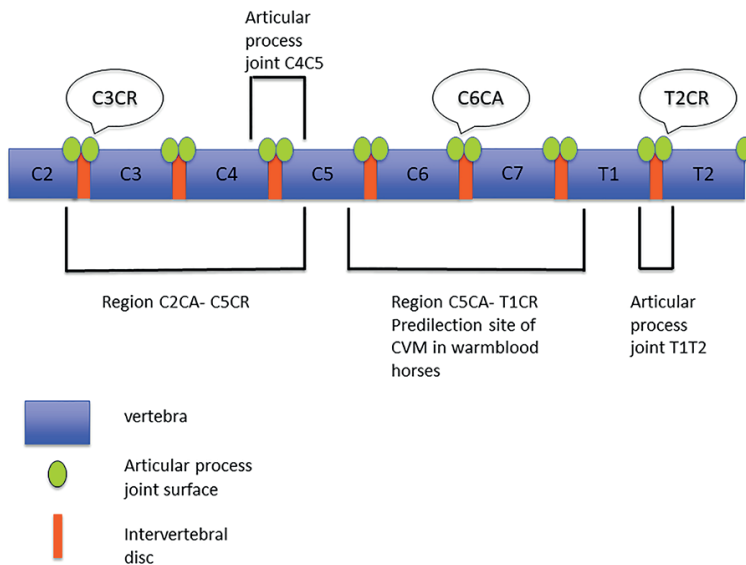


Figure 1. Schematic overview of the facets examined. C= cervical vertebra; T= thoracic vertebra; CR=cranial; CA=caudal; CVM=cervical malformation and malarticulation.

Model selection was done by stepwise backward elimination and the Akaike information criterion (AIC) was used to select the best model. Furthermore 95% log profile likelihood confidence intervals were used as effect size estimates.³ To see if the likelihood of the occurrence of OC increased if a neighbouring joint had OC could not be determined by this model due to identifiability problems that were likely due to intertwinement of the fixed effects. Instead the proportions of OC per joint were determined and subsequently the Pearson's correlation coefficient between the proportion of OC in a joint with the one before or after was determined.

The same logistic regression model was also used for the outcome severity of OC, with OC latens given a score 0, and OC manifesta a score 1. For this model the 144 OC positive facets were used. No OC dissecans was encountered and therefore not scored.

All calculations were performed with R (R Development Core Team, version 3.4.3, package lme4, R: A language and environment for statistical computing. R Foundation for Statistical Computing. <https://www.R-project.org>) and analysed using R studio: Integrated Development for R. RStudio, Inc., <http://www.rstudio.com/>).

Age turned out to have an effect on the likelihood to develop OC and therefore these calculations were repeated with one subset of foals within the age range of >1 month up to 5 months of age (n=7) and one subset of foals within the age range of 0 days up to 1 month of age (n= 20). Hereby, the fixed effect age was kept as a continuous variable. In the subset of foals within the age range of > 1 month up to 5 months of age only 1 female foal was present, and therefore the independent variable sex was for this set of foals not taken into account. For the outcome severity of OC 25 respectively 114 OC positive facets were used in these subsets of foals.

Results

Both foal 7 and foal 10 (Table S1) showed OC-like changes in many of the APJs due to a severe bacterial osteomyelitis affecting the osteochondral junction, and a vasculitis of bacterial origin respectively Therefore these two foals were omitted from further investigation.²¹

Osteochondrosis latens was characterised by necrotic epiphyseal cartilage. This cartilage contained hypereosinophilic, shrunken chondrocytes with pyknotic nuclei and was occasionally also hypocellular. The matrix showed loss of differential staining. Often nodular clusters of chondrocytes (chondrones) were visible surrounding areas of necrotic cartilage. Cartilage canal blood vessels in affected area's had lost their endothelium and very rarely swollen endothelial cells or endothelial cells with pyknotic nuclei were present. Occasionally the vessel lumen was filled with hyper-eosinophilic, fibrillar material, interpreted as fibrin (Figure S2).

In OC manifesta the ossification front was (also) affected and persistent necrotic cartilage could be seen (Figure S3). Occasionally, fissure formation was present in the necrotic cartilage, which often extended into the subchondral bone where bone lysis and fibrosis could be appreciated.

Commonly, multiple, up to 4, separate affected areas were visible and both OC latens and manifesta could be seen within the same facet. All foals but

one had OC lesions in one to 24 facets examined (mean number of lesions per foal 4.24 +/- 4.50 lesions). The foal removed from the uterus (foal 1; Table S1) during the necropsy of its dam had 2 facets with OC lesions (one latens, one manifesta).

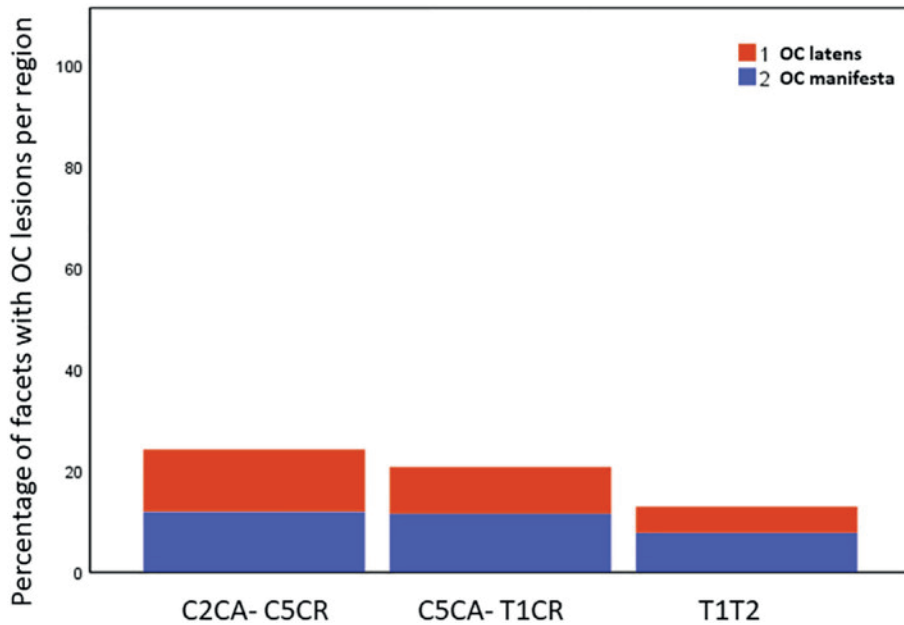
Osteochondrosis was identified in 144 / 700 facets (20.6 %), of which 66 (45.8 %) had OC latens and 78 (54.2%) OC manifesta. OC dissecans was not encountered (Table S1, Figure 2). Only 5 of the 144 facets with histologically confirmed OC lesions (3.5% of all facets with OC), had gross changes visible on the facet's surfaces, characterised by round to longitudinal indentation of the cartilage. All grossly visible affected facets had OC manifesta. There was no association between the frequency of OC lesions and sex, the different joints, regions within the vertebral column, nor the site (right/left) of the affected facet.

Taking all foals into account (age range of 0 up to 1 year), the likelihood of having OC did decrease with age (Table 1).

The odds of having OC lesions within the cranial facets of the cranial cervical region (C2CA-C5CR) and the CVM predilection site (C5CA-T1CR) were higher than of the caudal facets (Figure 3, Table 1). Odds of finding OC lesions within the caudal facets of the first thoracic APJ (T1T2) were higher than in the cranial facets (Figure 3, Table 1). There was no correlation between the proportion of OC in a joint and the proportion of OC in the joints cranial and caudal (lag-1 correlation -0.425; 95% CI -0.791-0.165). The likelihood of either mild or moderate OC did not differ between sex, different joints, region, site (left/right) or position (cranial/caudal). However, the likelihood of moderate OC did increase with age (Table 2).

In the subset of foals aged > 1-5 month none of the independent variables, including age, had an effect on the likelihood of OC lesions.

Similar to the entire population of foals aged 0 days up to 1 year, in the subset of foals aged 0 days to 1 month, the likelihood of OC lesions was higher for the cranial facets than the caudal facets in the cranial cervical region and the predilection site for CVM (Table 1). Also, the likelihood to develop OC was higher in the caudal facets than in the cranial facets of the first thoracic APJ in this age range (Table 1). As seen across the entire population, the likelihood of developing moderate OC increased with age in the subsets of foals with the younger age ranges (Table 2). The other independent variables had no effect on the likelihood to develop moderate OC.



2

FIGURE 2 Percentage of OC lesions found in each examined region in a group of warmblood foals. OC, osteochondrosis; C2CA-C5CR, region from the caudal articular process joints of the second cervical vertebra up to the cranial articular process joints of the fifth cervical vertebra; C5CA-T1CR, region from the caudal articular process joints of the fifth cervical vertebra up to the cranial articular process joint of the first thoracic vertebra; T1T2, articular process joints between the first and second thoracic joints

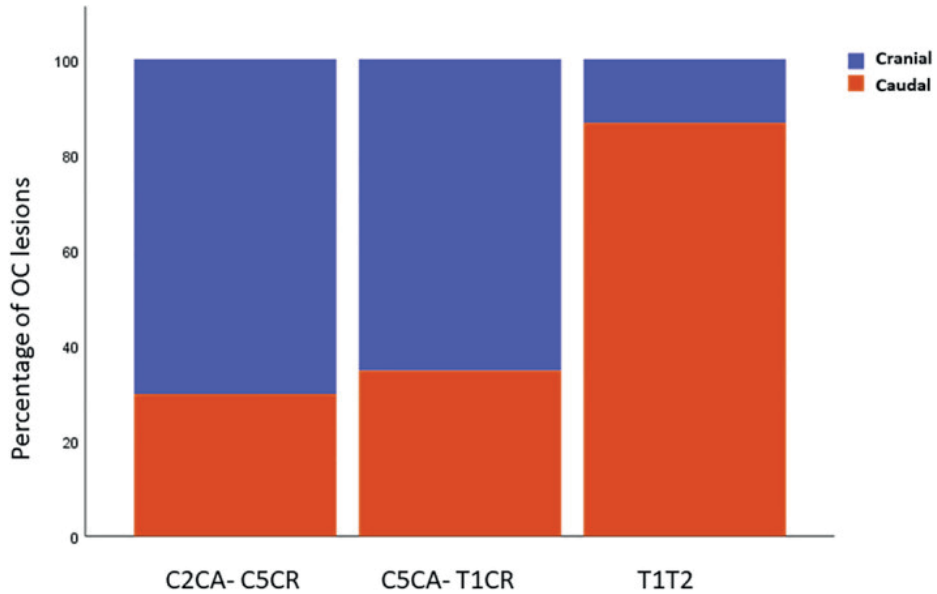


FIGURE 3 Distribution of OC lesions along the cranial and caudal position of the facets in each region examined in a group of warmblood foals aged 0 d to 1 y. C2CA-C5CR, from the caudal articular process joints of the second cervical vertebra to the cranial articular process joints of the fifth cervical vertebra; C5CAT1CR, from the caudal articular process joints of the fifth cervical vertebra to the cranial articular process joint of the first thoracic vertebra; T1T2, articular process joints between the first and second thoracic joint.

TABLE 1 Effective independent variables on the occurrence of osteochondrosis lesions in a group of warmbloods aged 0 d to 1 y

Age range	Independent variable	Odds ratio	95% profile likelihood confidence interval
0 d up to 1 y of age (N = 29)	Age	0.997	0.975-0.998
	Position (cranial vs. caudal)		
	Craniocervical (C2CA-C5CR)	0.364	0.170-0.745
	Caudocervical (C5CA-T1CR)	0.434	0.235-0.782
	First thoracic joint (T1T2)	7.665	1.615-66.553
0 d up to 1 mo of age (N = 20)	Position (cranial vs. caudal)		
	Craniocervical (C2CA-C5CR)	0.400	0.170-0.880
	Caudocervical (C5CA-T1CR)	0.351	0.172-0.700
	First thoracic joint (T1T2)	5.317	1.098-44.344

Abbreviations: C2CA-C5CR, region from the caudal articular process joints of the second cervical vertebra up to the cranial articular process joints of the fifth cervical vertebra; C5CA-T1CR, region from the caudal articular process joints of the fifth cervical vertebra up to the cranial articular process joint of the first thoracic vertebra; T1T2, articular process joints between the first and second thoracic joints; N, amount of foals examined.

TABLE 2 Effective independent variables on the severity of osteochondrosis lesions in a group of warmblood foals aged 0 d to 1 y

Age range	Independent variable	Odds ratio	95% profile likelihood confidence interval
0 d up to 1 y of age (N = 29)	Age	1.023	1.005-1.049
>1 mo up to 5 mo of age (N = 7)	Age	1.203	1.014e+00-1.921
0 d up to 1 mo of age (N = 20)	Age	1.114	1.041-1.228

Abbreviation: N, amount of foals examined.

Discussion

In this case series, predilection for OC was not identified in either the predilection site of CVM in warmblood horses or within the different examined joints and the cranial cervical region. This suggests that OC may not be a major contributor to CVM. This finding is supported by previous studies in which not only OC but also synovial cysts, degenerate joint disease and osteomyelitis have been described as cause for spinal cord compression in horses with CVM.^{13, 14} with the severity of both OC lesions and non-OC lesions being greater at sites of compression than at sites without compression.¹³ Compression has also been seen at sites with no lesions of the APJs.¹³ Furthermore no difference in frequency of OC lesions has been found between horses with and without CVM.¹³ However, the significant increase of frequency and severity of lesions of the APJs at both compression and non-compression sites and the increase in severity of OC lesions in

horses with CVM compared to control horses suggests a common developmental pathogenesis of OC and CVM.^{6, 13} The more frequent progression of OC lesions in horses with CVM may be the result of secondary biomechanical influences. In pigs the progression of the severity of OC has been suggested to be a consequence of local mechanical overload due to differences in joint and leg shape.^{4, 5} Also, in humans, increased biochemical stress seems to increase the prevalence and severity of gross OC lesions.² Therefore it is likely that minimal trauma, caused by normal movements, can lead to the progression of subclinical OC to clinical OC dissecans in horses with malformations of the vertebral column while these forces would have no effect in horses without CVM.

Osteochondrosis is a dynamic condition in which the time course of lesion development varies between joints.^{1, 18} Depending on the joint, there is a time window in which OC can develop and regress again.^{1, 18} Regression is common and just a few lesions will develop into clinical OC.^{1, 18} Although no susceptible period in particular has been described for APJ OC, it has been suggested that the majority of OC lesions will develop before the age of 5 months and that regression after the age of 11 months is no longer likely.¹⁸ The vast majority of foals examined here were less than 1 month of age and this age range showed the bulk of OC lesions. Only two foals were 5 months and older. Therefore, this case series consists of predominantly early onset OC. A relatively high incidence of OC lesions in the cervical APJs of warmblood foals reported earlier was considered to be due to the fact that these foals were specifically selected for being offspring of a sire having OC, and as such genetically predisposed.¹⁸ On the other hand, the foals used in the current study were assumed to be a representative sample of the general Dutch warmblood population and especially of the Royal Dutch Sport horse population as almost all foals belonged to this breed. However we used a convenience sample and therefore bias cannot be excluded and no details about the sire or dam were available to confirm this. Of the joints examined 20.6% showed OC making APJ OC common in the general population of warmblood foals. This is in line with OC development in other joints in which the prevalence of OC in domesticated horse breeds is much higher than those of feral horses, suggesting that OC could have unintentionally been introduced by selective breeding.^{15, 19, 20}

It is also possible that had these foals lived longer, more lesions on other

facets could have developed while others could have regressed. A larger group of foals between 5 and 12 months of age needs to be studied to see whether certain joints or regions might be a predilection site for lesions in this age range.

Within the foals we examined the presence of OC manifesta increased with age, however OC dissecans was not encountered. Biomechanical stress and trauma play a role in the progression of severity of OC.²² The level of biomechanical stress most of these foals had experienced is likely to be low as many were very young and this is a possible explanation for the lack of OC dissecans in the facets studied.

The odds of having OC lesions in the cranial facets of the cervical APJs and the cervical-thoracic APJs (C7T1) and the caudal facets of the first thoracic APJs (T1T2) were higher than having OC lesions in their opposite facets in the population of foals aged 0 days up to 1 year and the subset of foals aged 0 days up to 1 month of age. This difference between the cervical facets has been described before in foals of 5 months and 11 months of age.¹⁸ Although in the subset of foals aged > 1 month up to 5 months, 15 OC positive cranial facets were present in the cervical spinal column in contrast to only 7 OC positive caudal facets position was not an effective dependable variable for the occurrence of OC in this age range. Possibly, this was due to the small amount of foals and of OC positive facets in this subset of foals with subsequent limited statistical power. Micro-trauma is thought to be the initiating event for the development of OC²² and site-specific traits as cause for micro-trauma are likely due to the focal nature of OC.²² This suggests a different biomechanical environment between these two positions and these regions. In humans, APJ orientation is correlated with the development of APJ arthrosis due to changes in biomechanical forces.⁷ This difference in biomechanics could also be an explanation for the difference of the most likely affected facets between these regions in the horse as in the horse the orientation of the cervical and cervical/thoracic APJs is different than that of the first thoracic APJ with subsequent different biomechanics.

Less than one-fifth of the affected joint pairs examined here were affected bilaterally confirming that OC of the APJs not a bilateral symmetrical process^{14, 18} in contrast to most other joints.^{18, 22}

In conclusion, early onset OC is common in the cervical and cranial thoracic vertebral column of warmblood foals, without the presence of a predilection site, suggesting that OC is not the only contributor to CVM.

References

1. Barneveld A, van Weeren PR. Conclusions regarding the influence of exercise on the development of the equine musculoskeletal system with special reference to osteochondrosis. *Equine Vet J Suppl.* 1999(31):112-119.
2. Bohndorf K. Osteochondritis (osteochondrosis) dissecans: A review and new MRI classification. *Eur Radiol.* 1998;8(1):103-112.
3. Burnham K. Model selection and multimodel inference. Springer; 2002.
4. de Koning DB, van Grevenhof EM, Laurensen BF, et al. Associations of conformation and locomotive characteristics in growing gilts with osteochondrosis at slaughter. *J Anim Sci.* 2015;93(1):93-106.
5. Grondalen T. Osteochondrosis and arthrosis in pigs. VII. Relationship to joint shape and exterior conformation. *Acta Vet Scand Suppl.* 1974;46(0):1-32.
6. Janes JG, Garrett KS, McQuerry KJ, et al. Cervical vertebral lesions in equine stenotic myelopathy. *Vet Pathol.* 2015;52(5):919-927.
7. Kalichman L, Suri P, Guerhazi A, et al. Facet orientation and tropism: associations with facet joint osteoarthritis and degenerative spondylolisthesis. *Spine.* 2009;34(16):579.
8. Levine JM, Adam E, MacKay RJ, et al. Confirmed and presumptive cervical vertebral compressive myelopathy in older horses: a retrospective study (1992-2004). *J. Vet. Intern. Med.* 2007;21(4):812-819.
9. Levine JM, Scrivani PV, Divers TJ, et al. Multicenter case-control study of signalment, diagnostic features, and outcome associated with cervical vertebral malformation-malarticulation in horses. *J Am Vet Med Assoc.* 2010;237(7):812-822.
10. Nout YS, Reed SM. Cervical vertebral stenotic myelopathy. *Equine Vet Educ.* 2003;15(4):212-223.
11. Olstad K, Ekman S, Carlson CS. An update on the pathogenesis of osteochondrosis. *Vet Pathol.* 2015;52(5):785-802.
12. Powers BE, Stashak TS, Nixon AJ, et al. Pathology of the vertebral column of horses with cervical static stenosis. *Vet Pathol.* 1986;23(4):392-399.

13. Stewart RH, Reed SM, Weisbrode SE. Frequency and severity of osteochondrosis in horses with cervical stenotic myelopathy. *Am J Vet Res.* 1991;52(6):873-879.
14. Trostle SS, Dubielzig RR, Beck KA. Examination of frozen cross sections of cervical spinal intersegments in nine horses with cervical vertebral malformation: lesions associated with spinal cord compression. *J Vet Diagn Invest.* 1993;5(3):423-431.
15. Valentino LW, Lillich JD, Gaughan EM, et al. Radiographic prevalence of osteochondrosis in yearling feral horses. *Vet Comp Orthop Traumatol.* 1999;12(3):151-155.
16. van Biervliet J. An evidence-based approach to clinical questions in the practice of equine neurology. *Vet Clin North Am Equine Pract.* 2007;23(2):317-328.
17. van Biervliet J, Mayhew J, de Lahunta A. Cervical vertebral compressive myelopathy: diagnosis. *Clin Tech Equine Pract.* 2006;5(1):54-59.
18. van Weeren PR, Barneveld A. The effect of exercise on the distribution and manifestation of osteochondrotic lesions in the warmblood foal. *Equine Vet J Suppl.* 1999(31):16-25.
19. van Weeren R. Fifty years of osteochondrosis. *Equine Vet J.* 2018;50(5):554-555.
20. van Weeren R. Osteochondritis dissecans. In: McIlwraith CW, ed. *Joint Disease in the Horse.* 2nd ed. Saunders; 2016.
21. Wormstrand B, Østevik L, Ekman S, et al. Septic arthritis/osteomyelitis may lead to osteochondrosis-like lesions in foals. *Vet Pathol.* 2018;55(5):693-702.
22. Ytrehus B, Carlson CS, Ekman S. Etiology and pathogenesis of osteochondrosis. *Vet Pathol.* 2007;44(4):429-448.

Supplementary Table S1. Overview of the breed, age, sex, cause of death, number of osteochondral lesions, site of lesions and severity of lesions in foals examined. RDSH = Royal Dutch Sport Horse Netherlands; OC = osteochondrosis; C = cervical vertebra; T = thoracic vertebra; L = left; R = right; CR = cranial; CA = caudal

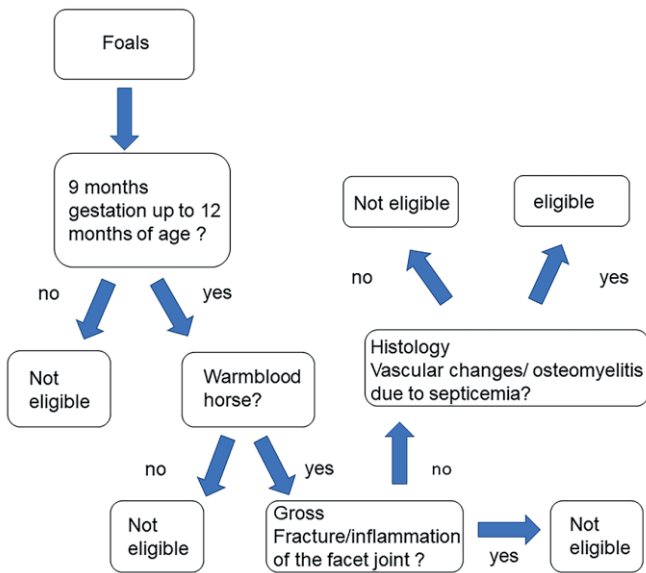
Foal	Breed	Age in days	Sex	Cause of Death	Facet surface affected	Number of OC latens	Number of OC manifesta
1	RDSH	0	Female	Intra uterine death (dam died due to typhlocolitis)	C5LCR T1RCA	1	1
2	RDSH	0	Female	Herpes viral hepatitis	C3RCR	0	1
3	RDSH	0	Male	Dystocia	C3RCR C3RCA C4LCR C6LCR C7LCR C7LCA C7RCA	2	5
4	RDSH	0	Male	Dystocia	C2RCA C4RCR C4LCA C5RCR C5LCA C6LCR C6RCR C6LCA C6RCA	7	2

5	RDSH	1	Female	Herpes viral pneumonia and hepatitis	C5LCR C6RCR C6LCR	2	1
6	RDSH	1	Female	Herpes viral pneumonia	C2LCA C3RCR C4RCA C6LCR C6RCR C7RCR C7LCA	5	2
7	RDSH	1	Female	Actinobacillus equuli sepsis	-	-	-
8	RDSH	1	Male	Perforative gastritis; bronchopneumonia	C6RCR C7LCA	1	1
10	Westphalian horse	1	Male	Neonatal asphyxia syndrome; sepsis	-	-	-
11	RDSH	2	Male	Euthanized due to malformation front legs	C6LCR	1	0
12	RDSH	3	Male	Bronchointerstitial pneumonia	C3LCA C4RCR C5LCR C6RCA T1LCR T1LCA T2LCR	6	1

13	RDSH	3	Female	White muscle disease; enteritis	C3RCR C3LCR C5LCR C5RCR C7RCR C7LCR T1LCR T1RCR T1RCA T1LCA	3	7
14	RDSH	4	Male	Interstitial pneumonia	C3RCR C5LCR C7LCA T2LCR	3	1
15	RDSH	5	Male	Enteritis	C3LCR C5RCR C6RCR C6LCR C7RCR T1LCR	5	1
16	RDSH	6	Female	Interstitial pneumonia	C2RCA C3LCR C3RCR T1RCA	1	3
17	RDSH	7	Female	Enteritis	C3RCA C3LCR C5RCR C6RCA T1RCR T1LCR T1LCA	4	3
18	RDSH	8	Male	Herpes viral pneumonia	C3LCR	1	0
19	RDSH	13	Male	Herpes viral pneumonia	C3RCR C3LCR C7RCR T1RCR	1	3

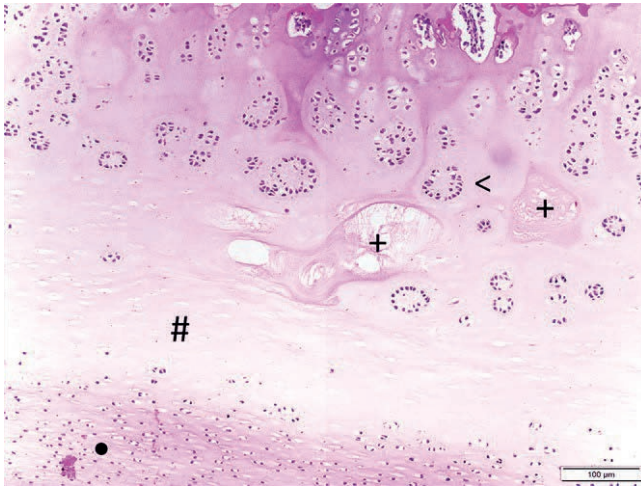
20	RDSH	18	Female	Euthanized due to malformation front legs	C6LCR C7RCA T1LCR T1LCA T2LCR	1	4
21	RDSH	18	Female	Bladder rupture	C3RCR C6RCR C6LCR T1RCR	1	3
22	RDSH	28	Male	Omphalitis	C3RCR C3LCR C5RCR C5LCA C6LCR C7LCA	0	6
23	Zangersheide Horse	47	Male	Hydrocephalus	C3RCR C5RCR C5LCR C7RCR C7LCR T1RCA T1LCA	3	4
24	RDSH	48	Male	Interstitial pneumonia	C2RCA C3RCR C6LCA C7RCR C7LCA C7RCA	5	1

25	RDSH	53	Male	Myocarditis	C3LCA C4LCR C4RCR C6LCA T1RCR	1	4
26	RDSH	54	Male	Rhodococcal pneumonia	C3LCR C6RCR	1	1
27	RDSH	83	Male	Typhlocolitis	C7RCR	0	1
28	RDSH	134	Male	Bladder rupture	C5LCA C5RCA C6LCR C7LCR	0	4
29	RDSH	149	Female	Euthanized due to a club foot	None	0	0
30	RDSH	157	Male	Stomach rupture	C3LCA C5LCA C6RCR C7LCR T1RCR	0	5
31	RDSH	365	Male	Trauma	T1RCR	0	1

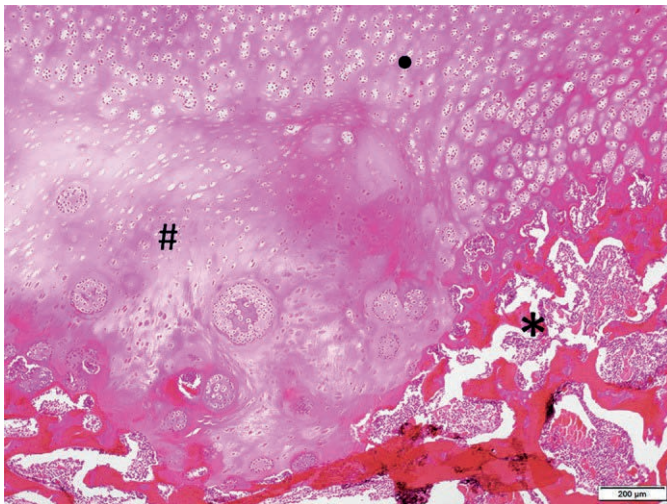


Supplementary Flowchart S1

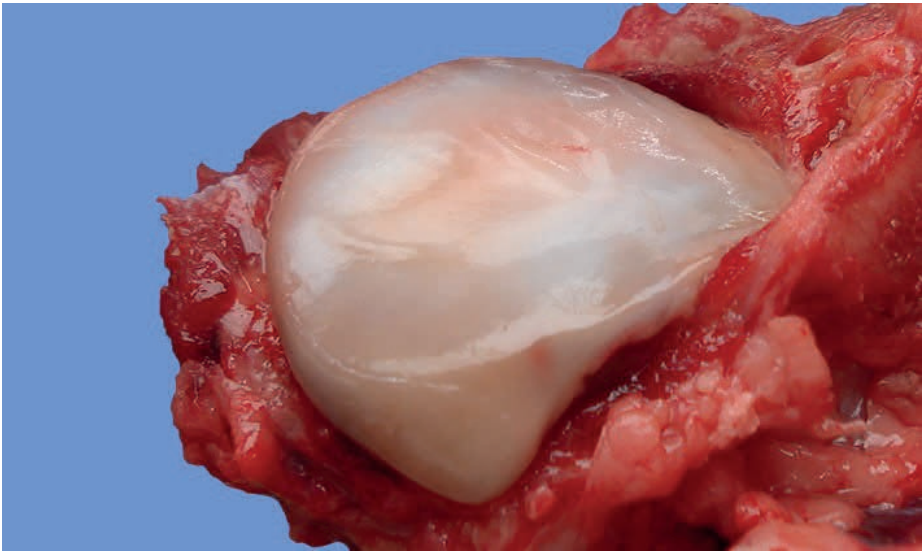
Flowchart for the eligibility of available foals for this research.



Supplementary Figure S2. Histological picture of osteochondrosis latens of Royal Dutch Sport Horse Netherlands foal 1 of 0 days; 100x magnification. Focally extensive necrosis (#) of the epiphyseal cartilage (.). Within the necrotic cartilage 2 necrotic blood vessels (+) are visible. Surrounding the necrotic cartilage chondrons (<) are present. Haematoxylin Eosin staining.



Supplementary Figure S3. Histological picture osteochondrosis manifesta of Royal Dutch Sport Horse Netherlands foal 26 of 54 days; 40x magnification. Focally extensive necrosis (#) of cartilage (.) which extends into the subchondral trabecular bone (*). Haematoxylin Eosin staining



Shapes of cervical
articular process joints
and association with
histological evidence of
osteocondrosis in
warmblood foals: a post-
mortem study

3

Accepted in Equine Veterinary Journal.

W. Bergmann
J.C.M. Vernooij
G.C.M. Grinwis
A. Gröne

Abstract

Background: Osteochondrosis dissecans (OCD) of articular process joints (APJs) is involved in cervical vertebral compressive myelopathy (CVM). Biomechanical forces, important in development of OCD, depend on joint conformation. Oval and flat APJ surfaces are considered normal.

Objectives: Identify and grade gross shape variation of cervical and cranial thoracic APJ surfaces and determine association with histological evidence of osteochondrosis.

Study design: Case series

Methods: 804 cervical and cranial thoracic APJ surfaces of 30 foals were evaluated for shape(s) and grades, and were correlated with osteochondrosis.

Result: Three top view shapes (oval, pointed, elongated) and 7 lateral view shapes (flat, convex, concave, stepped, bevelled, folded edge, raised edge) were regularly encountered. The oval top view shape was most common. Flat and bevelled were the most common lateral view shapes. General shape grade of caudal articular surfaces was significantly higher than of cranial surfaces.

Combination of an oval top view shape and the lateral view shapes folded edge, concave, or flat with additional raised edge and/or folded edge (flat +), were more likely to have OC than oval with convex, bevelled or flat lateral view shapes (normal versus oval and folded, odds Ratio (OR) 2.49 (95% confidence intervals (95%CI) 1.13-5.67); normal versus oval and flat +, OR 2.77 (95%CI 1.15-6.85); oval and convex versus oval and folded, OR 3.20 (95%CI 1.35-8.20); oval and convex versus oval and flat +, OR 3.56 (95%CI 1.43-9.54); oval and bevelled versus oval and concave, OR 2.02 (95%CI 1.14-3.60); oval and bevelled versus oval and folded, OR 3.50 (95%CI 1.91-6.60); oval and bevelled versus oval and flat +, OR 3.90 (95%CI 2.00-7.70)).

Main limitations: Most foals (21/30) were less than 1 month old. Lack of observer reliability scores for shape and shape grade.

Conclusion: APJs shape might contribute to CVM by increased likelihood to have OC.

Introduction

Cervical vertebral myelopathy (CVM) is the most common non-infectious, non-macro traumatic cause for neurological signs in horses. In this syndrome, neurological signs result from compression of the spinal cord and/or spinal nerves.^{15, 16, 20, 23, 24, 25}

Static compression occurs mostly in the caudal part of the neck (fifth cervical up to the first thoracic vertebra (C2-T1)) and often results from osteoarthritis/degenerative joint disease of the articular process joints (APJs) in older warmblood horses.^{15, 17, 20, 23, 24, 25}

Dynamic compression most commonly occurs in the cranial part of the neck (C2-C5).¹⁵ The cause of CVM is multifactorial and osteochondrosis dissecans (OCD), developmental malformation, repeated micro-trauma, sex and breed are factors thought to play a role in its development.^{15, 14, 16, 20, 22, 23}

Osteochondrosis tends to be more severe in CVM affected horses than in horses without CVM.²² OCD of the APJs can cause compression of the spinal cord and nerves due to joint capsule hypertrophy²³ and instability and malalignment of adjacent vertebrae.¹⁷ OCD can also lead to secondary osteoarthritis with resultant compression.^{17, 25} OC is common in several domestic species.^{18, 32} The development of subclinical OC latens results from vascular failure leading to ischemic chondronecrosis of the epiphyseal growth cartilage.^{18, 32} The cause of vascular failure is at this moment unknown. Although it is well known that there are predilection sites for OC, the previously suggested anatomy related microtrauma as cause for vascular failure could not be confirmed and therefore does not explain the occurrence of these predilection sites.^{19, 32} Currently, anatomical differences in the amount of blood vessels and cartilage thickness are thought to explain the presence of these predilection sites.¹¹ Progression into clinically relevant, grossly and radiographically detectable OCD is thought to result from biomechanical overload.^{18, 29, 32} Overload can result from external factors such as housing conditions,^{26, 29} but also from internal factors. For example, in pigs, certain joint - and leg shapes are thought to cause biomechanical overload,^{6, 9} and selective breeding against these shapes has decreased the prevalence of OCD.⁸ Also in equines, an association between conformation and the amount of biomechanical forces has been described,^{1, 30} although the effect of joint shapes on the occurrence of OC(D) has not been investigated in more detail.

Because the pathogenesis of OC in horses is similar to that in pigs, ⁴ it is likely that also in horses different joint shapes have different effects on progression of subclinical OC to clinically relevant OCD and possibly also on the initiation of subclinical OC.

This study had three aims. First, to determine by gross evaluation if there is variation in shape of cervical and cranial thoracic APJ surfaces in foals, and if so, to categorize and to grade these shapes. For this, foals were used instead of adult horses to establish a base of shape variations within a population that is most likely not affected by secondary shape changes due to degenerative processes such as osteoarthritis. ^{15, 20, 25} Second, to determine if there is a relationship between shape and shape grade and factors that are indicated as important in the development of CVM (e.g. location within the vertebral column and sex). Third, to investigate if there is an association between the shape of the articular surface and the histological evidence of OC in this articular surface or the opposite articular surface within the same APJ. It is hypothesised that there is variation in shape of the articular process joints, that certain shapes have a higher likelihood to develop OC and that these shapes are more common in the caudal part of the cervical vertebral column.

Materials and methods

Horses

The APJs of 30 warmblood foals were grossly examined. These foals were previously used to analyse the correlation of histological evidence of OC of the articular surface of APJ with age, sex and distribution along the cervical and cranial thoracic spine. ² The foals were privately owned by 24 different owners and either died spontaneously or were humanely euthanized for reasons unrelated to this study (supplemental Table S1). None of the foals were diagnosed with OC antemortem. 29 foals did not show neurological signs. One foal did show neurological signs caused by a hydrocephalus. Foals were submitted for post-mortem examination to the Division of Pathology of the Faculty of Veterinary Medicine of Utrecht University between July 2012 and July 2018 to investigate the cause of death or for explanation of clinical signs. The foals were of various breeds (28 Royal Dutch Sports Horses, one Zangersheide horse, one Westfalian horse), sex (19 males, 11 females) and age (from 9 months gestation up to 365 days).

Necropsy for this study was performed with the owner's informed consent for usage of tissue for general research. In two of the foals a bacterial sepsis with vasculitis respectively an osteomyelitis were seen in the APJs. Therefore these foals were used for evaluation of the APJ shapes but were excluded from evaluation of OC as these changes can lead to osteochondrosis-like lesions (supplemental Table S1 and supplemental Figure S1).^{12,31}

Data collection

The APJs were detached from the vertebrae by sawing through the pedicles and opened. To identify possible differences within the regions implicated in CVM, the vertebral column was divided in 3 subregions: cranial cervical (articular surface of the caudal APJs of the second cervical vertebra up to the articular surface of the cranial APJs of the fifth cervical vertebra (C2caudal -C5cranial)), caudal cervical (C5caudal -T1cranial) and the first thoracic APJ (T1caudal-T2cranial). Of 18 foals, the shape of the articular surface of the APJs C3 -T2cranial (26 articular surfaces each) and of 12 foals the articular surface of the APJs of C2caudal-T2cranial (28 articular surfaces each) were assessed macroscopically, making a total of 804 articular surfaces. Assessment was done by one board certified veterinary pathologist (WB). The articular surfaces of the APJs were analysed for the shape of the top view (visual perspective from directly above the articular surface) and of the lateral view (visual perspective from the side of the articular surface) resulting in a minimum of 2 shapes for each articular surface (Figure 1).

Unfortunately, no literature was found stating the normal shape of the articular surface of the APJ of foals. However, according to the literature, the normal APJ surface of horses of one year and older is oval in top view, and flat in lateral view, with thin, linear, smooth joint margins, irrespective of the localisation of the joint within the cervical vertebral column.^{5 10} Thus, the combination of an oval top view shape with a flat lateral view shape was assumed normal.

Lateral view shapes deviating from the normal flat shape were categorized. The degree of deviation from the normal shape (shape grade) was also recorded (minimal, mild, moderate, severe). Because grading was performed during necropsy and could therefore not be repeated, an intra-observer reliability score could not be determined. To optimize

reliable grading it was decided to make a 2-tier grading by combining minimal and mild grades, and moderate and severe grades. A minimal to mild grade has a slope of less than 30 degrees and/or could cover up to 1/3 of the articular surface, while a moderate to severe grade has a slope of 30 degrees or more and/or could take up more than 1/3 of the articular surface.

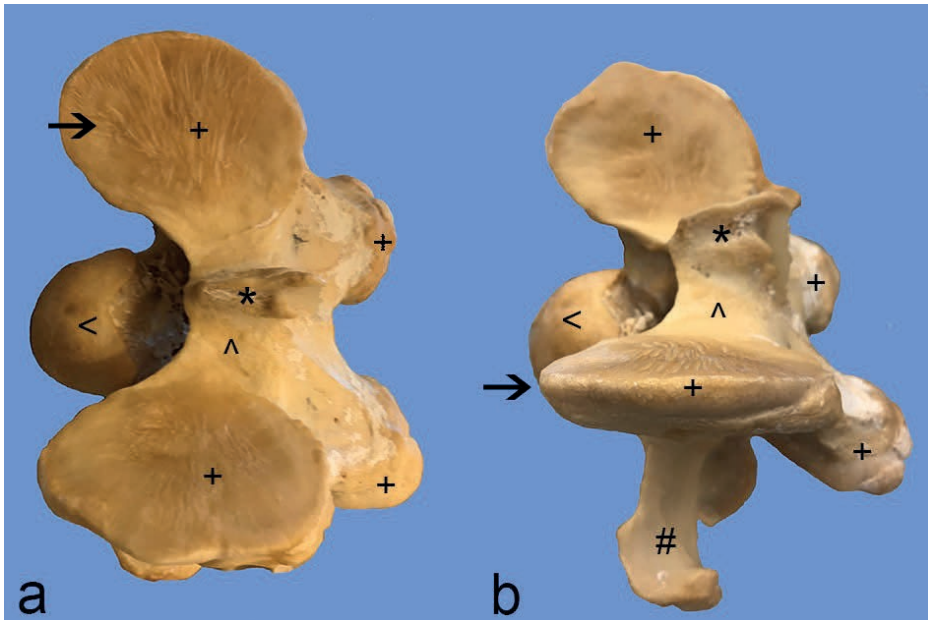


Figure 1. Macerated sixth cervical vertebra of a horse. A. Top view (view perpendicular to the plane of the articular surface of the APJ). B. Lateral view (view in the plane of the articular surface). + surface of the articular process, * spinous process, # transverse process, ^ dorsal lamina, < cranial extremity of the vertebral body.

Of 28 foals, histological data on the presence of osteochondrosis, as published previously,² were used to analyse the correlation of the combination of the top and lateral view shapes with OC. Histological samples were taken from areas with gross morphology that could be compatible with OC, which in these foals were (multi)focal round to longitudinal indentations of the cartilage.² When gross changes

suggestive of osteochondrosis were not present, a histological sample was taken from the centre of the articular surface. Histologically, osteochondrosis was characterized by necrotic epiphyseal cartilage (osteochondrosis latens) often associated with delayed ossification (osteochondrosis manifesta). Cartilage canal blood vessels in affected areas had lost their endothelium with occasionally presence of swollen endothelial cells or cells with pyknotic nuclei. This is consistent with osteochondrosis as described in literature.^{18, 32} Osteochondrosis dissecans was not seen. Foals were excluded from evaluation of OC if septic osteomyelitis or arthritis were present as this can mimic osteochondrosis.^{12, 31} Of the 28 foals previously evaluated², 27 foals had OC lesions in one up to 24 of the articular surfaces. Of the 678 articular surfaces evaluated 143 had OC (21.1%; 95% confidence interval (95%CI) 18.19-24.32%).

Data analyses

The distribution of the different shapes was first investigated by use of a binominal logistic regression model. In this model the distribution of normal (oval and flat) versus abnormal shaped articular surfaces was analysed with foal as random effect and sex, region within the vertebral column, and position (cranial or caudal) and side (left or right) of the articular surface as fixed effects. Model selection was done by stepwise backward elimination by use of the Akaike information criterion (AIC). The odds ratio with 95% log profile likelihood confidence intervals (95% CI) were used as effect size estimates.

Next, the distribution of the different shapes between sex, age, regions, side (left-right) and position (cranial -caudal) of the articular surface was investigated in more detail by the use of a multinominal model. In this model, normal shaped articular surfaces and articular surfaces with an oval top view shape and the 5 most frequently encountered lateral view shapes (convex, concave, bevelled, folded edge and raised edge) were included. Shapes with the lowest prevalence (pointed and elongated top view shapes and the stepped lateral view shape; N= 78) were excluded from calculations. Calculation was done with a multinomial Bayesian Multilevel Model using Stan (BMRS) with logit link and with foal as random effect and age (0-24 days or 25 -365 days), sex, region, side and position of the articular surface as independent variables. As reference, the normal shape combination (an oval top view shape and a flat lateral shape view) was

used. The correctness of the model was investigated by an intercept-only model and visualization of the chains and posterior distribution by use of trace plots, Z-base plots and density overlay plots. The best model was selected by Pareto smoothed importance sampling. Results were presented as odds ratio and significance was determined by use of the 95% credibility interval (95%CrI).

The shape grade was analysed with a binominal (minimal and mild versus moderate and severe) logistic regression model with foal as random effect and age (as a continuous variable), sex, region, and side and position of the articular surface as fixed effects. Model selection was done by stepwise backward elimination by use of the Akaike information criterion (AIC).

The association of OC incidence was analysed with a binomial logistic regression model. Two models were run: the first model with outcome OC in the observed articular surface and a second model with OC of the opposite articular surface within the same joint as outcome. Both models had foal as random effect and lateral view shape, grade, number of abnormal shapes (0,1, ≥ 2) and normal against abnormal shape combination as fixed effects. The first model with OC of the observed articular surface as outcome had additionally these variables of the opposite articular surface as fixed effects. Due to low incidence of OC, the shapes with the lowest prevalence (pointed and elongated top view shapes and stepped and raised edge lateral view shapes; N=121) were excluded from calculations. Also, because of the low prevalence of 3 abnormal shapes per articular surface, 2 and 3 abnormal shapes per articular surface were combined into 2 or more abnormal shapes. Model selection was done by stepwise backward elimination by use of the Akaike information criterion (AIC). To determine the different odds ratios between the different shapes (multinomial), the model was re-run using each shape once as reference shape.

All calculations were performed with R (The R Foundation for Statistical Computing Platform) version 3.6.1 and analysed using R studio version 1.2.1335 (RStudio: Integrated Development for R. RStudio, Inc., <http://www.rstudio.com/>). For BMRS analysis the bmrs package and for logistic regression the lme4 package were used.^{3, 7}

Results

Top and lateral view shapes

Ten different shapes were regularly encountered in 756 articular surfaces (Table 1; Figures 2,3 and 4). 48 articular surfaces had a more unique shape, and those shapes were not further examined. Of the 10 common shapes, 3 were different top view (view perpendicular to the plane of the articular surface) shapes (oval, pointed and elongated; Figure 2) and 7 were different lateral view (in the plane of the articular surface) shapes (flat, convex, concave, stepped, bevelled, folded and raised edge; Figures 3 and 4).

An oval top view shape (Figures 2a and b) has an egg-shaped circumference (ratio short to long axis approximately 1:2). In the pointed top view shape (Figures 2 c and d), the two opposite poles have a different width, resulting in a triangular shape. In the elongated top view shape (Figures 2e and f), the articular surface resembles a stretched oval (ratio short to long axis 1: > 2). The convex lateral view shape has a domed instead of a flat surface, while the concave lateral view shape has a depressed surface (Figures 3a, b, c and d). A stepped articular surface has a cartilage-covered surface with 2 or more regions with a different height resembling stairs (Figures 3e and f). The bevelled lateral view shape has a cartilage-covered, oblique-sloped edge (Figures 4 a and b). The folded and the raised edge lateral view shapes have focal cartilage-covered bony projections perpendicular to the joint surface, originating from the margins and pointing downwards to the bony part of the articular surface or upwards towards the corresponding articular surface of the APJ respectively (Figures 4c,d,e and f).

Distribution of top view shapes

The most common top view shape was oval (86 (95%CI 82.3-89.5%; N=343) -98% (95%CI 95.6-98.7%; N=413), irrespective of the region, side, position, and sex (Table 1).

Table 1 Distribution of absolute numbers and percentages of shapes of the Articular surface of cervical and cranial thoracic articular process joint of a group of warmblood foals (N=30) aged 0 days to 1 year †

	<i>Entire examined vertebral column</i>	<i>Cranial cervical</i>	<i>Caudal cervical</i>	<i>Cranial thoracic</i>	<i>Male</i>	<i>Female</i>	<i>Left</i>	<i>Right</i>	<i>Cranial</i>	<i>Caudal</i>
	N (%)	N (%)	N (%)	N (%)	N (%)	N (%)	N (%)	N (%)	N (%)	N (%)
Top view shape										
<i>oval</i>	699 (93)	290 (95)	319 (92)	90 (88)	447 (94)	252 (90)	346 (92)	353 (93)	403 (98)	296 (86)
<i>pointed</i>	24 (3)	7 (2)	9 (2)	8 (8)	12 (3)	12 (4)	14 (4)	10 (3)	8 (2)	16 (5)
<i>elongated</i>	33 (4)	10 (3)	19 (6)	4 (4)	16 (3)	17 (6)	18 (4)	15 (4)	2 (< 1)	31 (9)
Side view shape										
<i>flat</i>	269 (26)	90 (21)	127 (26)	52 (37)	186 (28)	83 (22)	136 (26)	133 (26)	133 (21)	136 (32)
<i>convex</i>	64 (6)	38 (9)	21 (4)	5 (3)	50 (8)	14 (4)	35 (7)	29 (5)	15 (2)	49 (10)
<i>concave</i>	186 (18)	90 (21)	64 (13)	32 (23)	107 (16)	79 (20)	96 (18)	90 (17)	179 (29)	7 (2)
<i>beveled edge</i>	283 (27)	116 (27)	149 (31)	18 (13)	144 (22)	139 (36)	136 (26)	147 (28)	135 (22)	148 (35)
<i>stepped</i>	15 (1)	6 (1)	9 (2)	0 (0)	15 (2)	0 (0)	7 (1) (2)	8 (2)	0 (0)	15 (4)
<i>folded edge</i>	191 (18)	62 (15)	97 (20)	32 (23)	140 (21)	51 (13)	97 (18)	94 (18)	124 (20)	67 (16)
<i>raised edge</i>	43 (4)	23 (6)	17 (4)	3 (1)	22 (3)	21 (5)	23 (4)	20 (4)	38 (6)	5 (1)
<i>other ‡</i>	48	14	16	18	35	13	24	24	19	29

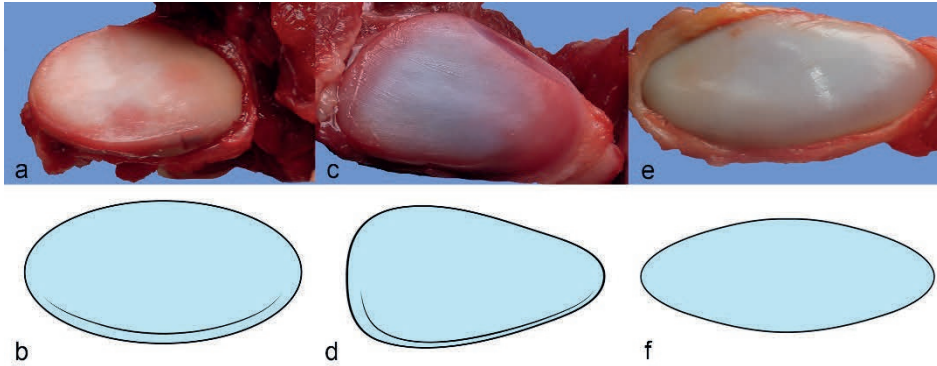


Figure 2. Different top view shapes found in the examined group of warmblood foals. Both representative photos and schematic drawings for clarification are shown.

(a) (photo) and (b) (drawing). oval top view shape. The circumference of the articular surface of the APJ is egg-shaped (ratio of the short axis to the long axis is 1:2).

(c) (photo) and (d) (drawing). pointed top view shape. The width of the circumference varies at the two opposite poles, giving the articular surface a triangular shape.

(e) (photo) and (f) (drawing). elongated top view shape. The circumference of the articular surface resembles a stretched oval with narrow opposite poles; the ratio of the short axis to the long axis is 1:>2.

Distribution of lateral view shapes

Bevelled (22 (95%CI 18.6-25.0%; N= 624) -36% (95%CI 30.3-39.8%; N=387)) and flat (21 (95%CI 17.6-25.3%; N= 425) -32% (95%CI 27.6-36.4%; N=427)) were the two most common lateral view shapes in the entire examined part of the vertebral column, the cranial and caudal neck but not the cranial thoracic region, both sexes, left, right and caudal articular surfaces but not the cranial articular surfaces. In the cranial thoracic region the most common lateral view shapes were flat (37% (95%CI 29.2-44.8%; N=142), concave and folded (both 23% (95%CI 16.4-30.1%, N= 142). Cranial articular surfaces were mostly concave (29% (95%CI 25.3-32.4%; N=624)) and bevelled (22% (95%CI 18.6-25.0%, N=624)) (Table 1).

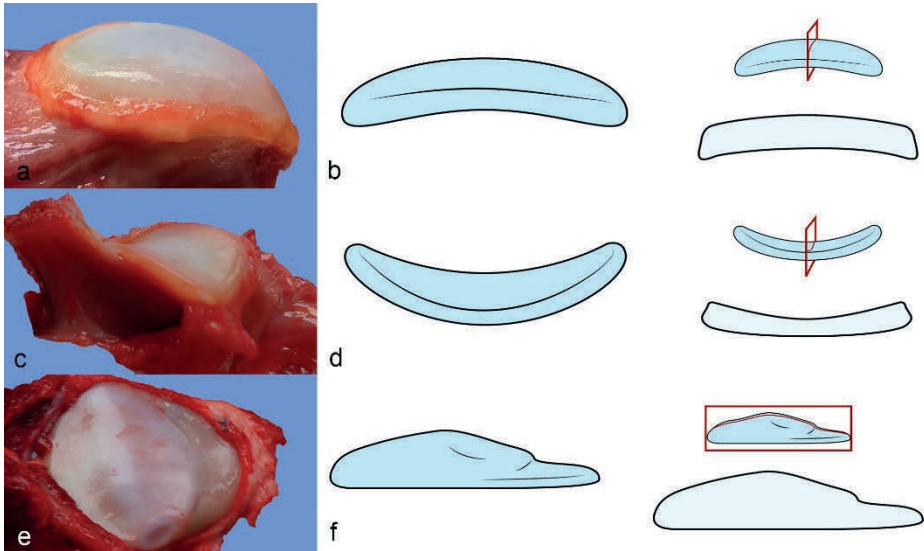


Figure 3. Different lateral view shapes found in the examined group of warmblood foals. Both representative photos and schematic drawings for clarification are shown. The drawings show the lateral view shape and the shape view on cut surface (red rectangle).

(a) (photos) and (b) (drawing). Convex lateral view shape. The convex shape has a domed instead of a flat surface.

(c) (photo) and (d) (drawing). Concave lateral view shape. The concave shape has a depressed surface instead of a flat surface.

(e) (photo) and (f) (drawing). Stepped lateral view shape. The articular surface of the APJ has cartilage covered differences in height, resembling a stair. At circa 5 O'clock a cut artefact is visible in the photo.

Distribution of top and lateral view shape combinations

A normal shape (oval and flat) was observed in 14.2% (95%CI 11.9-16.8%; N=756) of the articular surfaces. 60.6% (95%CI 57.1-64.0%; N=756) of the articular surfaces had one shape different from normal, 24.7% (95%CI 21.8-27.9%; N=756) 2 shapes (for example the left C7caudal articular surface of a female foal of 149 days had an oval top view shape and a flat lateral view shape with both a raised edge and a folded edge at lateral view) and 0.5 % (95%CI 0.2-1.4%; N=756) of

articular surfaces had 3 shapes (for example the left T1caudal articular surface of a female foal of 18 days had and elongated top view shape and both a bevelled and folded lateral view shape) different from normal.

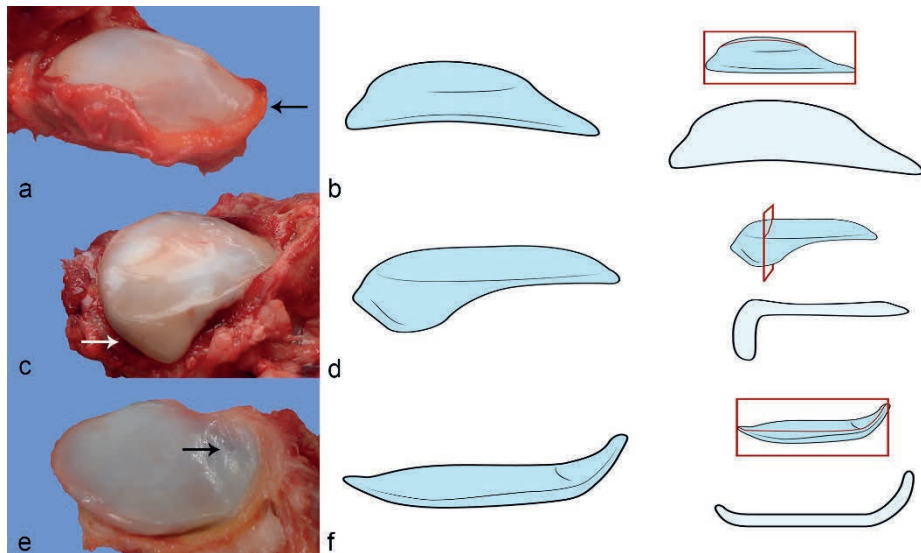


Figure 4. Different lateral view shapes found in the examined group of warmblood foals. Both representative photos and schematic drawings for clarification are shown. The drawings show the lateral view shape and the shape view on cut surface (red rectangle).

(a) (photo) and (b) (drawing). Bevelled lateral view shape. The edge of the articular surface is sloped and cartilage covered (arrow).

(c) (photo) and (d) (drawing). Folded edge lateral view shape. The articular surface of the APJ has a cartilage covered bony projection pointing downward (arrow).

(e) (photo) and (f) (drawing). Raised edge lateral view shape. The articular surface of the APJ has a cartilage covered bony projection pointing upwards (arrow).

The normal shape combination versus an abnormal shape combination (binomial) was not associated with sex, region, side or position of the articular surface.

Within the entire examined part of the vertebral column, but also within the two separate cervical regions, and the left, right and caudal articular surfaces, the two most common shape combinations were oval and flat (flat as singular shape or flat combined with a raised and/or a folded edge lateral view shape (flat +) (20 (95%CI 16.7-23.3%, N=425) -27% (95%CI 22.9-31.3%, N=427)) and oval and bevelled (23 (95%CI 20.1-27.1%; N=531) -30% (95%CI 25.4-34.0%; N=427)). The most common shape combinations in the cranial thoracic region were oval and flat (singular or flat + (33%, (95%CI 25.9-41.2%; N=142)) and oval and concave or folded (both 22% (95%CI 15.8-29.3%; N=142)). The most common shape combinations of cranial articular surfaces were oval with a concave lateral view shape (29% (95%CI 25.1-32.2%, N=624)) and oval with a flat (singular or flat +) or a bevelled edge lateral view shape (both 21% (95%CI 17.8-24.2%; N=624)) (Supplemental Table S2).

The significant odds ratios and 95%CRIs of the multinomial comparison for distribution can be found in Table 2. The total random effect (i.e. animal level + measurement level) due to animal level (i.e. the effect of the individual foal on the results) of this multinomial BMRS model used for assessment of the distribution of shapes was 18%. Significant odds ratios were only found with the variables age, position on the vertebra (cranial/caudal) and region. Only two abnormal shape combinations were associated with age: oval and concave and oval and bevelled. The likeliness for the presence of both these shape combinations, compared to normal shaped articular surfaces, was tenfold lower in foals of 25- 365 days compared to 0-24 days of age. The distribution of the different abnormal shaped articular surfaces between the cranial versus caudal position on the vertebrae and the regions within the vertebral column is very variable (Table 2). However, the likelihood of an abnormal shape combination (oval and concave, folded or raised edge) is higher in articular surfaces cranially positioned on the vertebrae compared to caudally positioned articular surfaces, and in cervical articular surfaces compared to articular surfaces in the thoracic region (oval and convex, bevelled, or raised edge). For example an articular surface with an oval top view and a raised edge side view is approximately a third less likely to be present caudally than cranially on the vertebrae and tenfold less likely to be present in the cranial thoracic region than the cranial cervical region compared to normal shaped articular surfaces.

Table 2. Significant odds ratio and 95% credibility interval of the shape combination distribution in a group of warmblood foals (N=30) age 0 day to 1 year with the assumed normal shape combination (oval top view and flat lateral view) as reference shape combination

Variable	Odds ratio	95% Credibility interval
Age (0-24 days versus 25-365 days)		
Normal versus oval and concave	0.1	0.1-0.3
Normal versus oval and bevelled	0.1	0.0-0.4
Cranial versus caudal position		
normal versus oval and convex	4.3	2.2-8.7
normal versus oval and concave	0.0	0.0-0.1
normal versus oval and bevelled	1.6	1.1-2.5
normal versus oval and folded edge	0.5	0.3-0.8
normal versus oval and raised edge	0.1	0.0-0.4
Region		
<i>cranial cervical versus caudal cervical</i>		
normal versus oval and convex	0.3	0.2-0.7
<i>cranial cervical versus cranial thoracic</i>		
normal versus oval and convex	0.1	0.0-0.4
normal versus oval and bevelled	0.2	0.1-0.4
normal versus oval and raised edge	0.3	0.1-0.9
<i>caudal cervical versus cranial thoracic</i>		
normal versus oval and concave	2.2	1.1-4.1
normal versus oval and bevelled	0.2	0.1-0.3

The most common combinations of lateral view shapes of opposing articular surfaces within the same joint were bevelled with bevelled (12.9 % (95%CI 10.42-15.75 %; N=607)), bevelled with a concave

articular surface (8.0% (95%CI 6.16-10.51%; N=607)) and a folded edge with folded edge (7.3 % (95%CI 5.44-9.59 %;N= 607) . 4.3 % (95%CI 2.94-6.20 %; N=607) of joints had two, assumed, normal shaped articular surfaces (Supplemental Table S3).

Shape grade

Of the abnormal lateral view shapes, 75% (95% CI 72.5-78.7 %, N=732) had a minimal to mild and 25% (95%CI 21.4-27.6%, N=732) a moderate to severe grade.

The convex, concave and raised edge lateral view shapes had mostly a minimal to mild grade (37 (95%CI 24.4-52.1%; N=43) -58% (95%CI 43.3-71.6%; N=43)). Bevelled and folded shapes had generally a minimal, mild and moderate grade (23 (95%CI 18.4-28.3%; N=274) -39% (95%CI 32.3-46.2%; N=187). (Supplemental Table S4).

The total random effect (i.e. animal level + measurement level) due to animal level of the binominal logistic regression model used for examination of the distribution of shape grade was 11%.

Caudal articular surfaces had significantly higher grades than cranial articular surfaces in all 3 regions combined (Figure 5, Supplemental Table S5) and within the separate cervical regions (Supplemental Table S5).

Incidence of OC

The total random effect (i.e. animal level + measurement level) due to animal level of the binominal logistic regression model used for examination of the correlation between shape and OC was 33%. Articular surfaces with an oval top view shape and a flat +, concave or folded lateral view shape were significantly more likely to have OC latens or manifesta than oval articular surfaces with a flat only (normal), convex or bevelled lateral view (Table 3, Figure 6).

The grade, number of abnormal shapes per articular surface, and normal compared to an abnormal shape combination were not associated with a significant likelihood to have OC. None of the variables was associated with significant likelihood to have OC in the opposite articular surface within the same joint.

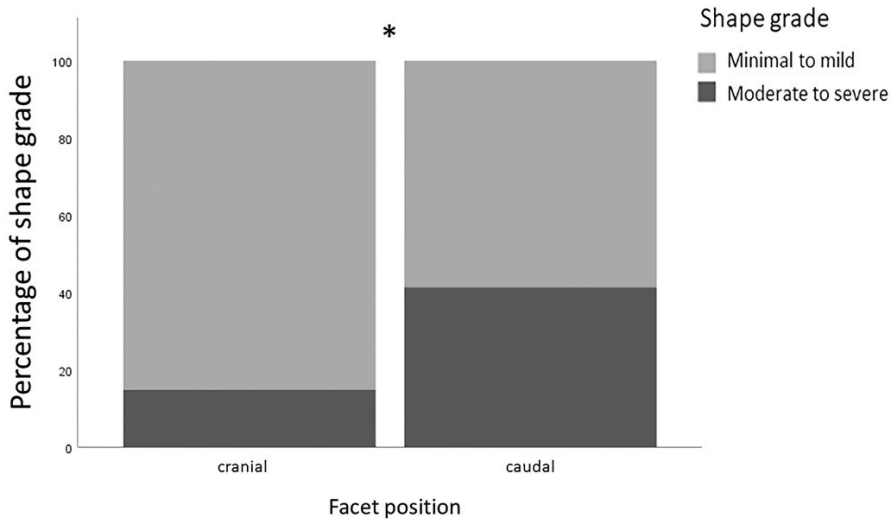


Figure 5. Distribution of general shape grade between cranial and caudal articular surfaces of the APJs. Distribution of general shape grade between cranial and caudal articular surfaces on the vertebrae of the entire examined part of the vertebral column. Caudal articular surfaces are significantly more likely to have moderate to severe shape grades than minimal to mild shape grades compared to cranial articular surfaces of the APJs. Minimal to mild shape grades are represented by the light grey colour. The dark grey colour represents the moderate to severe shape grades.

Discussion

The shape combination which in the literature is suggested to be normal (i.e. oval and flat), ^{5, 10} is expected to be most commonly encountered. However, this was not the case in the warmblood foals examined. There was substantial variation in shape and there was not one combination more dominantly present, suggesting that variation in APJ morphology is normal for warmblood foals. Yet, in the examined part of the vertebral column the oval and bevelled combination (24%) and the suggested normal shape combination (23%) were most prevalent and therefore both combinations should maybe be considered normal in warmblood foals, especially as the assumed normal shape of the articular surface of APJs has only been described

Table 3. Significant odds ratios and 95% confidence intervals of osteochondrosis of articular surfaces of the APJs in a group of warmblood foals (N=28) age 0 day to 1 year of the final model[†]

Shape combination (absolute number)	Odds ratio	95% profile likelihood confidence interval
normal (oval and flat) (107)	reference	
oval and folded edge (186)	2.5	1.13-5.67
normal (oval and flat) (107)	reference	
oval and flat with additional lateral view shape (138)	2.8	1.15-6.85
oval and convex (60)	reference	
oval and folded edge (186)	3.2	1.35-8.20
oval and convex (60)	reference	
oval and flat with additional lateral view shape (138)	3.6	1.43-9.54
oval and bevelled (256)	reference	
oval and concave (184)	2.0	1.14-3.60
oval and bevelled (256)	reference	
oval and folded edge (186)	3.5	1.91-6.60
oval and bevelled (256)	reference	
oval and flat with additional lateral view shape (138)	3.9	2.00-7.70

[†] The first initial model for osteochondrosis (with binary outcome variables osteochondrosis/no osteochondrosis) of the observed articular surface, included explanatory variables osteochondrosis of the opposite articular surface, (opposite) shape combination, (opposite) shape grade, (opposite) number of abnormal shapes and (opposite) normal against abnormal shape combination. The second initial model for osteochondrosis of the opposite articular surface in the same joint, included the explanatory variables shape combination, shape grade, number of abnormal shapes and normal against abnormal shape combination. The final model included only the shape combination of the observed articular surface.

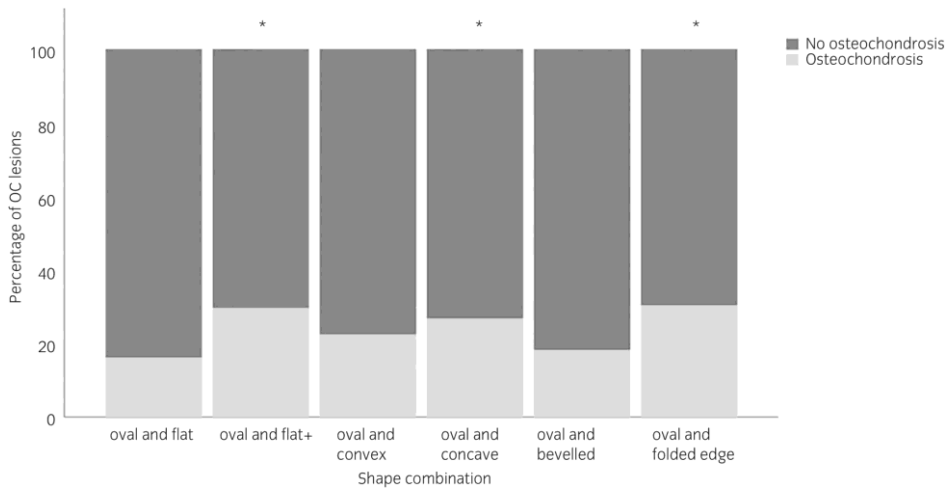


Figure 6. Percentage of osteochondrosis in the articular surface of APJs with different shape combinations. Articular surfaces with an oval top view shape and a flat lateral view shape with an additional raised edge and/ or a folded edge combined (flat +), a concave or a folded edge lateral view shape are significantly more likely to have osteochondrosis than an oval top view shape with solely a flat lateral view shape, a convex or a bevelled lateral view shape. The percentage of articular surfaces not affected by osteochondrosis are depicted with the dark grey colour. The percentage of articular surfaces that do have osteochondrosis are depicted with the light grey colour.

in horses of 1 year and older.¹⁰ This suggestion is further supported by the fact that oval and bevelled and oval and concave shape combinations are more commonly found in younger than in older foals compared to the normal articular surface shape. Further research concerning the evolution of the shape of the articular surface of the APJ, by use of repetitive computer tomography and MRI, starting already with fetuses, would be highly informative. The assumed normal shape was taken as reference for statistic calculations, because of the slight difference in prevalence of these two most commonly encountered combinations within the entire examined vertebral column. However, sampling bias cannot be completely excluded as the foals in our study were a convenience sample. Interestingly, previous studies describing the normal shape of APJs, in which 1870 respectively 22 articular surfaces were examined, shape details were

not specified for each breed.^{5, 10} Therefore breed-related variation as an explanation for different results cannot be ruled out. The present study suggests that the shape of the articular surface of APJs per se is not a major contributor to the development of CVM as there was no overrepresentation of any one shape combination within the different regions, sexes (factors of importance in the development of CVM), position and side of the articular surfaces.

In a recent study, bony changes of cervical and cranial thoracic APJs were described in a mixed population of horses of one year and older, without a distinction between top and lateral view.¹⁰ In that study, a considerable variation in morphology was reported also. That study described, amongst others, two shapes, named 'lipping' and 'flattening', that are comparable with respectively the raised edge and folded edge lateral view shapes as described in this study. In that other study, these shapes were considered pathologic and progressive. In the present study, these shapes were already existent in new-born foals and can therefore in any case be considered congenital. An age related prevalence of these two shapes could not be established. The folded lateral view shape (in combination with an oval top view shape) was positively associated with OC and therefore indeed associated with pathology in foals. Whether these two shapes are also associated with pathology in older horses, such as increased likelihood to develop osteoarthritis, needs to be investigated.

OC's first developmental stage, OC latens, is characterized by necrosis of the epiphyseal cartilage and results from necrosis of blood vessels in the cartilage canals.^{4, 18} These cartilage canals are symmetrically present in contralateral joints, only present within a certain age-range, and their course is consistent within species. Therefore, OC lesions develop in young animals, tend to occur in certain predilection sites and are frequently bilaterally symmetric.^{4, 18, 32} Local differences in amount of blood vessels and thickness of the cartilage are thought to account for the occurrence of these predilection sites.¹¹ In the present study, several specific shape combinations were more likely to have OC latens and OC manifesta while OCD was not observed. The cause for this difference in likelihood is not clear, however shape-associated differences in number of blood vessels and thickness of cartilage cannot be excluded. Still, it is possible that the other shape combinations are just as likely to result in OC in older foals, as half of

the foals examined were less than one week old, and the time window for development of radiologically and grossly detectable APJ OC is suggested to last up to approximately 5 months.²⁸ Variances in joint shape likely lead to changes in biomechanical stress and therefore differences in likelihood to develop OCD.³² It is to be expected that environmental stress, such as housing conditions but also normal movement, increases the biomechanical forces on a joint and can as such potentially contribute to OCD development.³² As half of the foals examined were less than one week old, the contribution of biomechanical stress caused by movement was most likely limited and therefore it cannot be excluded that certain shape combinations are associated with OCD in older foals.

Sepsis can cause a vasculitis and subsequently OC-like lesions.^{12, 31} Thus, all examined joints were carefully evaluated for septic changes and the articular surfaces of two foals which showed signs of sepsis after histological evaluation were excluded from further assessment. Although sepsis as cause for OC lesions in the remaining foals seems highly unlikely, several of the foals included did die or were euthanized because of infection. As no histological serial sections of the articular surfaces, nor bacterial culture of the joints were performed, OC-like lesions due to sepsis cannot be ruled out completely.

OC can lead to gross changes, including focal thickening of cartilage, soft and red cartilage, flattening of cartilage and irregular cartilage with possible invaginations.^{13, 27, 32} All articular surfaces included, had smooth, white cartilage and the concave and convex lateral shapes compromised the entire articular surface. Also, the folded and raised edge shapes were composed of cartilage covered bone, seamlessly and firmly attached to the rest of the articular surface, and were therefore not loose cartilage flaps. Only 5 of the articular surfaces with histologically confirmed OC had gross changes suggestive for OC. These changes consisted of (multi) focal round to longitudinal indentations of the cartilage.² Therefore the different shapes described in this study are most probably conformational shape differences and not the result of OC. This is supported by the relative limited numbers of different shapes.

The suspected differences in biomechanical loading associated with different shapes could influence the likelihood to develop osteoarthritis as seen in other joints.²¹ Non-congruent shapes of

opposite articular surfaces within one APJ can result in mal-articulation which may directly lead to compression of nervous tissue, or secondary to compression by developing osteoarthritis. Indeed, the development of CVM in older horses has been suggested to result from progression of subclinical malformation-mal-articulation leading to chronic microtrauma.¹⁵ Therefore, certain shape combinations could still contribute to the development of CVM, although they do not have increased likelihood to have OC. However, to confirm the suspected role of shape in the development of osteoarthritis leading up to CVM, more research, for example long term computer tomographic evaluation with eventually pathological evaluation, is necessary.

Both shape categorization and scoring of the shape grade were made as objective as possible by use of ratios of the axis's, width at the poles, measurements of slope degree and ratio to the articular surface. Objectivity could not be substantiated by use of an intra- or inter-observer reliability score as scoring was only done once during necropsy by a single person (WB). The reliability and reproducibility of the shape categorisation was however improved by the use of representative pictures and schematic drawings. The reliability of grading of the shapes was increased by reducing the original 4-tier grading scale to a 2-tier grading scale.

In conclusion, articular surface shape of the cervical and cranial thoracic APJs is highly variable in warmblood foals. Certain shape combinations are associated with a higher incidence of OC in young warmblood foals and thus might contribute to the development of CVM.

References

1. Back W, Remmen JL, Knaap J, et al. Effect of lateral heel wedges on sagittal and transverse plane kinematics of trotting Shetland ponies and the influence of feeding and training regimes. *Equine Vet J*. 2003;35(6):606-612.
2. Bergmann W, de Mik-van Mourik M, Veraa S, et al. Cervical articular process joint osteochondrosis in warmblood foals. *Equine Vet J*. 2020.
3. Burkner P. brms: An R Package for Bayesian multilevel models using Stan. *J. Stat. Softw*. 2017;80(1):1-28.
4. Carlson CS, Cullins LD, Meuten DJ. Osteochondrosis of the articular-epiphyseal cartilage complex in young horses: evidence for a defect in cartilage canal blood supply. *Vet Pathol*. 1995;32(6):641-647.
5. Claridge HAH, Piercy RJ, Parry A, et al. The 3D anatomy of the cervical articular process joints in the horse and their topographical relationship to the spinal cord. *Equine Vet J*. 2010;42(8):726-731.
6. de Koning DB, van Grevenhof EM, Laurensen BF, et al. Associations of conformation and locomotive characteristics in growing gilts with osteochondrosis at slaughter. *J Anim Sci*. 2015;93(1):93-106.
7. Douglas B, Maechler M. Fitting linear mixed-effects models using lme4. *J. Stat. Softw*. 2015;67(1):1-48.
8. Grondalen T. Osteochondrosis and arthrosis in Norwegian slaughter-pigs in 1980 compared to 1970. *Nord Vet Med*. 1981;33(9-11):417-422.
9. Grondalen T. Osteochondrosis and arthrosis in pigs. VII. Relationship to joint shape and exterior conformation. *Acta Vet Scand Suppl*. 1974;46(0):1-32.
10. Haussler KK, Pool RR, Clayton HM. Characterization of bony changes localized to the cervical articular processes in a mixed population of horses. *PLoS One*. 2019;14(9):e0222989.
11. Hendrickson EHS, Olstad K, Nodtvedt A, et al. Comparison of the blood supply to the articular-epiphyseal growth complex in horse vs. pony foals. *Equine Vet J*. 2015;47(3):326-332.
12. Hendrickson EHS, Lykkjen S, Dolvik NI, et al. Prevalence of osteochondral lesions in the fetlock and hock joints of standardbred horses that survived bacterial infection before 6 months of age. *BMC Vet Res*. 2018;14(1):390-3.

13. Janes JG, Garrett KS, McQuerry KJ, et al. Cervical vertebral lesions in equine stenotic myelopathy. *Vet Pathol.* 2015;52(5):919-927.
14. Laugier C, Tapprest J, Foucher N, et al. A necropsy survey of neurologic diseases in 4,319 horses examined in Normandy (France) from 1986 to 2006. *J Equine Vet Sci.* 2009;29(7):561-568.
15. Levine JM, Adam E, MacKay RJ, et al. Confirmed and presumptive cervical vertebral compressive myelopathy in older horses: A retrospective study (1992-2004). *J. Vet. Intern. Med.* 2007;21(4):812-819.
16. Levine JM, Scrivani PV, Divers TJ, et al. Multicenter case-control study of signalment, diagnostic features, and outcome associated with cervical vertebral malformation-malarticulation in horses. *J Am Vet Med Assoc.* 2010;237(7):812-822.
17. Nout YS, Reed SM. Cervical vertebral stenotic myelopathy. *Equine Vet Educ.* 2003;15(4):212-223.
18. Olstad K, Ekman S, Carlson CS. An update on the pathogenesis of osteochondrosis. *Vet Pathol.* 2015;52(5):785-802.
19. Olstad K, Cnudde V, Masschaele B, et al. Micro-computed tomography of early lesions of osteochondrosis in the tarsus of foals. *Bone.* 2008;43(3):574-583.
20. Powers BE, Stashak TS, Nixon AJ, et al. Pathology of the vertebral column of horses with cervical static stenosis. *Vet Pathol.* 1986;23(4):392-399.
21. Sprackman L, Dakin SG, May SA, et al. Relationship between the shape of the central and third tarsal bones and the presence of tarsal osteoarthritis. *Vet J.* 2015;204(1):94-98.
22. Stewart RH, Reed SM, Weisbrode SE. Frequency and severity of osteochondrosis in horses with cervical stenotic myelopathy. *Am J Vet Res.* 1991;52(6):873-879.
23. Trostle SS, Dubielzig RR, Beck KA. Examination of frozen cross sections of cervical spinal intersegments in nine horses with cervical vertebral malformation: Lesions associated with spinal cord compression. *J Vet Diagn Invest.* 1993;5(3):423-431.
24. Van Biervliet J. An evidence-based approach to clinical questions in the practice of equine neurology. *Vet Clin North Am Equine Pract.* 2007;23(2):317-328.
25. van Biervliet J, Mayhew J, de Lahunta A. Cervical vertebral compressive myelopathy: diagnosis. *Clin Tech Equine Pract.* 2006;5(1):54-59.

26. van Grevenhof EM, Gezelle Meerburg ARD, van Dierendonck MC, et al. Quantitative and qualitative aspects of standing-up behavior and the prevalence of osteochondrosis in Warmblood foals on different farms: could there be a link?. *BMC Vet Res.* 2017;13(1):324-y.
27. van Grevenhof EM, Ott S, Hazeleger W, et al. The effects of housing system and feeding level on the joint-specific prevalence of osteochondrosis in fattening pigs. *Livest Sci.* 2011;135(1):53-61.
28. van Weeren PR, Barneveld A. The effect of exercise on the distribution and manifestation of osteochondrotic lesions in the warmblood foal. *Equine Vet J Suppl.* 1999(31):16-25.
29. van Weeren PR, Denoix JM. The Normandy field study on juvenile osteochondral conditions: conclusions regarding the influence of genetics, environmental conditions and management, and the effect on performance. *Vet J.* 2013;197(1):90-95.
30. van Weeren RP, Olstad K. Pathogenesis of osteochondrosis dissecans: How does this translate to management of the clinical case?. *Equine Vet Educ.* 2016;28(3):155-166.
31. Wormstrand B, Østevik L, Ekman S, et al. Septic arthritis/osteomyelitis may lead to osteochondrosis-like lesions in foals. *Vet Pathol.* 2018;55(5):693-702.
32. Ytrehus B, Carlson CS, Ekman S. Etiology and pathogenesis of osteochondrosis. *Vet Pathol.* 2007;44(4):429-448.

Supplementary Table S1. Foals used in the study

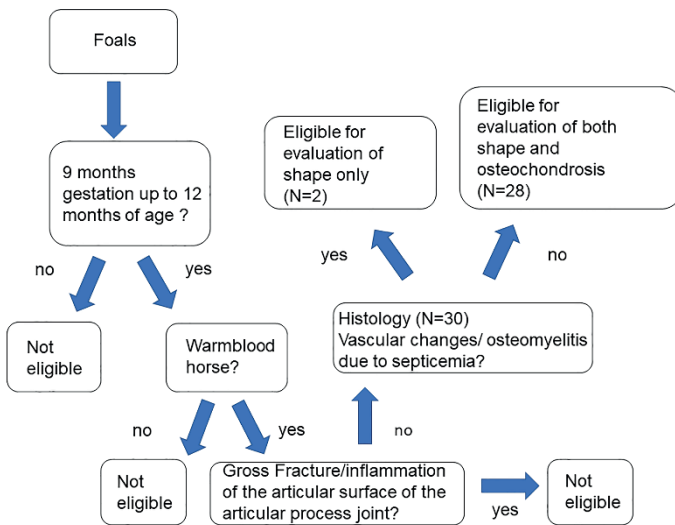
Foal	Breed	Age in days	Sex	Cause of Death	Evaluation of facet shapes	Evaluation of presence of osteochondrosis
1	RDSH	0	Female	Intra uterine death (dam died due to typhlocolitis)	yes	yes
2	RDSH	0	Female	Herpes viral hepatitis	yes	yes
3	RDSH	0	Male	dystocia	yes	yes
4	RDSH	0	Male	dystocia	yes	yes
5	RDSH	1	Female	Herpes viral pneumonia and hepatitis	yes	yes
6	RDSH	1	Female	Herpes viral pneumonia	yes	yes
7	RDSH	1	Female	Actinobacillus equuli sepsis	yes	No ¹
8	RDSH	1	Male	Perforative gastritis; bronchopneumonia	yes	yes
9	RDSH	1	Male	Subepiglottic cyst with resultant dyspnoea and dysphagia	yes	yes
10	Westphalian horse	1	Male	Neonatal asphyxia syndrome; sepsis	yes	No ¹

11	RDSH	3	Male	Bronchointerstitial pneumonia	yes	yes
12	RDSH	3	Female	White muscle disease; enteritis	yes	yes
13	RDSH	4	Male	Interstitial pneumonia	yes	yes
14	RDSH	5	Male	Enteritis	yes	yes
15	RDSH	6	Female	Interstitial pneumonia; enteritis	yes	yes
16	RDSH	7	Female	enteritis	yes	yes
17	RDSH	8	Male	Herpes viral pneumonia	yes	yes
18	RDSH	13	Male	Herpes viral pneumonia	yes	yes
19	RDSH	18	Female	Malformation front legs	yes	yes
20	RDSH	18	Female	Bladder rupture	yes	yes
21	RDSH	28	Male	Omphalitis	yes	yes
22	Zangers heide Horse	47	Male	Hydrocephalus	yes	yes
23	RDSH	48	Male	Interstitial pneumonia	yes	yes
24	RDSH	53	Male	Myocarditis	yes	yes
25	RDSH	54	Male	Rhodococcal pneumonia	yes	yes
26	RDSH	83	Male	typhlocolitis	yes	yes

27	RDSH	134	Male	Bladder rupture	yes	yes
28	RDSH	149	Female	Euthanized due to club foot	yes	yes
29	RDSH	157	Male	Stomach rupture	yes	yes
30	RDSH	365	Male	Trauma	yes	yes

RDSH= Royal Dutch Sport Horse Netherlands

¹ Because sepsis can cause osteochondrosis- like lesions, presence of osteochondrosis was not evaluated in these foals



Supplementary Figure S1

Flowchart for the eligibility of available foals for this research.

Supplemental Table S2. Distribution of absolute numbers and percentages of the shapes combinations of articular surfaces of cervical and cranial thoracic articular process joints of a group of warmblood foals (N=30) aged 0 days to 1 year †

Entire vertebral column

Top view	Side view N (%)							Sum
	Flat	Convex	Concave	Bevelled	Stepped	Folded edge	Raised edge	
Oval	107 (10) ‡ 138 (13) §	60 (6)	184 (18)	256 (24)	186 (18)	43 (4)	15 (1)	989 (94)
Pointed	12 (1)	2 (<1)	0 (0)	10 (1)	0 (0)	0 (0)	0 (0)	24 (2)
Elongated	13 (1)	2 (<1)	2 (<1)	17 (2)	5 (1)	0 (0)	0 (0)	39(4)
Sum	270 (25)	64 (6)	186 (18)	283 (27)	191 (19)	43 (4)	15 (1)	

Cranial Cervical

Top view	Side view N (%)							Sum
	Flat	Convex	Concave	Bevelled	Stepped	Folded edge	Raised edge	
Oval	46 (11) † 40 (9) §	36 (9)	89 (21)	105 (25)	62 (15)	23 (5)	6 (1)	407 (96)
Pointed	3 (1)	2 (<1)	0 (0)	2 (<1)	0 (0)	0 (0)	0 (0)	7 (1)
Elongated	1 (<1)	0 (0)	1 (<1)	9 (2)	0 (0)	0 (0)	0 (0)	11 (3)
Sum	90 (21)	38 (9)	90 (21)	116 (28)	62 (15)	23 (5)	6 (1)	

Caudal cervical

Top view	Side view N (%)							Sum
	Flat	Convex	Concave	Bevelled	Stepped	Folded edge	Raised edge	
Oval	43 (9) † 68 (14) §	19 (4)	64 (13)	139 (29)	93 (19)	17 (4)	9 (2)	452 (94)
Pointed	6 (1)	0 (0)	0 (0)	3 (<1)	0	0 (0)	0 (0)	9 (1)
Elongated	10 (2)	2 (<1)	0 (0)	7 (2)	4 (1)	0 (0)	0 (0)	23 (5)
Sum	127 (26)	21 (4)	64 (13)	149 (31)	97 (20)	17 (4)	9 (2)	

Cranial thoracic

Top view	Side view N (%)							Sum
	Flat	Convex	Concave	Bevelled	Stepped	Folded edge	Raised edge	
Oval	18 (13) † 29 (20) §	5 (4)	31 (22)	12 (9)	31 (22)	3 (2)	0 (0)	129 (92)
Pointed	3 (2)	0 (0)	0 (0)	5 (4)	0	0 (0)	0 (0)	8 (6)
Elongated	2 (<1)	0 (0)	1 (<1)	1 (<1)	1 (<1)	0 (0)	0 (0)	5 (2)
Sum	52 (36)	5 (4)	32 (22)	18 (14)	32 (22)	3 (2)	0 (0)	

Male

Top view	Side view N (%)							Sum
	Flat	Convex	Concave	Bevelled	Stepped	Folded edge	Raised edge	
Oval	69 (11) [‡] 103 (16) [§]	47 (7)	107 (17)	133 (21)	136 (21)	22 (3)	15 (2)	632 (95)
Pointed	6 (<1)	2 (<1)	0 (0)	4 (<1)	0	0 (0)	0 (0)	12 (2)
Elongated	8 (1)	1 (<1)	0 (0)	7 (1)	4 (<1)	0 (0)	0 (0)	20 (3)
Sum	186 (28)	50 (8)	107 (16)	144 (22)	140 (21)	22 (3)	15 (2)	

Female

Top view	Side view N (%)							Sum
	Flat	Convex	Concave	Bevelled	Stepped	Folded edge	Raised edge	
Oval	38 (10) [‡] 34 (9) [§]	13 (3)	77 (20)	123 (32)	50 (13)	21 (5)	0 (0)	356 (92)
Pointed	6 (2)	0 (0)	0 (0)	6 (2)	0 (0)	0 (0)	0 (0)	12 (3)
Elongated	5 (1)	1 (<1)	2 (<1)	10 (3)	1 (<1)	0 (0)	0 (0)	19 (5)
Sum	83 (22)	14 (4)	79 (20)	139 (36)	51 (13)	21 (5)	0 (0)	

Left

Top view	Side view N (%)							Sum
	Flat	Convex	Concave	Bevelled	Stepped	Folded edge	Raised edge	
Oval	46 (9) [‡] 73 (14) [§]	33 (4)	96 (18)	124 (23)	95 (18)	23 (4)	7 (1)	497 (93)
Pointed	11 (2)	1 (<1)	0 (0)	2 (<1)	0 (0)	0 (0)	0 (0)	14 (3)
Elongated	6 (1)	1 (<1)	0 (0)	11 (2)	2 (<1)	0 (0)	0 (0)	20 (4)
Sum	136 (26)	35 (7)	96 (18)	137 (26)	97 (18)	23 (4)	7 (1)	

Right

Top view	Side view N (%)							Sum
	Flat	Convex	Concave	Bevelled	Stepped	Folded edge	Raised edge	
Oval	61 (12) [‡] 64 (12) [§]	27 (5)	88 (17)	133 (26)	91 (18)	20 (4)	8 (2)	492 (94)
Pointed	1 (<1)	1 (<1)	0 (0)	8 (2)	0 (0)	0 (0)	0 (0)	10 (2)
Elongated	7 (1)	1 (<1)	2 (<1)	6 (1)	3 (<1)	0 (0)	0 (0)	19 (4)
Sum	133 (26)	29 (6)	90 (17)	147 (28)	94 (18)	20 (4)	8 (1)	

Cranial

Top view	Side view N (%)							Sum
	Flat	Convex	Concave	Bevelled	Stepped	Folded edge	Raised edge	
Oval	51 (8) [‡] 78 (13) [§]	14 (2)	178 (29)	130 (21)	124 (20)	38 (6)	0 (0)	613 (98)
Pointed	3 (<1)	1 (<1)	0 (0)	4 (1)	0 (0)	0 (0)	0 (0)	8 (1)
Elongated	1 (<1)	0 (0)	1 (<1)	1 (<1)	0 (0)	0 (0)	0 (0)	3 (1)
Sum	133 (21)	15 (2)	179 (29)	135 (22)	124 (20)	38 (6)	0 (0)	

Caudal

Top view	Side view N (%)							Sum
	Flat	Convex	Concave	Bevelled	Stepped	Folded edge	Raised edge	
Oval	56 (13) [‡] 59 (14) [§]	46 (11)	6 (2)	126 (30)	62 (15)	5 (<1)	15 (4)	375 (88)
Pointed	9 (2)	1 (<1)	0 (0)	6 (1)	0 (0)	0 (0)	0 (0)	16 (4)
Elongated	12 (3)	2 (<1)	1 (<1)	16 (4)	5 (<1)	0 (0)	0 (0)	36 (8)
Sum	136 (32)	49 (12)	7 (1)	148 (35)	67 (16)	5 (1)	15 (3)	

† The sum of all cells per table per region is 100%

‡ Shape combination of an oval top view shape with only a flat side view (normal)

§ Shape combination of an oval top view shape with a flat side view and an extra side view

< Less than

Supplemental Table S3: Percentage of side view shape combinations of the articular surfaces within the same articular process joint in a group of warmblood foals age 0 to 1 year (N=30) †

shape	normal	convex	concave	stepped	bevelled	folded	raised
normal	4.3	0.7	2.2	0.8	3.2	3.0	0.4
convex	0.7	1.0	3.5	0.0	1.6	1.8	0.2
concave	2.2	3.5	2.0	1.2	8.0	2.1	0.2
stepped	0.8	0.0	1.2	0.0	0.3	0.0	0.0
bevelled	3.2	1.6	8.0	0.3	12.9	5.3	1.5
folded	3.0	1.8	2.1	0.0	5.3	7.3	0.1
raised	0.4	0.2	0.2	0.0	1.5	0.1	0.3

† N= 607 combinations from 384 joints examined. Joints including an articular surface with a more unique shape were excluded. 150 joints had at least one articular surface with 2 and 4 joints had a least one articular surface with 3 abnormal shapes. The total sum of the cells of the table is 100%.

Supplemental Table S4. Absolute number of shapes graded and percentage of different grades per side view shape

Shape	Absolute number of shapes graded	Percentage of shape grade			
		minimal	mild	moderate	severe
convex	48	40	44	10	6
concave	174	54	43	2	1
bevelled	274	28	37	23	12
folded edge	187	28	39	24	10
raised edge	43	58	37	5	0
stepped	6	0	17	67	17

Supplemental Table S5. Significant odds ratio and 95% confidence interval of shape grade of a articular surface in a group of warmblood foals (N=30) age 0 day to 1 year of the final model†

Fixed variable	Absolute number (and percentages) of articular surfaces graded minimal and mild	Absolute number (and percentages) of articular surfaces graded moderate and severe	Odds ratio	95% profile likelihood confidence interval
All regions				
cranial position	403 (72)	71 (40)	reference	
caudal position	154 (28)	109 (60)	4.61	3.16-6.81
Cranial cervical region				
cranial position	194 (78)	20 (31)	reference	
caudal position	54 (22)	44 (69)	14.32	6.76-33.33
Caudal cervical region				
cranial position	173 (69)	39 (43)	reference	
caudal position	79 (31)	52 (57)	3.08	1.80-5.22

† The initial model, for shape grade (with binary outcome variables minimal to mild/ moderate to severe) of the observed articular surface, included explanatory variables age, sex, region, side and position.

The final model for all regions included age and position of the observed articular surface. The final model for the cranial cervical region included only position of the observed articular surface. The final model of the caudal cervical region included age and the position of the observed articular surface.



Intervertebral Disc
Degeneration in
Warmblood Horses:
Morphology, Grading,
and Distribution of
Lesions

4

Published in: Veterinary Pathology.
2018;55(3):361–478

W. Bergmann
N. Bergknut
S. Veraa
A. Gröne
H. Vernooij
I. D. Wijnberg
W. Back
G. Grinwis

Abstract

Equine intervertebral disc degeneration is thought to be rare and of limited clinical relevance, although research is lacking. To objectively assess pathological changes of the equine intervertebral disc and their clinical relevance, description of the normal morphology and a practical, biologically credible grading scheme are needed. The objectives of this study are to describe the gross and histological appearance of the equine intervertebral discs and to propose a grading scheme for macroscopic degeneration. Spinal units from 33 warmblood horses were grossly analysed and scored. Of the 286 intervertebral discs analysed, 107 (37%) were assigned grade 1 and grade 2 (considered normal) and were analysed histologically. A nucleus pulposus and an annulus fibrosus could be identified macroscopically and histologically. Histologically, the nucleus pulposus was composed of a cartilaginous matrix and the annulus fibrosus of parallel collagenous bands. A transition zone was also histologically visible. Intra- and inter-observer reliability scores were high for all observers. Higher grades were associated with greater age. Gross changes associated with equine intervertebral disc degeneration (grades 3–5) —that is, yellow discoloration, cleft formation (tearing), and changes in consistency of the nucleus pulposus— were largely similar to those in humans and dogs and were most prevalent in the caudal cervical spine. Equine intervertebral disc degeneration was not associated with osteophyte formation. Changes of the vertebral bone were most common in the thoracolumbar spine but were not correlated with higher grades of intervertebral disc degeneration. Thus, changes of the vertebral bone should be excluded from grading for equine intervertebral disc degeneration.

Introduction

Neurological conditions originating from the equine neck are common.⁵⁷ Non-infectious, nontraumatic causes have mostly been attributed to space-occupying changes of the facet joints, vertebral dorsal laminae, and ligamentum flavum, leading to static compression of the spinal cord and nerves or to cervical vertebral instability characterized by dynamic narrowing of the spinal canal during movement of the neck.^{12, 28, 35} Although cervical neurological abnormalities in horses have been related to intervertebral discs (IVDs) in case reports^{15-17, 24, 30, 32, 33, 38, 44, 45, 48, 55, 56}, degeneration of the IVD is thought to be clinically less relevant,^{7, 26, 33, 36, 53} and a detailed morphological description is missing. However, numerous studies in humans and dogs do show a compelling relationship between IVD degeneration (IVDD) and clinical signs,^{2, 9, 29, 31, 46} but systematic studies of equine IVD disease seem to be lacking.

Moreover, there is absence of consensus among authors about the anatomical characteristics of the equine IVD. Some publications claim the lack of a nucleus pulposus (NP),^{7, 53} while in others, a fibrous^{33, 36, 52, 53} or fibrocartilaginous^{26, 58} NP is acknowledged. Nonetheless, like humans and dogs,^{5, 8} it is agreed that there is also a peripheral annulus fibrosus (AF) in horses,^{17, 24, 44, 56, 58} which is composed of collagenous bands.⁵⁸ To be able to determine the clinical importance of equine IVDD, a precise definition of the anatomical structures and the morphological characteristics of degeneration is required.

Therefore, this study had 3 objectives: (1) to describe the gross and histological appearance of the normal equine IVD, as well as facilitate the development of a grading scheme for gross changes of the IVDs and the vertebral bone, including changes of the subchondral bone (vertebral endplate) and changes of the ventral part of the vertebral body since these anatomical structures are also included in grading of human and canine IVDs;^{5,51} (2) to develop a grading scheme of the gross pathological changes of the equine IVD; and (3) to evaluate the prevalence of IVDD within different spinal regions.

Materials and methods

Vertebral columns were harvested post-mortem from 33 warmblood horses that either died unexpectedly or were humanly euthanized for reasons unrelated to the current study and referred for necropsy to the Department of Pathobiology, Faculty of Veterinary Medicine, Utrecht University (Suppl. Table S1). All but 2 of the horses used in this study were privately owned. One horse was used for police work. Necropsy was performed with the owner's informed consent to investigate the cause of death or the cause for the clinical signs. One of the horses was owned by the Faculty of Veterinary Medicine, Department of Equine Sciences of the Utrecht University and used for teaching purposes, which included obtaining surgical skills with subsequent euthanasia with approval of the local ethics committee (DEC number 2013.III.01.012). Horses were of different ages, varying from 8 months to 21 years (mean age, 8.8 + 6.1 years), different breeds (28 Royal Dutch Sport horses, 2 Zangersheide horses, 1 Trakehner, 1 Holsteiner, 1 Westphalian horse), and different sexes (15 mares, 6 stallions, 12 geldings).

Sampling

The vertebral columns were dissected and cut mid-sagittally using a K430 band saw (Kolbe, Elchingen, Germany; blades Munkfors, Värmland, Sweden). The cut surfaces of the IVDs were photographed with a Nikon D80 digital single-lens reflex camera (Nikon, Tokyo, Japan), and the analysis was based on the spinal unit (subchondral bone-IVD-subchondral bone). Only 1 IVD was visible per photograph to allow unbiased evaluation. Only pictures of good quality to evaluate subtle changes were used, resulting in a total of 286 spinal units (86% of the number photographed) being analysed. Four different regions were selected for examination, based on common sites of IVDD and related diseases in humans and in non-chondrodystrophic dogs, the 2 most commonly studied species affected by IVDD.^{3, 23} The IVDs of the cervical spine (C2- T1) were selected because in humans, this is the second most common region showing IVDD after the lumbar region.^{22, 49} In addition, in non-chondrodystrophic dogs, the caudal cervical spine is predisposed to develop IVDD-related diseases.⁹ The IVDs of the cervical spine were further

subdivided into 2 regions—(1) cranial to mid-cervical region (IVDs between the cervical vertebrae C2 and C5¹⁰) and (2) the caudal cervical region (IVDs between C5 and the thoracic vertebra T1^{11, 28})—to identify possible differences in the distribution of IVDD in the equine cervical spine as seen in the dog.⁹ In humans and dogs, severe IVDD can lead to osteophyte formation (spondylosis).^{3, 51} To investigate whether IVDD is also important in the development of osteophytes (spondylosis) in the horse, the intervertebral discs between thoracic vertebrae T11 and T13, the most common region for horses to develop spondylosis,^{25, 53} were selected. Finally, the lumbosacral region (IVDs between the lumbar vertebrae L4 and the sacral vertebrae S1) was chosen, as this is the most common location for IVDD in humans and for diseases associated with IVDD in non-chondrodystrophic dogs.^{2, 22, 49} To make sure not to damage the IVD between C7 and T1 during necropsy, the cervical and thoracic parts of the spine were separated by sawing through vertebra T2. Consequently, the IVD between T1 and T2 was readily available and therefore also used to develop and validate the grading scheme.

Development of a macroscopic grading scheme for IVDD and the vertebral bone

The photographs of the IVDs were analysed for morphologic changes of the NP, AF, and vertebral bone using a human grading scheme,⁵¹ which is also validated for the dog³ and was subsequently adjusted for the horse as deemed necessary. In short, for grading of the IVD, the annulus fibrosus and the nucleus pulposus were evaluated for its texture, colour, and the presence of clefts. IVD considered normal showed a gelatinous, semi-translucent nucleus and white shiny lamellae. Degenerated discs were characterized by a fibrillary nucleus pulposus, with yellow (-whitish) discoloration of both the nucleus and the annulus with or without clefts (i.e. tears) (Table 1, Figures 1–9). For grading of the vertebral body, both the subchondral bone and the ventral part of the vertebral body were evaluated. With increasing grades, the subchondral bone changed from trabecular to more compact. The ventral part of the vertebral bone was being reviewed for the loss of rounded margins and the development of osteophytes (Table 2, Figures 1 and 10–14). For human and canine discs, grades 1 and 2 are considered normal and grades 4 and 5 degenerated, with grade 3 representing a transitional stage.^{6, 50} In a preceding pilot study (results not

shown), the grading of morphological changes of the subchondral bone as well as osteophyte formation and spondylosis of the ventral part of the vertebral body did not correlate with the grades for changes of the AF and NP, and therefore these morphological aspects were graded in 2 separate schemes.

Validation of the macroscopic grading schemes

The photographs were assigned a random number using an online randomization program and graded twice each by 3 independent observers with a time lapse of at least a week between grading sessions of each observer. Inter- and intraobserver reliabilities were calculated by using a Cohen's weighted k analysis (quadratic weights of 1, 0.9375, 0.75, 0.4375, and 0). A k value of less than 0.00 is considered poor, a value between 0.00 and 0.20 as slight, between 0.21 and 0.40 as fair, between 0.41 and 0.60 as moderate, between 0.61 and 0.80 as substantial, and a value between 0.81 and 1.00 as almost perfect.^{3,27} The grades assigned during the second round of grading by each observer were added and averaged for a total averaged final grade per spinal unit. If the assigned grade from the second grading differed by more than 1 between the observers, the image was reviewed by the 3 observers and a consensus grade was allotted.

Statistical analysis

To evaluate the association of the grade for IVDD and the grade for changes of the vertebral bone with age and distribution, the final grades were log-transformed to meet the model assumptions for normality and constant variance. The outcomes were analysed using a linear mixed model with explanatory continuous variable age and factor variable region, and horse was added to the model as random effect to take the correlated observations within horse into account. The Akaike information criterion was used to select the best model, and Bonferroni correction was applied to correct for multiple comparisons. Residuals were used to investigate the correctness of the model assumptions.

A scatterplot showed a linear association between the grades for IVDD and

the grades for the changes of the vertebral bone within the same spinal unit only up to grade 3 (Figure. 15). Therefore, correlation was determined with a Spearman's rank-order correlation test.

All statistical analyses were performed using SPSS version 22 (SPSS, Inc, an IBM Company, Chicago, IL).

Table 1. Macroscopic grading scheme for intervertebral disc degeneration in horses.

Grade	Nucleus	Annulus
1	Gelatinous, semi-translucent to white, shiny	White shiny lamellae
2	Partially gelatinous, partly fibrillar	White shiny lamellae
3	Fibrillar	Slightly yellow lamellae
4	Fibrillar, slightly yellow, vertical clefts	Slightly yellow, focal disruptions
5	Yellow discoloration, vertical clefts through nucleus and one or two annuli	Yellow discoloration, clefts through nucleus and one or two annuli

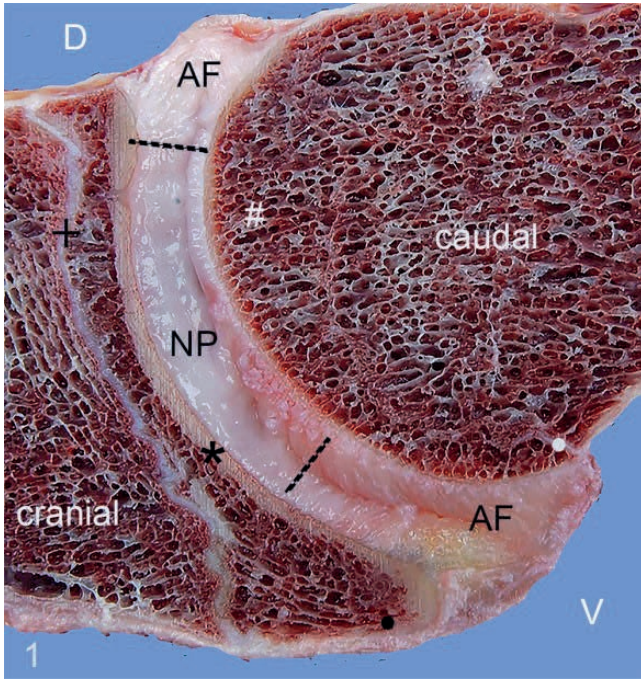


Figure 1. Normal intervertebral disc, C7 to T1 (intervertebral disc between cervical vertebra 7 and thoracic vertebra 1), mid-sagittal spinal section, 2-year-old horse. Grade 1 (normal) for intervertebral disc degeneration and grade 2 for changes of the vertebral bone. The gelatinous, semi-translucent, white, and shiny nucleus pulposus (NP) is visible between the dotted lines. The annulus fibrosus (AF) is white and contains horizontal

lamellae. The dorsal AF shows minimal dorsal bulging. Cranially, there is a rim of subchondral compact bone (*), whereas the caudal subchondral bone is trabecular. The ventral part of the vertebral body (•) is rounded.

D, dorsal; V, ventral; +, growth plate; *, compact subchondral bone/vertebral endplate; #, subchondral trabecular bone/vertebral endplate; •, ventral part of the vertebral body.

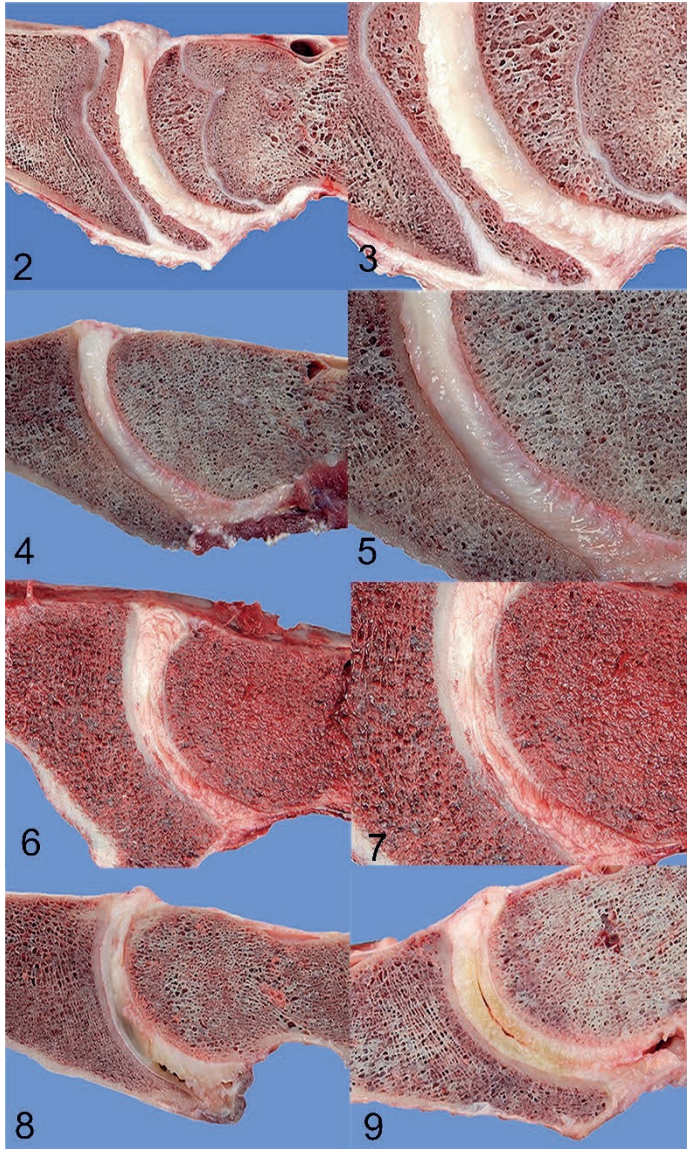
Normal histology

For analysis of the histological characteristics of the normal equine IVD, 107 discs assigned grade 1 and grade 2 (37%) were cut into 0.5-cm-thick slices and fixed in 10% neutral buffered formalin and then decalcified in 10% EDTA before routine processing into 4-mm sections that were stained with hematoxylin and eosin (HE) and with Alcian blue/picrosirius red (AB/PSR).^{4, 18, 37} Depending on the size of the IVD, 2 to 5 histological sections were necessary to encompass the entire IVD.

Results

Macroscopically, the AF and the NP could be identified using mid-sagittal sections in all dissected regions of the vertebral column (Figures. 1–9). The IVD was convex on the cranial aspect and concave at the caudal aspect, and this shape was most prominent in the cervical region. The NP was characterized by a gelatinous, nonlamellar texture compared to the AF and was placed slightly eccentrically toward the dorsal part of the IVD (Figure. 1). The NP of a normal disc was defined as shiny, blue-white, semi-translucent, and pulpy. A firmer, more solid NP with a fibrillar texture and often with yellow-white discoloration was interpreted as mild, early degeneration. Cleft formation of the NP was interpreted as severe degeneration occurring in later stages. The normal AF was defined as a lamellar structure with the ventral AF mildly broader and about twice the height of the dorsal AF. Cleft formation of the lamellae in a dorsoventral direction, nearly always accompanied by a yellow discoloration, was interpreted as degeneration. Bulging of a few millimetres of the dorsal AF into the spinal canal was seen commonly in all grades (Figures. 1, 2, 8, 9). However, in none of the IVDs was this deemed extensive enough to have caused pressure on the spinal cord as visible on mid-sagittal sections of the vertebral column. Herniation of the nucleus pulposus was not seen in any of the IVDs examined.

Histologically, the normal IVD was dorsally and ventrally composed of approximately 10 parallel bands that stained brightly red with the AB/PSR stain, consistent with an AF that is rich in collagen type I. The more centrally located part of the IVD consisted of a blue intercellular matrix, compatible with a proteoglycan-rich (mucinous) cartilaginous NP. Between these 2 parts, a rather poorly demarcated transition zone was visible in which there was a gradual transition of the staining characteristics of the intercellular matrix (Figure. 16). This histological difference was colocalized with the grossly visible different morphological characteristics of the peripheral annulus region and the central nucleus region of the equine IVD. At the cranial and caudal margins, the NP and AF were bordered by a rim of hyaline cartilage of approximately 8 chondrocytes thick, compatible with a cartilaginous endplate (Figures. 16, 17).



Figures 2-9. Grades 1 to 5 for intervertebral disc degeneration, mid-sagittal sections of the spinal column, horse.

Figures 2-3. Grade 1, C5 to C6, 8 months old. The nucleus pulposus (NP) is white, gelatinous, and shiny. The dorsal and ventral parts of the annulus fibrosus (AF) are white and shiny, and horizontal lamellae are easily visible ventrally. The dorsal AF shows minimal dorsal bulging.

Figures 4-5. Grade 2, C2 to C3, 6 years old. The NP is partially gelatinous and partially fibrillar and has a more condensed consistency than in grade 1. The AFs are white and shiny. The horizontal lamellae of the ventral AF are visible (Figure. 5).

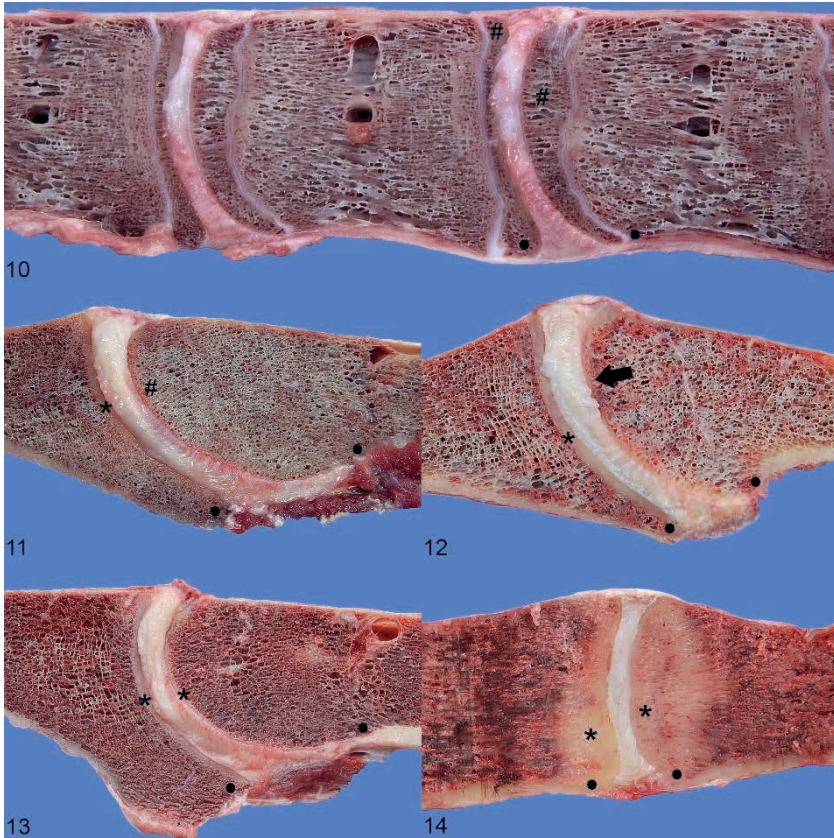
Figures 6-7. Grade 3, C3 to C4, 12 years old. The NP is completely fibrillar and has a more condensed consistency than grade 2. The dorsal and ventral parts of the AF are still white with reduced visibility of the lamellae.

Figure 8. Grade 4, C6 to C7, 10 years old. The NP is fibrillar. The ventral AF has a vertical cleft. The dorsal AF shows minimal dorsal bulging.

Figure 9. Grade 5, C7 to T1, 15 years old. The NP and the AF are slightly yellow with clefting through both. The dorsal AF shows minimal dorsal bulging.

Table 2. Macroscopic grading scheme for changes of the vertebral bone in horses.

Grade	Subchondral bone	Ventral part of the vertebral body
1	Only trabecular subchondral bone, no compact subchondral bone	Margins rounded
2	Cranially compact subchondral bone, caudal trabecular subchondral bone	Margins rounded
3	Cranially compact subchondral bone, caudally areas of increased density of trabecular subchondral bone (sclerosis)	Margins pointed
4	Cranially compact subchondral bone, caudally small line of compact subchondral bone (less than ½ of the thickness cranially)	Osteophyte formation
5	Cranially compact subchondral bone, caudally compact subchondral bone (½ or more of cranial thickness)	Bony bridging of vertebrae



Figures 10–14. Grades 1 to 5 for changes in the vertebral bone, mid-sagittal sections of the spinal column, horse.

Figure 10. Grade 1, T11 to T12, 1 year old. The cranial and caudal subchondral bone are composed of trabecular bone (#). The ventral part of the vertebral body has rounded margins (•).

Figure 11. Grade 2, C2 to C3, 6 years old. Cranially, there is a rim of subchondral compact bone (*). The caudal subchondral bone is composed of trabecular bone (#). The ventral part of the vertebral body is rounded (•).

Figure 12. Grade 3, C3 to C4, 15 years old. Cranially, there is a rim of subchondral compact bone (*). Caudally, the subchondral trabecular bone is multifocally more compact (arrow). The ventral part of the vertebral body is rounded (•).

Figure 13. Grade 4, C4 to C5, 10 years old. Cranially, there is a rim of subchondral compact bone (*). Caudally, there is a smaller rim of compact bone (*). The ventral part of the vertebral body is rounded (•).

Figure 14. Grade 5, L5 to L6, 10 years old. Both cranially and caudally, there are thick bands of compact bone (*). The ventral part of the vertebral body is rounded (•).

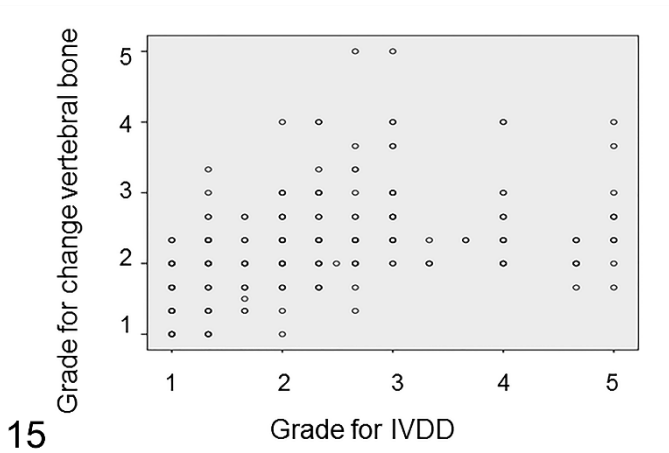
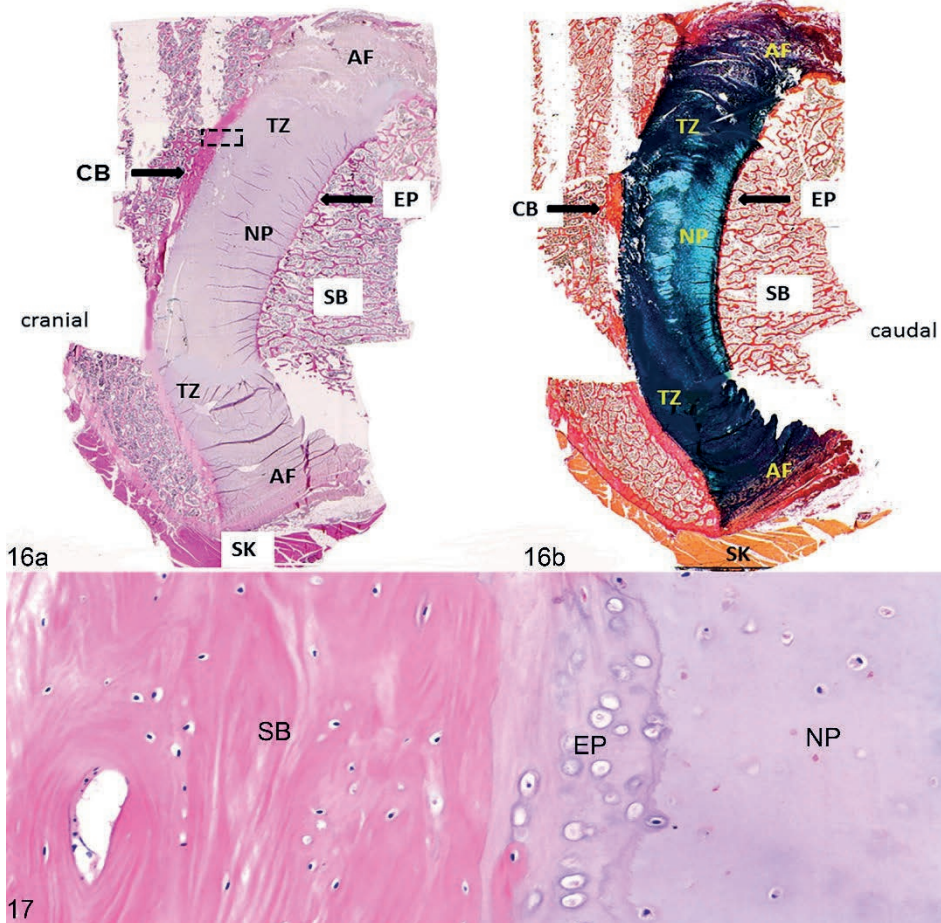


Figure 15. Correlation between the total averaged final grade for intervertebral disc degeneration (IVDD) and for changes of the vertebral bone. Changes in the vertebral bone are linearly associated with grades 1 to 3 for IVDD but are not associated with grades 4 to 5 for IVDD.

IVDD was significantly more severe in the caudal cervical region (C5–T1) with a mean + standard deviation (SD) grade of 2.69+1.64 compared with the cranial cervical region (2.00 + 0.89), thoracic region (2.02 + 0.86), and lumbosacral region (2.08 + 0.87) (Figure. 18, Table 3; $P < .05$). The grade for IVDD increased significantly with age: grade 1, 4.12 + 4.15 years of age (mean + SD); grade 2, 8.10 + 4.91 years; grade 3, 11.52+ 5.84 years; grade 4, 11.13+ 5.35 years; and grade 5, 14.20 + 3.31 years ($P < .05$). The grades for changes of the vertebral bone also increased significantly with age: grade 1, 2.05 +1.99 years of age (mean + SD); grade 2, 8.12 + 5.2 years; grade 3, 11.79 + 6.08 years; and grade 4, 14.5 + 3.8 years ($P < .05$). The formation of subchondral compact bone was significantly more extensive in the thoracic and lumbosacral regions (mean + SD grade of 2.34 + 0.75) compared to the cervical segments (2.01 + 0.67) (Figure. 19, Table 4; $P < .05$). The cartilaginous endplate was not visible without microscopic magnification in any of the IVDs examined.



Figures 16–17. Normal intervertebral disc, C3 to C4, 11-year-old horse. Grade 1 for intervertebral disc degeneration and grade 2 for changes of the vertebral bone. Figure 16. There is no obvious distinction between the annulus fibrosus (AF) and the nucleus pulposus (NP) with the haematoxylin and eosin stain (Figure. 16a). However, the Alcian blue/picrosirius red stain (Figure. 16b) does show a clear difference between the red collagenous AF and the blue proteoglycan-rich NP, and these are separated by a transition zone (TZ). On the cranial and caudal margins, the intervertebral disc is bordered by a cartilaginous endplate (EP) composed of hyaline cartilage, and on the cranial aspect, a rim of subchondral compact bone (CB) is visible. SB, subchondral bone; SK, skeletal muscle. The rectangle indicates the area of the intervertebral disc enlarged in Figure 17. Figure 17. The cartilaginous NP is flanked by an EP composed of hyaline cartilage. Haematoxylin and eosin.

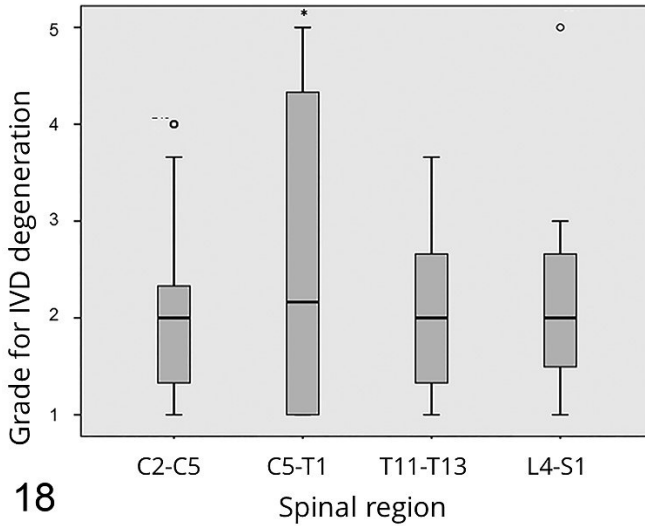


Figure 18. Distribution of grades for intervertebral disc degeneration (IVDD) within the different spinal regions. IVDD was significantly more severe in the caudal cervical region (C5-T1) compared to the cranial cervical, thoracic, and lumbosacral regions. *P < 0.05. The box spans the first to the third quartiles (interquartile range). The line inside the box represents the median. The whiskers show the minimum and maximum. o, outliers.

18

There was a significant correlation between the grade for IVDD and the grade for changes of the vertebral bone ($r_s \approx 0.56$, $P < .01$), which was almost exclusively due to the changes of the subchondral bone. Changes of the ventral part of the vertebral body were only present at the 2 thoracic IVDs of the oldest horse and were characterized by a partially bony, partially fibrous bridge with involvement of the outer layers of the ventral AF between the corresponding vertebrae. These IVDs were both assigned a grade 3.

The intraobserver reliability was substantial to almost perfect, with mean k scores of 0.78, 0.87, and 0.87 for the 3 observers when using the grading scheme for IVDD. The interobserver reliability for this grading scheme was also substantial to almost perfect, with k scores of 0.75 and 0.82.

The intraobserver reliability for the scoring scheme for changes of the vertebral bone was moderate to substantial, with mean k scores of 0.50, 0.70, and 0.77. The interobserver reliability for this grading scheme was fair to moderate, with mean k scores of 0.39 and 0.56.

Table 3. Grades for intervertebral disc degeneration distributed among the different spinal regions. ^a

Region	Total	grade 1	grade 2	grade 3	grade 4	grade 5
Cranio-cervical	81	24 (30)	41 (50)	8 (10)	8 (10)	0 (0)
Caudo-cervical ^b	80	29 (36)	16 (20)	6 (8)	9 (11)	20 (25)
Thoracic	56	19 (34)	18 (32)	18 (32)	1 (2)	0 (0)
Lumbo--sacral	48	13 (27)	20 (42)	14 (29)	0 (0)	1 (2)

^a The data show the number (and percentage) of discs with each grade for each of the anatomic regions.

^b Intervertebral disc degeneration was significantly more severe in this region than in the other regions.

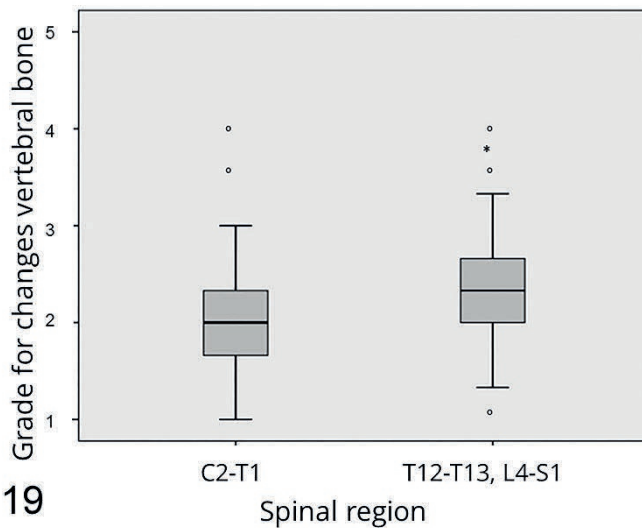


Figure 19. Distribution of grades for changes of the sub chondral bone within the different spinal regions. Increased density of subchondral bone was significantly more extensive in the thoracic and lumbosacral regions compared to the cervical segments. *P < 0.05. The box

spans the first to the third quartiles (interquartile range). The line inside the box represents the median. The whiskers show the minimum and maximum. o, outliers.

Table 4. Grades for changes of the vertebral bone distributed among the different spinal regions. ^a

Region	Total	grade	grade	grade	grade	grade
		1	2	3	4	5
Cranio-cervical	81	14 (17)	54 (67)	9 (11)	4 (5)	0 (0)
Caudo-cervical ^b	80	15 (19)	54 (67)	9 (11)	2 (3)	0 (0)
Thoracic	56	5 (9)	33 (59)	15 (27)	3 (5)	0 (0)
Lumbo--sacral	48	3 (6)	28 (58)	13 (27)	3 (6)	1 (2)

^a The data show the number (and percentage) of discs with each grade for each of the anatomic regions.

^b The changes of the vertebral bone were significantly more severe in these 2 regions combined, compared to the other 2 regions combined.

Discussion

In contrast to previous publications,^{7, 53} this study showed that the equine IVD does have a grossly and histologically discernible proteoglycan-rich NP that is distinct from the lamellar collagenous AF. This is similar to the situation in humans and dogs (Figure. 1).^{5, 6, 8, 37, 51} Furthermore, cranially and caudally located cartilaginous endplates separated the IVD from the bony vertebral endplates, and a transition zone was present between the AF and the NP, which is also comparable to the situation in humans and dogs.^{6, 37} In literature on the human and canine intervertebral disc, the bony vertebral endplate adjacent to the cartilaginous endplate of the IVD is commonly referred to as subchondral bone. As shown in this study and described previously,^{44, 58} a rim of cartilage between the IVD and the vertebral bone is also present in the horse. To be consistent with the vast majority of literature, the vertebral endplate is called subchondral bone in this study. The distinction between the AF and the NP was much less clear, both macroscopically and histologically (in the HE stain), in horses compared to

human and dogs (Figures. 1, 16). Grossly, in horses of all ages, the NP was never as translucent as in normal human and canine IVDs, making it more difficult to distinguish the NP from the AF. Presumably, this is why in previous publications,^{7, 53} the equine IVD was said to lack a NP. Nevertheless, the AB/PSR stain clearly showed a morphological and biochemical difference between the AF and NP, and this histological difference was colocalized with the different gross morphological characteristics of the peripheral annulus region and the central nucleus region of the equine IVD. Bulging of a few millimetres of the dorsal AF into the spinal canal was commonly seen in all grades and was considered too small to have caused pressure on the spinal cord, suggesting that minimal bulging of the dorsal AF occurs in normal horses.

Gross changes that were in accordance with degeneration as described for human and canine IVDs could be identified in all parts of the IVD.^{1, 5, 6, 51} The presence of yellow discoloration and cleft formation are the only features previously described for equine IVDD,^{7, 53} whereas the present study identified additional morphological characteristics like a reduced gelatinous and an increased fibrillary appearance of the NP. This interpretation is likely to also apply to horses.

Although the correlation between grades for IVDD and changes of the vertebral bone was statistically significant, this significance seemed to be present for grades 1 to 3 only (Figure. 15). The more severe grades for IVDD (grades 4 and 5) were not associated with a substantial increase in changes of the vertebral bone, suggesting that age is a more dominant factor for these changes than IVDD. Furthermore, grades for IVDD were significantly associated with localization in the caudal cervical spine, whereas grades for changes of the vertebral bone were significantly associated with the thoracolumbar spine. Therefore, macroscopic grading of equine IVDD should only include the morphology of the NP and the AF to prevent under- or overinterpretation of the severity of IVDD.

It has been suggested that osteophyte formation in the horse is not secondary to IVDD.⁷ The findings in the present study support this assumption. Of the 39 IVDs assigned a grade 4 or a grade 5, none showed changes of the ventral part of the vertebral body. In addition, ventral bridging was seen only between 3 thoracic vertebrae of 1 horse, and in that case, both associated IVDs were assigned a grade 3 for IVDD.

An age-related increase in the bone density of the equine cervical subchondral bone, directly adjacent to the cartilaginous endplate, was found

in this and a previous study.⁵⁸ The increased density of the subchondral bone is probably a common feature of aging in horses, as we have found no correlation with pronounced IVDD (grades 4 and 5). The density of the subchondral trabecular bone was significantly less in the cervical than in the thoracic and lumbosacral segments, perhaps because the former trabeculae are oriented less horizontally, possibly leading to less axial compression stress and subsequently lower bone density as dictated by Wolff's law.⁴²

The equine grading scheme presented here was based on a commonly used human grading scheme that does not include the parameters' joint space width (considered indicative of IVDD on radiographs in both humans and dogs^{40, 46}) or dorsal bulging and herniation of the IVD. These parameters were not included in the human grading scheme because they are considered consequences of and not part of the degenerative process,²⁰ and therefore these parameters were also not incorporated in the equine scheme.

When investigating the pathogenesis and the clinical relevance of equine IVDD, a standardized method for evaluation and grading is necessary to assess the gross characteristics and the severity of degeneration. Such a method will allow reliable comparison of results in future research. A good grading scheme is reproducible, which is reflected in high k scores for intra- and interobserver reliability,⁵¹ as was the case in the adapted grading scheme used in the present publication. A good grading scheme should also be biologically credible.⁵¹ In humans, dogs, and also horses, IVDD is correlated with age.^{1, 7, 36, 54} The grades for IVDD assigned in the present study were also significantly associated with age, supporting its biological credibility.

In accordance with the existing literature,^{7, 36} IVDD was significantly more prevalent in the caudal cervical segment compared to the other segments examined. In addition to the age-related component, IVDD in humans and dogs is thought to be influenced by genetic and mechanical factors, as well as reduced nutrient supply.^{2, 19, 31, 39} In humans, IVDs undergo microstructural changes to a similar extent in all regions, and age-related degeneration affects the entire spine.^{1, 49} A higher prevalence of degeneration in certain regions in both humans and dogs can occur due to locally increased mechanical loading.^{1, 19, 39, 43, 49} Also in horses, increased mechanical load has been suggested as a cause for the increased prevalence of IVDD in the caudal cervical spine.⁷ In addition, dorsoventral mobility may promote IVDD in the horse.⁵³ According to the literature, the movements in

the caudal cervical spinal joints are larger than those in the cranial cervical spine,⁴¹ which might explain the observed difference in prevalence of IVDD between these 2 regions. The lower incidence of IVDD in the thoracic spine of humans and dogs has been attributed to the stabilizing effect of the ribcage with resultant reduced mechanical stress on the IVDs.^{29,47} The horse has a comparably rigid thoracolumbar spine that, as in humans and dogs, might at least partially explain the low incidence of IVDD in this region.^{26,34,52} An increased prevalence of degeneration in the equine lumbosacral disc has been previously described,^{36,53} but this was not confirmed by the present study. In these earlier publications, the breeds of horses, if specified, did not belong to the group of warmblood horses. This suggests that the breed or the work the animal is used for might influence which IVD has the highest mechanical loading and subsequently the highest risk for development of degeneration. It might be that the lumbosacral area is more affected in the racing Thoroughbred than in warmblood horses, as the former breed performs exclusively at the gallop. Ventrodorsal flexion-extension is known to be largest at canter or gallop, and the lumbosacral junction is known to show by far the largest range of motion.^{13,14,21} Unfortunately, the type of work the horses were used for was not mentioned in these publications.

In conclusion, the equine IVD had a grossly and histologically discernible proteoglycan-rich NP and a lamellar collagenous AF, which is similar to the situation in humans and dogs. The morphological changes associated with equine IVDD are largely similar to those found in humans and dogs. A grading scheme for equine IVDD, based on a generally accepted human scheme, was developed, which proved useful, as reflected in high k values for intra- and interobserver reliability. IVDD, as evaluated by the use of this grading scheme, was associated with increasing age, confirming the biological credibility of the scheme. IVDD was most prevalent in the caudal cervical spine (C5–T1). In horses, subchondral bone changes were not correlated with IVDD and therefore should be graded separately, in contrast to the case in humans and dogs. We suggest using this grading scheme in further research into the pathogenesis of equine IVDD, possible breed-related differences, its effect on the vertebral column, and its relevance for the development of neurological conditions arising from diseases of the spinal column in horses.

References

1. Adams MA, Roughley PJ. What is intervertebral disc degeneration, and what causes it? *Spine*. 2006;31(18):2151-2161.
2. Bergknut N, Egenvall A, Hagman R, et al. Incidence of intervertebral disk degeneration-related diseases and associated mortality rates in dogs. *J Am Vet Med Assoc*. 2012;240(11):1300-1309.
3. Bergknut N, Grinwis G, Pickee E, et al. Reliability of macroscopic grading of intervertebral disk degeneration in dogs by use of the Thompson system and comparison with low-field magnetic resonance imaging findings. *Am J Vet Res*. 2011;72(7):899-904.
4. Bergknut N, Meij BP, Hagman R, et al. Intervertebral disc disease in dogs - Part 1: A new histological grading scheme for classification of intervertebral disc degeneration in dogs. *Vet J*. 2013;195(2):156-163.
5. Bergknut N, Rutges JPHJ, Kranenburg H-C, et al. The dog as an animal model for intervertebral disc degeneration?. *Spine*. 2012;37(5):351-358.
6. Bergknut N, Smolders LA, Grinwis GC, et al. Intervertebral disc degeneration in the dog. Part 1: Anatomy and physiology of the intervertebral disc and characteristics of intervertebral disc degeneration. *Vet J*. 2013;195(3):282-291.
7. Bollwein A, Hänichen T. Age-related changes in the intervertebral disks of the cervical vertebrae of the horse. *Tierärztl Prax*. 1989;17(1):73-76.
8. Boos N, Weissbach S, Rohrbach H, et al. Classification of age-related changes in lumbar intervertebral discs: 2002 Volvo award in basic science. *Spine*. 2002;27(23):2631-2644.
9. Cherrone KL, Dewey CW, Coastes JR, et al. A retrospective comparison of cervical intervertebral disk disease in nonchondrodystrophic large dogs versus small dogs. *J Am Anim Hosp Assoc*. 2004;40(4):316-320.
10. Clayton HM, Kaiser LJ, Lavagnino M, et al. Dynamic mobilisations in cervical flexion: effects on intervertebral angulations. *Equine Vet J*. 2010;42(suppl):688-694.
11. Down SS, Henson FMD. Radiographic retrospective study of the caudal cervical articular process joints in the horse. *Equine Vet J*. 2009;41(6):518-524.
12. Dyson SJ. Lesions of the equine neck resulting in lameness or poor performance. *Vet Clin North Am Equine Pract*. 2011;27(3):417-437.

13. Faber M, Johnston C, Schamhardt H, et al. Basic three-dimensional kinematics of the vertebral column of horses trotting on a treadmill. *Am J Vet Res.* 2001;62(5):757-764.
14. Faber M, Johnston C, Schamhardt HC, et al. Three-dimensional kinematics of the equine spine during canter. *Equine Vet J Suppl.* 2001;33(suppl):145-149.
15. Foss RR, Genetzky RM, Riedesel EA, et al. Cervical intervertebral disc protrusion in two horses. *Can Vet J.* 1983;24:188-191.
16. Fuentealba IC, Weeks BR, Martin MT, et al. Spinal cord ischemic necrosis due to fibrocartilaginous embolism in a horse. *J Vet Diag Invest.* 1991;3(2):176-179.
17. Furr MO, Anver M, Wise M. Intervertebral disk prolapse and diskospondylitis in a horse. *J Am Vet Med Assoc.* 1991;198(12):2095-2096.
18. Gruber HE, Ingram J, Hanley Jr. EN. An improved staining method for intervertebral disc tissue. *Biotech Histochem.* 2002;77(2):81-83.
19. Hadjipavlou AG, Tzermiadianos MN, Bogduk N, et al. The pathophysiology of disc degeneration: a critical review. *J Bone Joint Surg - Series B.* 2008;90(10):1261-1270.
20. Hansen HJ. A pathologic-anatomical study on disc degeneration in dog, with special reference to the so-called enchondrosis intervertebralis. *Acta Orthop Scand.* 1952;11(suppl):1-117.
21. Haussler KK, Bertram JE, Gellman K, et al. Segmental in vivo vertebral kinematics at the walk, trot and canter: a preliminary study. *Equine Vet J.* 2001;33 (suppl):160-164.
22. Ho-Pham LT, Lai TQ, Mai LD, et al. Prevalence and pattern of radiographic intervertebral disc degeneration in Vietnamese: a population-based study. *Calcif Tissue Int.* 2015;96(6):510-517.
23. Ikegawa S. The genetics of common degenerative skeletal disorders: osteoarthritis and degenerative disc disease. *Annu Rev Genomics Hum Genet.* 2013;14:245-256.
24. Jansson N. What is your diagnosis? Multiple cervical intervertebral disk prolapses. *J Am Vet Med Assoc.* 2001;219(12):1681-1682.
25. Jeffcott LB. Disorders of the thoracolumbar spine of the horse--a survey of 443 cases. *Equine Vet J.* 1980;12(4):197-210.
26. Jeffcott LB, Dalin G. Natural rigidity of the horse's backbone. *Equine Vet J.* 1980;12(3):101-108.

27. Landis JR, Koch GG. The measurement of observer agreement for categorical data. *Biometrics*. 1977;33(1):159-174.
28. Levine JM, Adam E, MacKay RJ, et al. Confirmed and presumptive cervical vertebral compressive myelopathy in older horses: A retrospective study (1992-2004). *J Vet Int Med*. 2007;21(4):812-819.
29. McLnerney J, Ball PA. The pathophysiology of thoracic disc disease. *Neurosurg Focus* 2000;9(4).
30. McKelvey WAC, Owen RR. Acquired torticollis in eleven horses. *J Am Vet Med Assoc*. 1979;175(3):295-297.
31. Meij BP, Bergknut N. Degenerative lumbosacral stenosis in dogs. *Vet Clin North Am Small Anim Pract*. 2010;40(5):983-1009.
32. Nappert G, Vrins A, Breton L, et al. A retrospective study of nineteen ataxic horses. *Can Vet J*. 1989;30(10):802-806.
33. Nixon AJ, Stashak TS, Ingram JT, Norrdin RW, Park RD. cervical intervertebral disk protrusion in a horse. *Vet Surg*. 1984:154-158.
34. Pagger H, Schmidburg I, Peham C, et al. Determination of the stiffness of the equine cervical spine. *Vet J* 2010;186(3):338-341.
35. Powers BE, Stashak TS, Nixon AJ, et al. Pathology of the vertebral column of horses with cervical static stenosis. *Vet Pathol*. 1986;23(4):392-399.
36. Rooney JR. The horse's back: biomechanics of lameness. *Vet Clin: Equine Pract*. 1982;4(2):17-27.
37. Rutges JPHJ, Duit RA, Kummer JA, et al. A validated new histological classification for intervertebral disc degeneration. *Osteoarthr Cartil*. 2013;21(12):2039-2047.
38. Sebastian MM, Giles RC. Fibrocartilaginous embolic myelopathy in a horse. *J Vet Med Series A*2004;51(7-8):341-343.
39. Seiler GS, Häni H, Busato AR, et al. Facet joint geometry and intervertebral disk degeneration in the L6-S1 region of the vertebral column in German shepherd dogs. *Am J Vet Res*. 2002;63(1):86-90.
40. Sharp NIH, Wheeler SJ, Cofone M. Radiological evaluation of 'wobbler' syndrome -caudal cervical spondylomyelopathy. *J Small Ani Pract*. 1992;33(10):491.

41. Sleutjens J, Voorhout G, Van Der Kolk JH, et al. The effect of ex vivo flexion and extension on intervertebral foramina dimensions in the equine cervical spine. *Equine Vet J Suppl.* 2010;(38):425-30. doi(38):425-430.
42. Smit TH. The use of a quadruped as an in vivo model for the study of the spine - biomechanical considerations. *Europ Spine J.* 2002;11(2):137-144.
43. Smolders LA, Bergknut N, Grinwis GCM, et al. Intervertebral disc degeneration in the dog. Part 2: chondrodystrophic and non-chondrodystrophic breeds. *Vet J* 2013;195(3):292-299.
44. Speltz MC, Olson EJ, Hunt LM, et al. Equine intervertebral disk disease: a case report. *J Equine Vet Sci.* 2006;26(9):413-419.
45. Stadler P, van den Berg SS, Tustin RC. Cervical intervertebral disk prolapse in a horse. *J S Afr Vet Assoc.* 1988;59(1):31-32.
46. Taher F, Essig D, Lebl DR, et al. Lumbar degenerative disc disease: current and future concepts of diagnosis and management. *Adv Orthop.* 2012;2012:970752.
47. Takeuchi T, Abumi K, Shono Y, et al. Biomechanical role of the intervertebral disc and costovertebral joint in stability of the thoracic spine: a canine model study. *Spine.* 1999;24(14):1414-1420.
48. Taylor HW, Vandeveld M, Firth EC. Ischemic myelopathy caused by fibrocartilaginous emboli in a horse. *Vet Pathol.* 1977;14(5):479-481.
49. Teraguchi M, Yoshimura N, Hashizume H, et al. Prevalence and distribution of intervertebral disc degeneration over the entire spine in a population-based cohort: the Wakayama spine study. *Osteoarthr Cartil.* 2014;22(1):104-110.
50. Thompson JP, Pearce RH, Ho B. Correlation of gross morphology and chemical composition with magnetic resonance images of human lumbar intervertebral discs. *Transactions Ann Meeting Orthopaed Res Soc.* 1988(13):276.
51. Thompson JP, Pearce RH, Schechter MT, et al. Preliminary evaluation of a scheme for grading the gross morphology of the human intervertebral disc. *Spine.* 1990;15(5):411-415.
52. Townsend HG, Leach DH. Relationship between intervertebral joint morphology and mobility in the equine thoracolumbar spine. *Equine Vet J.* 1984;16(5):461-465.
53. Townsend HG, Leach DH, Doige CE, et al. Relationship between spinal biomechanics and pathological changes in the equine thoracolumbar spine. *Equine Vet J.* 1986;18(2):107-112.

54. Urban JPG, Roberts S. Degeneration of the intervertebral disc. *Arthritis Res Ther.* 2003;5(3):120-130.
55. Walling BE, Stewart MC, Valli VE. Pathology in practice. *J Am Vet Med Assoc.* 2011;239(2):199-201.
56. Whitwell KE. Causes of ataxia in horses. *Pract Equine Pathol.* 1980;2(4):17-25.
57. Wijnberg D, Bergmann W, Veraa S. Neurological neck problems, diagnostics and prognosis in the horse. *Prakt Tierarzt.* 2015;96(2):150-158.
58. Yovich JV, Powers BE, Stashak TS. Morphologic features of the cervical intervertebral disks and adjacent vertebral bodies of horses. *Am J Vet Res.* 1985;46(11):2372-2377.

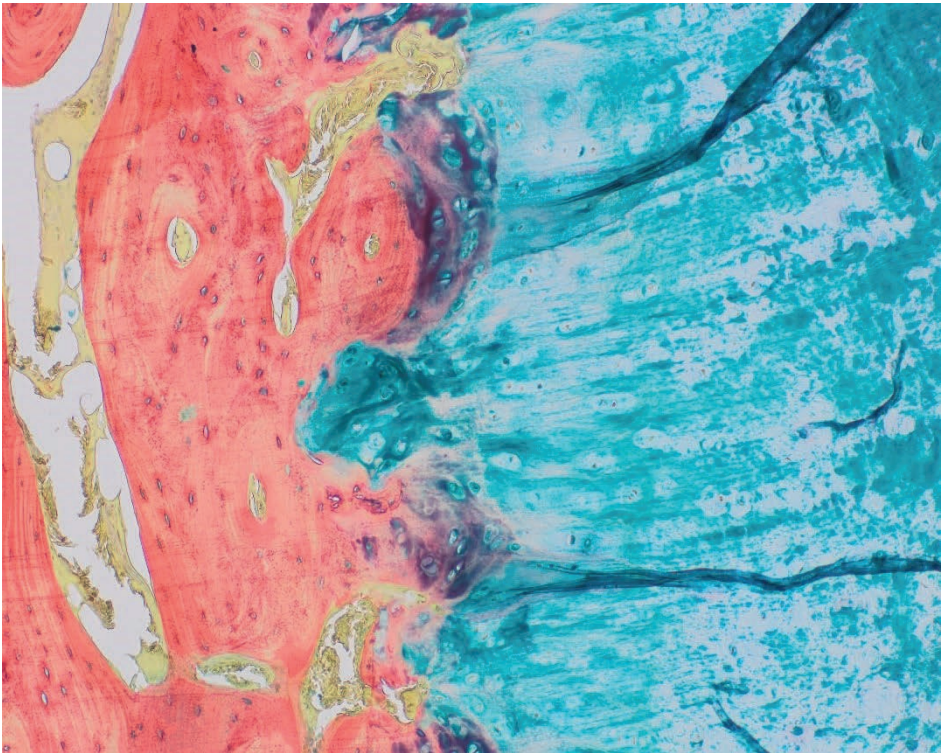
Supplemental Table S1 Signalment of the Warmblood Horses in this study.

Case	Breed	Age	Sex	Number of cranio-cervical IVDs (C2-C5)	Number of caudo-cervical IVDs (C5-T1)	Number of cranio-thoracic IVDs (T1-T2)	Number of mid-thoracic IVDs (T11-T12)	Number of lumbo-sacral IVDs (L4-S1)
1	RDSH	8 months	Stallion	3	3	1	2	2
2	RDSH	9 months	Stallion	2	3	1	2	2
3	RDSH	11 months	Mare	2	3	1	2	0
4	Zangersheide	1 year	Stallion	3	3	0	2	2
5	RDSH	1 year	Mare	3	3	1	2	2
6	Trakehner	2 years	Stallion	1	1	1	2	1
7	RDSH	2 years	Stallion	3	3	1	2	2
8	RDSH	2 years	Stallion	3	3	1	2	2
9	RDSH	3 years	Mare	3	3	1	2	2
10	Holsteiner	4 years	Gelding	3	3	0	2	0
11	RDSH	5 years	Mare	2	3	0	1	1
12	RDSH	5 years	Mare	3	3	1	2	2
13	RDSH	6 years	Gelding	3	1	0	0	2
14	RDSH	6 years	Gelding	3	3	1	2	2
15	RDSH	7 years	Mare	3	3	1	2	2
16	RDSH	7 years	Gelding	3	3	1	0	0
17	RDSH	10 years	Mare	3	3	1	2	1
18	RDSH	10 years	Mare	3	2	0	2	2
19	RDSH	11 years	Gelding	3	2	1	0	0
20	RDSH	11 years	Gelding	3	3	1	2	2
21	RDSH	11 years	Gelding	3	3	1	2	2
22	Westfaler	12 years	Mare	1	1	0	2	1
23	RDSH	12 years	Gelding	1	2	0	2	2
24	RDSH	12 years	Gelding	3	3	1	2	2
25	Zangersheide	12 years	Mare	3	2	1	2	2
26	RDSH	15 years	Gelding	3	3	1	2	2
27	RDSH	15 years	Mare	1	1	0	2	1

28	RDSH	15 years	Mare	0	1	0	1	2
29	RDSH	16 years	Mare	3	3	1	2	0
30	RDSH	18 years	Mare	1	1	0	0	0
31	RDSH	18 years	Mare	3	3	0	2	2
32	RDSH	18 years	Gelding	3	3	1	2	1
33	RDSH	21 years	Gelding	1	0	0	2	2

RDSH=Royal Dutch Sport Horse

IVD= intervertebral disc



Intervertebral disc
degeneration in
warmblood horses:
histological and
biochemical
characterization

5

Published in: Veterinary Pathology.
2022;59(2):284-298

W. Bergmann
C. van de Lest
S. Plomp
H Vernooij
I. D. Wijnberg
W. Back
A. Gröne
M. Delany
N. Caliskan
M. Tryfonidou
G. Grinwis

5

Abstract

Gross morphology of healthy and degenerated intervertebral discs (IVDs) is largely similar in horses as in dogs and humans. For further comparison, the biochemical composition and the histological and biochemical changes with age and degeneration were analysed in 41 warmblood horses. From 33 horses, 139 discs and 2 foetal vertebral columns were evaluated and scored histologically. From 13 horses, 73 IVDs were assessed for hydration, DNA, glycosaminoglycans, total collagen, hydroxyl-lysyl-pyridinoline, hydroxylysine, and advanced glycation end-product (AGE) content. From 7 horses, 20 discs were assessed for aggrecan, fibronectin, and collagen type 1 and 2 content. Histologically, tearing of the nucleus pulposus (NP) and cervical annulus fibrosus (AF), and total histological score (tearing and vascular proliferation of the AF, and chondroid metaplasia, chondrocyte like cell proliferation, presence of notochordal cells, matrix staining, and tearing of the NP) correlated with gross degeneration. Notochordal cells were not seen in IVDs of horses. Age and gross degeneration were positively correlated with AGEs and a fibrotic phenotype, explaining gross degenerative changes. In contrast to dogs and humans, there was no consistent difference in glycosaminoglycan content and hydration between AF and NP, nor decrease of these variables with age or degeneration. Hydroxylysine decrease and collagen 1 and AGEs increase were most prominent in the NP, suggesting degeneration started in the NP. In caudal cervical NPs, AGE deposition was significantly increased in grossly normal IVDs and total collagen significantly increased with age, suggesting increased biomechanical stress and likelihood for spinal disease in this part of the vertebral column.

Introduction

Neurological signs originating from the neck are common in the horse.⁶² The most common non-infectious, non-traumatic cause is cervical vertebral myelopathy.^{33, 37} In this syndrome, neurological signs are caused by compression of the spinal cord and spinal nerves in which vertebral instability and enlargement of the articular process joints and thickening of the vertebral dorsal laminae and ligamentum flavum are important factors.^{16, 35, 41} However, a link between cervical vertebral myelopathy and intervertebral disc degeneration (IVDD) has not been definitively established. This study aims to assess IVDD in horses, as a basis for considering its possible role in cervical vertebral myelopathy in horses. Cervical neurological signs due to compression of nervous tissue have also been commonly described in dogs and humans, and in these species IVDD and subsequent disc disease is one of the main underlying lesions.^{6, 30} Degeneration of the canine and human intervertebral disc (IVD) is characterized by changes of the cellular composition and the extracellular matrix of the nucleus pulposus (NP), annulus fibrosus (AF), transition zone, and end plate.^{7, 9} On a cellular level, disc maturation in humans and degeneration in dogs and humans is characterized by replacement of physaliferous notochordal cells in the NP and fibroblasts in the AF by smaller, non-vacuolated chondrocyte-like cells with corresponding matrix deposition^{12, 26} (chondroid metaplasia), and in the AF by subsequent disorganization of the collagenous lamellae.^{7, 9, 12, 46}

In both canine and human NPs, the most characteristic biochemical finding associated with degeneration is loss of proteoglycans and their attached sulphated glycosaminoglycans (GAGs) with subsequent dehydration of the NP.^{1, 2, 8} A second important biochemical change seen in dogs and humans is the development of a fibrotic matrix, which is characterized by an increase in the total amount of collagen in the NP and the AF^{1, 9} and a decrease in the amount of type 2 collagen in the NP with a simultaneous increase of type 1 collagen.^{4, 7, 9, 66} Furthermore, fibronectin, which is implicated in fibrosis,⁵⁷ increases in the degenerated NP in dogs and in the degenerated AF and NP in humans.^{17, 38, 66}

Collagen cross-links, such as hydroxyl-lysyl-pyridinoline (HP), are vital for the biomechanical properties of the extracellular matrix including that of the IVD.^{20, 29, 63} Hydroxylysine is important for the formation of these cross-links and is formed post translationally by hydroxylation of the amino acid

lysine.¹⁴ Furthermore, hydroxylysine may undergo posttranslational enzymatic O-glycosylation. Although the exact function of these attachments of sugar groups is yet unknown, recent literature suggests that the extent and pattern of glycosylation of hydroxylysine may regulate cross-link maturation in collagen and therefore modulate its properties.^{14, 53, 56}

In equine and in human IVDD, yellow discoloration of the disc is a prominent gross finding.^{1, 10} A likely cause for this change in colour is increased nonenzymatic glycation of proteins leading to the formation of advanced glycation end-products (AGEs). AGEs form abnormal collagen cross-links resulting in structural tissue modifications with subsequent changes in the biomechanical properties of the disc.^{1, 3, 20, 63}

Ultimately, these cellular and biochemical changes can lead to structural and functional failure of the IVD, resulting in subsequent failure to limit spinal movement and an inability to resist compression. This can further affect other parts of the spinal unit such as the articular process joints.^{1, 4, 9}

Cervical IVDD is common in warmblood horses and grossly comparable to dogs and humans.¹⁰ Herniation or protrusion of the IVD are considered rare in horses,^{11, 52} and systematic studies on the relation with clinical signs are missing. Clinical signs due to functional failure of the degenerated IVD and subsequent pathological changes of other parts of the spinal unit seem likely and might be underreported or under diagnosed.

The overall objectives of this study were to investigate the association of cellular and biochemical changes of the equine IVD with age and degeneration. For this, a histological scoring scheme for degenerative changes was developed in which also the presence of notochordal cells was included. Furthermore, the biochemical changes associated with age and IVDD in dogs and humans (changes in hydration, GAG, aggrecan, and collagen content) were examined in horses. Additionally, changes of the quality of collagen with age and degeneration were investigated by evaluation of hydroxylysine and HP content and degree of nonenzymatic glycation by quantifying the AGE biomarker pentosidine.^{47, 48} It was hypothesized that the cellular and biochemical changes in equine IVD are similar to those of dogs and humans.

Materials and Methods

Horses

Vertebral columns of 41 warmblood horses, including 2 fetuses (approximately 45 days and 61 days of gestation²⁴), were harvested post-mortem (Supplemental Table S1). Of these, 38 privately owned horses were referred for necropsy, with the owner's informed consent, to the Division of Pathology, Faculty of Veterinary Medicine, Utrecht University. These horses had either died unexpectedly or were humanly euthanized for reasons unrelated to the current study. The foetal IVDs were derived from a pregnant mare undergoing necropsy and from an aborted foetus from an unrelated reproduction study (approved by the university's Animal Experimentation Committee [permission number 2007.III.02.036]). Finally, one experimental horse was included, which was owned by the Division of Equine Sciences of Utrecht University and used for teaching purposes, which included obtaining surgical skills with subsequent euthanasia (permission number 2013.III.01.012). The age ranged from approximately 45 days gestation up to 21 years with a mean age of 7.0 ± 7.4 years. The horses were of different breeds (38 Royal Dutch Sport horses, 2 Zangersheide horses, 1 Holsteiner) and sex (19 mares, 8 stallions, 11 geldings, and 3 of unknown sex). The IVDs of horses of 8 months and older ($n = 26$), were examined in a previous study concerning macroscopic grading and distribution of equine IVDD along 4 different regions of the spine.¹⁰ These regions were the cranial cervical region from cervical vertebrae (C)2–C5, the caudal cervical region from C5 to thoracic (T)1, T11–T13, and the lumbosacral region L4–S1.

To meet the desired minimum number of 10 IVDs per gross grade for biochemical evaluation, 2 T1–T2 IVDs with gross grade 5 were also collected. These vertebral regions were dissected, sectioned mid-sagittally, photographed, and macroscopically graded as described.¹⁰ In this previously developed 5-point grading scheme, grades 1 and 2 were considered normal, grade 3 a transitional grade, and grades 4 and 5 severely degenerated.

Histological Preparation

Of a subgroup of 33 horses (Supplemental Table S1), 139 IVDs and 2 complete foetal vertebral columns were evaluated histologically .IVDs

containing the NP, AF, cartilaginous endplate, and subchondral bone of 9 months gestation and older horses were cut into 0.5-cm-thick slices using a band saw, fixed in 10% (v/v) neutral buffered formalin, and decalcified for about 9 months in 10% (w/v) ethylenediaminetetraacetic acid with a pH of 7, before routine processing and staining with haematoxylin/eosin and with Alcian blue/picrosirius red for optimal detection of both collagen and proteoglycan-containing matrix

Validation of the Histologic Scoring Scheme

After initial histological evaluation of the IVDs, it was strongly suspected that certain histological differences were age-dependent, and a provisional histologic scoring scheme for equine IVDD was devised (Supplemental Table S2) that was largely based on the validated scoring scheme for the dog.⁷ For validation of this histological scoring scheme, 10 IVDs with each macroscopic grade for degeneration (1 to 5) were selected. This total of 50 IVDs were assigned a random number using an online randomization program and subsequently scored blindly twice by 3 independent observers with a time lapse of at least a week between scoring sessions for each observer.

Notochordal Cells

To evaluate the presence of notochordal cells, the vertebral columns of the 2 fetuses and 1 adult horse (11 years old) were immunolabeled for cytokeratin^{18, 45}. The positive controls were an IVD of a non-chondrodystrophic dog with notochordal cells in the NP, and kidneys of an adult horse and the fetus of 45 days gestation.^{43, 45} After deparaffinization and rehydration of the sections, antigen retrieval was achieved by incubating with citrate buffer (Dako Target Retrieval Solution, Dako) of pH 6 at 97 °C with Dako PT-link (Dako) for 20 minutes. To prevent nonspecific binding, peroxidase blocking solution (Dako) and 10% normal goat serum were added for 5 minutes and 15 minutes, respectively, at room temperature (RT). Thereafter, the slides were incubated with the primary antibody for cytokeratin18 (0.5 µg/mL, monoclonal, goat anti-mouse, Abcam [C-04] ab668, lot: GR3196069-6) in normal antibody diluent (Bright Diluent Green, VWR; 60 minutes, RT). Then, the sections were incubated with the secondary antibody (Brightvision Goat Anti-Mouse/Rabbit, VWR; 30 minutes, RT), and subsequently with AEC (Agilent; 20 minutes, RT). Nuclei were counterstained with haematoxylin for 20 seconds at RT.

Biochemical analyses were performed on a subgroup of 13 horses (Supplemental Table S1) with a total of 73 IVDs that were collected within 24 hours after death, including 22 IVDs with grade 1 for gross degeneration, 30 with grade 2, 11 with grade 3, 1 with grade 4, and 9 with grade 5. The IVDs with grades 4 and 5 were combined to form a group of 10 severely degenerated discs. The distribution of the grades along the different examined spinal regions is shown in Supplemental Table S3. IVDs with grades 4 and 5 for gross degeneration were only found in the caudal cervical and cranial thoracic regions (C5–T2). These 2 regions did not contain any IVDs with grade 3 for gross degeneration. Biochemical evaluation was done for all examined IVDs combined (all IVDs from all researched vertebral regions), but also for the different regions separately, except for region T1–T2 from which only 2 IVDs were sampled. Within 24 hours after death, IVDs were photographed during necropsy and a sagittal full-thickness, 0.5-cm-thick section was prepared including the AF, transition zone, and the NP. This section was cut into 6 equally sized pieces representing the AF (areas A1 and A2), the NP (areas C1 and C2), and the transitional zone between AF and NP (areas B1 and B2; Figure. 1). Subsequently, these pieces of tissue were snap frozen in liquid nitrogen and stored at –80 °C until further analysis. Each of the samples of the IVD were further randomly cut into 4 equal portions, put into microcentrifuge safe-lock tubes (Eppendorf), and wet weights were measured with a high-resolution analytical balance scale (Mettler Toledo AB). Dry weights were determined after overnight lyophilization by using a SpeedVac Vacuum Concentrator (Thermo-Fisher). Two of the 4 portions of each sample were used for further biochemical analysis. Because there was no statistically significant difference in hydration between the AF and NP, nor a statistically significant correlation with hydration and age or degeneration, the DNA, GAG, and total collagen content are expressed in milligrams (DNA, GAG) or grams (total collagen) per gram wet weight.

Two samples of AF and NP per IVD were digested with papain as described before.⁵⁹ To determine the cellularity of the tissue, DNA content was determined by fluorometric quantitation with a Quant-iT dsDNA Broad-Range assay kit in combination with Qubit (Invitrogen) according to the manufacturer's protocol. Subsequently, a modified 1.9-dimethylmethylene blue assay was performed to establish the GAG content.¹⁹ Both DNA and GAG content are expressed as mg/g wet weight.

After papain digestion, 2 samples of AF and NP per IVD were hydrolysed in a 6 M hydrochloric acid solution in milliQ water (Millipore). Subsequently, the hydroxyproline (to determine the collagen content), hydroxylysine, HP, and pentosidine contents were quantified by high-performance liquid chromatography mass spectrometry (HPLC/MS) as described previously.⁵¹ Only samples with a minimal recovery of 30% were included in further analysis. Total collagen content is expressed as g/g wet weight. Hydroxylysine is expressed as percentage of total lysine. HP and pentosidine are expressed as mole per mole of collagen.

Of the IVDs used for biochemical analysis, 20 cervical IVDs of 7 horses (mean age 16 ± 1 years, all Royal Dutch Sport horses, 4 mares, 3 geldings) were used to determine the difference in the amount of aggrecan, collagen type 1 α 1 and type 1 α 2, collagen type 2 α 1, and fibronectin between normal IVDs (1 IVD with grade 1, 9 IVDs with grade 2) and severely degenerated discs (1 IVD with grade 4, 9 IVDs with grade 5). From these samples, 40- μ m cryosections were collected on glass slides and dried. The tissue sections were washed twice in 0.1 M HCl and further processed as described.²⁸ The identified peptides are expressed as percentage of the total signal.

Statistical Analysis

To validate the histological scoring system, pairwise interobserver and intra-observer reliabilities were calculated for each individual variable with a Cohen's weighted κ analysis with quadratic weights of 1, 0.9375, 0.75, 0.4375, and 0. A κ -value of less than 0.00 is considered poor, a value between 0.00 and 0.20 as slight, between 0.21 and 0.40 as fair, between 0.41 and 0.60 as moderate, between 0.61 and 0.80 as substantial, and a value between 0.81 and 1.00 as almost perfect.³² Also, the percentages of intra-observer and interobserver agreement per variable were calculated.

If the reliability of the histological scoring was considered sufficient (weighted κ values of fair or higher or observer agreement percentages of ≥ 80), the correlation between the individual histological variable and the macroscopic grade (1 to 5) and normal (grades 1 and 2) versus severely degenerated (grades 4 and 5) was determined. For this the 3 different scores obtained during the second round of scoring were averaged and a Pearson correlation test was performed. The strength of the correlation r was considered very weak (0.00–0.19), weak (0.20–0.39), moderate (0.40–0.59), strong (0.60–0.79), or very strong (0.80–1.00).¹⁸ Correlation of the total

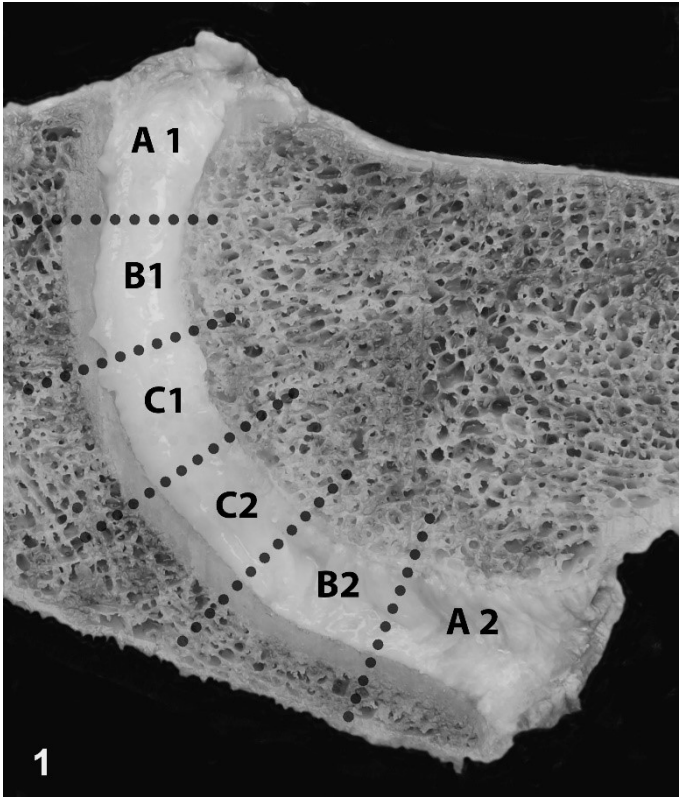


Figure 1. Normal intervertebral disc (IVD), C3–C4, horse. Midsagittal vertebral section. For biochemical evaluation, IVDs were cut into 6 equally large pieces representing the annulus fibrosus (areas A1 and A2), the nucleus pulposus (areas C1 and C2), and the transition zone (areas B1 and B2).

histological score of an IVD (determined by the sum of the averaged scores of those variables that could be scored reliably) with degeneration was also determined. Calculations were also performed for the cervical IVDs only ($n = 32$) because IVDD in this part of the vertebral column is most prevalent.¹⁰ Statistical significance was set at $P \leq .05$. Analysis was conducted with SPSS 16.0 (IBM).

The results of the collagen, aggrecan, and fibronectin analyses were further processed using LCMS2 proteomics data analyses in R version 3.4.3 using the package MSGF plus version 1.19.1. The data of all biochemical variables, except for hydration, were not normally distributed. Due to the large number of variables, the initial use of a linear mixed model, which would

take out horse-dependent variation, was not considered executable. Instead, in order to enable descriptive analysis of the data it was decided to first evaluate the composition of the IVDs and correlation of the variables with age and with gross degeneration by using heat maps of Spearman rank correlation coefficients. Heat maps were created for the IVDs of all regions combined, and for IVDs of the cranial cervical (C2–C5), caudal cervical (C5–T1), thoracic (T11–T13), and lumbosacral (L4–S1) regions separately. Furthermore, heat maps were created with only the data of normal discs (to determine the difference in composition of the AF and the NP, and to determine age-related changes), and the results of all grades (to determine degeneration-related differences). Also, separate heat maps were created for the AF and NP separately. Significance was set at $P < .05$. Interpretation of the strength of the correlation was the same as for the Pearson correlation coefficients.¹⁸ Furthermore, 2 linear mixed models were conducted to further investigate the formation of AGEs in the different spinal regions and the caudal cervical region more specifically. Therefore, one mixed model was used to determine regional differences in the initial formation of AGEs that may explain the higher prevalence of IVDD in the caudal cervical spine.¹⁰ For this purpose, the pentosidine content of the normal IVDs (grade 1 and grade 2) in the different regions was examined. By use of the second linear mixed model the pentosidine content in the different grades within this caudal cervical region were assessed. For this, the results of the pentosidine analyses were log-transformed to meet the model assumptions for normality and constant variance. In both models, “horse” was set as random effect and “region” and respectively “grade” as factor variables. Bonferroni correction was used to correct for multiple comparisons. To check for the correctness of the model, residuals were used. All linear mixed model calculations were done for the AF and NP separately. Heat maps and subsequent mixed models were performed in R version 3.4.3 using the *corrplot* and *nlme* packages.^{39, 55}

Results

Histological Changes With Age

The foetal AF was composed of spindle cells with a small amount of cytoplasm, which formed about 20 layers of slightly convex rows. The spindle cells of the AF merged dorsally and ventrally into more loosely arranged

rows of spindle cells belonging to the longitudinal ligaments (Figure. 2). With the Alcian blue/picrosirius red stain, the stroma of the AF was a mixture of blue (mucinous) and slightly red (collagenous) stroma. The foetal NP was composed of more plump spindle cells with a small to moderate amount of eosinophilic cytoplasm, haphazardly embedded in a looser stroma (Figure. 2) that was bright blue in the Alcian blue/picrosirius red stain, compatible with mucinous stroma. No cells with the typical phenotype of notochordal cells as seen in other species (clusters of large cells with cytoplasmic vesicles)^{7, 46} were encountered.

In foals from 9 months gestation up to 13 weeks, the AF was composed of fibrous tissue with few small to medium-sized blood vessels in the peripheral two thirds of the AF. With the Alcian blue/picrosirius red stain, the AF appeared to consist of about 10 concave/convex-oriented lamellae of fibroblasts with intercellular collagen fibres (red) and a small (outer layers) to moderate (inner layers) amount of fibrillar pale blue (mucinous) matrix, which increased in amount with age (Figure. 3). From the age of 6 weeks onward, oval cells in lacunae (chondrocyte-like cells) were embedded in this mucinous matrix material, which partly disrupted the lamellae. The NP of foals of 9 months gestation up to 13 weeks was composed of small spindle to oval chondrocyte-like cells in lacunae embedded in a looser stroma. These cells were either solitary, in small groups, or in horizontal or vertical rows (Figure. 4). Rows were most prominent in the cranial and caudal periphery near the cartilaginous end plate. With the Alcian blue/picrosirius red stain, the cytoplasm of these cells stained blue (proteoglycan-rich) and the stroma consisted of a combination of red (collagenous) and blue fibres. The dominant colour of these fibres varied by IVD and by location within the NP. Cranially and caudally, the NP was flanked by an often irregular cartilaginous endplate composed of 3 to 6 cell rows of chondroid cells. The trabeculae of the vertebral trabecular bone/subchondral bone flanking the cranial side of the IVD were typically thicker than those of the caudal side with resultant smaller bone marrow spaces.

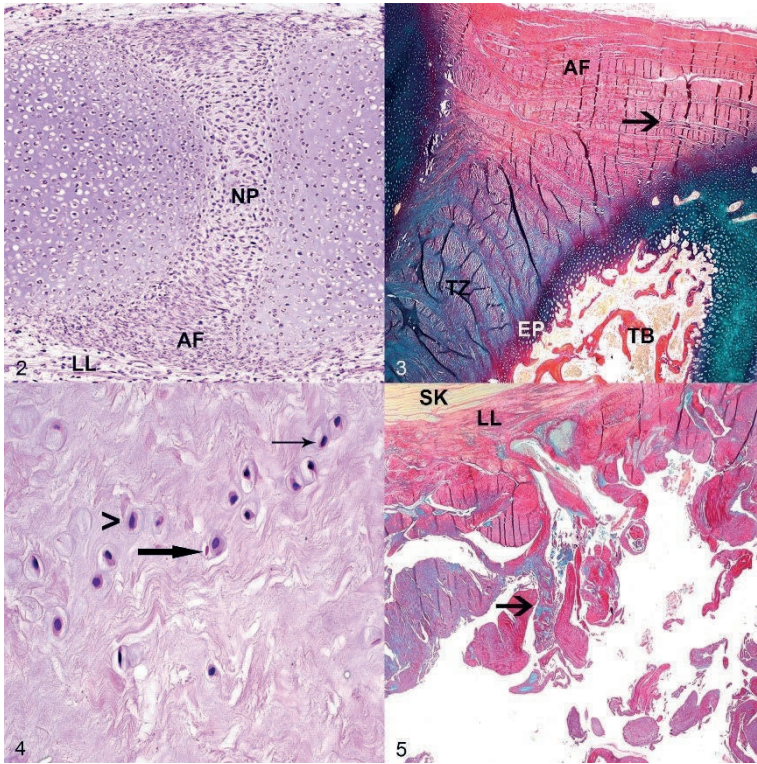
In 8- to 11-month-old foals, the lamellae of the normal fibroblast-rich AF were increasingly disorganized due to the presence of mucinous extracellular matrix material containing chondrocyte-like cells, with partial effacement of the inner lamellae closest to the NP. In the NP of these foals, more oval than spindle chondrocyte-like cells were present. Occasionally, 2 cells were clustered together. With Alcian blue/picrosirius red stain, the NP stroma was a combination of red and blue fibres without a clear dominant

colour suggesting an equal distribution of proteoglycans and collagen in the stroma. Increasing numbers of chondrocyte-like cells with a pyknotic nucleus and hyper eosinophilic cytoplasm were visible, without the presence of an inflammatory reaction (consistent with apoptosis; Figure. 4).

In 1- to 21-year-old horses, the lamellae of the AF were moderately to extensively disorganized up to the longitudinal ligament, due to the presence of chondrocyte-like cells embedded in mucinous intercellular matrix with almost complete loss of the inner one third of the lamellar architecture. Often the AF contained few to large numbers of tears with well-demarcated yet irregular borders (Figure. 5), and occasionally the AF was completely ruptured. In these 1- to 21-year-old horses, the NP contained almost exclusively oval (rather than spindle-shaped) chondrocyte-like cells. Within the NP, occasional clones of 3 to 10 chondrocyte like cells were formed (Figure. 6). Apoptotic chondrocyte-like cells were commonly present, and cell-poor areas became more common with increasing age. With Alcian blue/picrosirius red stain, the stroma of the NP consisted of a combination of red and blue fibres with blue often being the dominant colour, suggesting the presence of a more proteoglycan-rich matrix. Infrequently, the NP showed irregular yet well-demarcated tears (Figure. 7). Occasionally, the end plate was disrupted with herniation of NP material into the vertebral subchondral bone (Schmorl nodule; Figure. 8). Also, with increasing age, the vertebral subchondral bone flanking the cranial border of the cartilaginous endplate of the IVD was commonly composed of a rim of compact instead of trabecular bone (Figure. 9). The vertebral bone flanking the caudal border of the IVD also had increasing occurrence of a rim of compact bone, although this started at a later age.

Validation of the Histological Scoring Scheme

All tissue sections were evaluated and scored histopathologically (Supplemental Table S2) and the percentages and weighted kappa coefficients of the interobserver and intra-observer reliabilities and agreements of the histological variables were determined (Table 1, IVDs of all regions; Table 2, cervical IVDs). Many of the variables showed only limited variation, including morphology of the lamellae of the AF, chondroid metaplasia of the AF, presence of vascular proliferation in the AF, chondroid metaplasia of the NP, cellularity of the NP, presence of notochordal cells in the NP, and subchondral bone sclerosis (Supplemental Table S4).



Figures 2-5. Histological features of the equine intervertebral disc
 Figure 2 Normal intervertebral disc (IVD), equine foetus of 45 days gestation. The annulus fibrosus (AF) is composed of spindle cells, which form slightly convex rows. The nucleus pulposus (NP) is composed of plumper

spindle cells haphazardly embedded in a looser stroma. No cells of notochordal cell phenotype are visible. LL, longitudinal ligament. Haematoxylin and eosin (HE).

Figure 3. Normal IVD, T1-T2, 6-week-old horse. The AF is composed of ~10 collagenous lamellae separated by a small amount of mucinous material in some areas (arrow). Alcian blue/picrosirius. TZ, transition zone; EP, end plate; TB, trabecular bone.

Figure 4. Normal NP, IVD C7-T1, 6-week-old horse. The NP is composed of small spindle to oval chondrocyte-like cells in lacunae within a loose stroma (parameter C, score 1, and parameter E, score 2 [see Table 3]). These cells are either solitary or in rows (thin arrow; parameter D, score 1). Apoptotic chondrocyte-like cells with a pyknotic nucleus and hyper-eosinophilic cytoplasm are occasionally visible (thick arrow), without the presence of an inflammatory reaction. No tears or clefts are visible (parameter G, score 0). A viable chondrocyte-like cell is shown (>). HE.

Figure 5. IVD degeneration, C6-C7, horse. Within the severely degenerated AF, the lamellae are torn to the level of the longitudinal ligament (parameter A, score 4) and are interspersed with mucinous material (arrow) with almost complete effacement of the lamellae. SK, skeletal muscle; LL, longitudinal ligament. Alcian blue/picrosirius red.

When including IVDs of all regions in the validation of the scoring scheme, 6 variables could be scored reliably: the presence of vascular proliferation in the AF, chondroid metaplasia of the NP, chondrocyte-like cell proliferation of the NP, presence of notochordal cells, matrix staining of the NP, and tears and cleft formation of the NP. The histological score of these 6 variables combined (i.e., the total histological score) was weakly correlated with gross degeneration when taking all gross grades into account, and was moderately correlated when comparing normal IVDs to severely degenerated discs. Of these variables separately, only the presence of tears and clefts in the NP was statistically significantly, but weakly correlated with gross degeneration when comparing normal IVDs (grades 1 and 2) to severely degenerated discs (grades 4 and 5).

The other variables (morphology of the AF, chondroid metaplasia of the AF, tearing of the AF, cellularity of the NP, endplate morphology, subchondral bone sclerosis) could not be scored reliably as revealed by a low percentage for interobserver and/or intra-observer agreement and a low weighted κ interobserver and/or intra-observer agreement coefficient.

When including only the cervical IVDs in the validation of the scoring scheme, tears and clefts of the AF could also be scored reliably but chondrocyte-like cell proliferation of the NP could not. The total score of these 6 histological variables that could be scored reliably in the cervical discs was moderately correlated with gross degeneration.

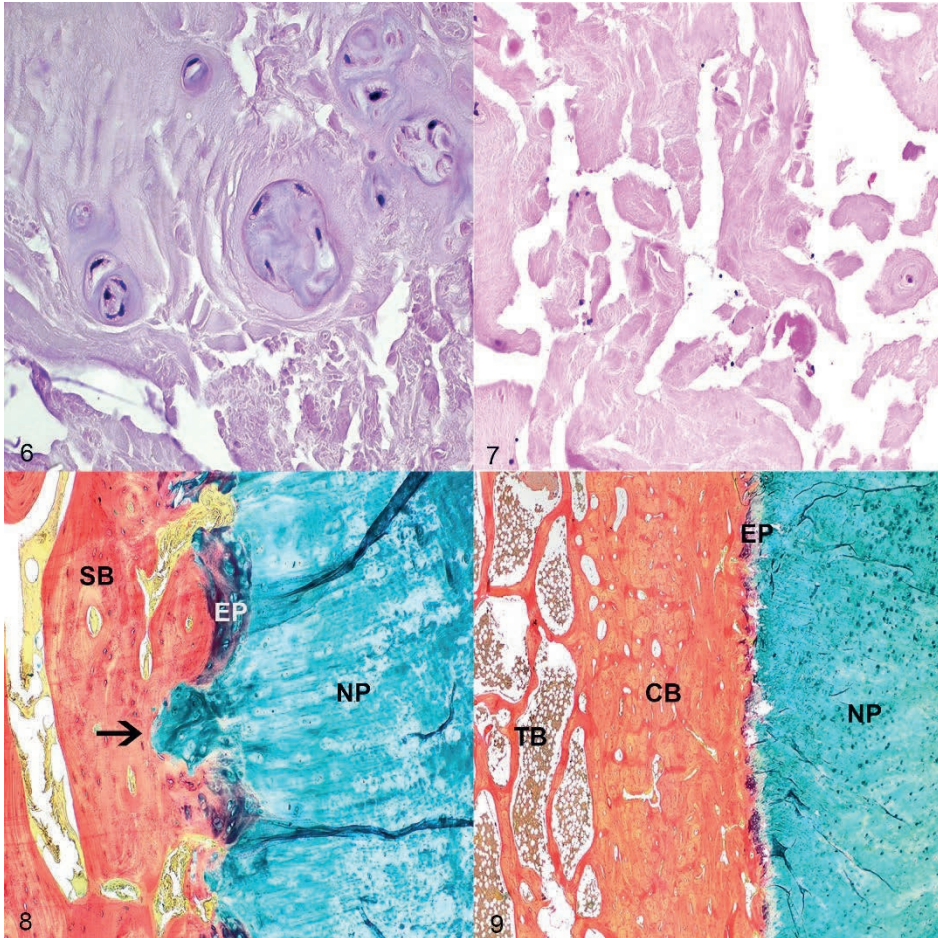
Of the separate variables, tears and clefts of the AF when including all gross grades, and tears and clefts of both the AF and NP when comparing normal discs to severely degenerated discs, were moderately to strongly correlated with gross degeneration.

These observations taken together formed the basis of a histological scoring scheme for equine IVDs which assesses tears and cleft formation and vascular proliferation of the AF, and chondroid metaplasia, proliferation of chondrocyte-like cells, presence of notochordal cells, matrix staining, and tears and cleft formation of the NP (Table 3).

Furthermore, the total histological score is important to histologically assess degeneration of the equine IVD by histology.

Immunohistochemistry

No cells in the foetal or adult IVDs were immunolabeled for cytokeratin 18. However, labelling for cytokeratin 18 was present in the cell membrane of



Figures 6–9. Histological features of equine intervertebral discs

Figure 6 Intervertebral disc (IVD) degeneration, C7–T1, horse. Within the severely degenerated nucleus pulposus (NP), clones of 4 to 6 chondrocyte-like cells form groups (Table 3; parameter C, score 3, parameter D, score 4, parameter E, score 2). The matrix of the NP has intermediate amounts of tears (parameter G, score 2). Haematoxylin and eosin (HE).

Figure 7. IVD degeneration, C7–T1, horse. The severely degenerated NP is cell-poor and has irregular yet well-demarcated tears (parameter G, score 3). HE.

Figure 8. IVD degeneration, C6–C7, horse. The end plate (EP) is disrupted with herniation of chondroid NP tissue into the subchondral bone (SB; Schmorl nodule, arrow). Alcian blue/picosirius red.

Figure 9. IVD degeneration, C7–T1, horse. The subchondral vertebral bone flanking the cranial site of the IVD is composed of a rim of compact bone (CB) instead of trabecular bone (TB). Alcian blue/picosirius red.

notochordal cells (Supplemental Figure.S1) but not the chondrocyte-like cells in the canine control IVD. Renal tubular cells of adult and foetal horses were also immunolabeled for cytokeratin 18 (Supplemental Figure. S2).

Biochemistry

Details on the composition of the normal IVD and the biochemical changes with age and degeneration are depicted in Figures 10 and S3-S8. The most notable, statistically significant biochemical findings are summarized below.

Comparison of normal NP versus normal AF.

The detailed information on the composition of the normal IVD is depicted in Supplemental Figure S3.

The collagen 1 content of the AF was moderately higher than that of the NP. In the NP the GAG content was slightly higher than in the AF. However, there was no difference in aggrecan or collagen type 2 content and hydration between the AF and the NP. The water content of the AF and NP were similar (AF, $69 \pm 12\%$ [mean \pm SD]; NP, $70 \pm 15\%$).

The mean pentosidine content was higher in the caudal cervical NPs than the NPs of the cranial cervical region, and the NPs of both the cranial and the caudal cervical regions had a higher mean pentosidine content than those of the thoracic and the lumbosacral regions (cranial cervical vs caudal cervical: mean 0.32, 95% confidence interval [CI] 0.03–0.61, $P < .05$; thoracic vs cranial cervical: mean 0.30, 95% CI 0.03–0.57, $P < .05$; thoracic vs caudal cervical: mean 0.62, 95% CI 0.27–0.97, $P < .001$; lumbosacral vs cranial cervical: mean 0.45, 95% CI 0.14–0.76, $P < .01$; lumbosacral vs caudal cervical: mean 0.76, 95%CI 0.37–1.16, $P < .001$; Figure. 11).

For the normal AFs, there was no statistically significant difference in the mean pentosidine content between the different regions.

Association with age.

Detailed information can be found in the Supplemental Figures S4 and S5.

A strong to very strong increase in pentosidine (with exception of the caudal cervical NPs) and a moderate to very strong decrease of hydroxylysine was noted in both the AF and the NP. Furthermore, there was a strong increase

Table 1. Reliability of histologic scores for equine intervertebral disc degeneration: all vertebral regions.

	To evaluate reliability, 50 NVDs were scored twice by 3 independent observers					
	intra-observer agreement (%)	intra-observer reliability (weighted kappa)	inter-observer agreement (%)	inter-observer reliability (weighted kappa)	correlation with gross grade 1-5	correlation with normal versus severe degeneration
AF: morphology	49, 50, 66	0.18, 0.38, 0.53	12, 25	0.12, 0.25	n/a	n/a
AF: chondroid metaplasia	70, 78, 94	0.00, 0.50, 0.53	60, 70	0.00, 0.33	n/a	n/a
AF: tears and cleft formation	51, 56, 62	0.42, 0.62, 0.68	30, 63	0.22, 0.66	n/a	n/a
AF: presence of vascular proliferation	96, 96, 98	0.48, 0.48, 0.85	96, 96	0.44, 0.48	$r = -0.09; p = 0.56$	$r = -0.03; p = 0.84$
NP: chondroid metaplasia	80, 88, 88	0.26, 0.48, 0.59	82, 96	0.36, 0.86	$r = 0.13; p = 0.36$	$r = 0.24; p = 0.13$
NP: chondrocyte-like cell proliferation	54, 60, 74	0.36, 0.62, 0.66	44, 46	0.40, 0.42	$r = 0.30; p = 0.17$	$r = 0.28; p = 0.08$
NP: cellularity	70, 86, 100	n/a ^a , 0.17, 0.48	76, 78	0.00, 0.49	n/a	n/a
NP: presence of notochordal cells	100, 100, 100	n/a ^a	100, 100, 100	n/a ^a	$r = 0; p = 1$	$r = 0; p = 1$
NP: matrix staining	76, 78, 78	0.69, 0.73, 0.78	62, 74	0.56, 0.73	$r = 0.20; p = 0.16$	$r = 0.18; p = 0.26$
NP: tears and cleft formation	34, 54, 64	0.29, 0.61, 0.73	34, 38	0.36, 0.58	$r = 0.26; p = 0.07$	$r = 0.36; p = 0.02$ ^c
Endplate morphology	63, 65, 84	0.17, 0.32, 0.34	8, 84	0.02, 0.14	n/a	n/a
Subchondral bone sclerosis	69, 76, 89	0.00, 0.09, 0.50	69, 83	0.00, 0.27	n/a	n/a
Total histological score	n/a ^b	n/a ^b	n/a ^b	n/a ^b	$r = 0.32; p = 0.02$ ^c	$r = 0.43; p = 0.01$ ^c

n/a: analysis of the correlation with the gross grade was not applicable because of lack of histological grading reliability

n/a^a: the weighted kappa could not be determined because of the high observer agreement

n/a^b: analyses of the observer agreement or weighted kappa was not applicable

^c: this parameter was significantly correlated with the gross grade of degeneration

AF: annulus fibrosis

NP: nucleus pulposus

r: Pearson correlation coefficient

Table 2. Reliability of histologic scores for equine intervertebral disc degeneration: cervical vertebral regions.

	intra-observer agreement (%)	intra-observer reliability (weighted kappa)	inter-observer agreement (%)	inter-observer reliability (weighted kappa)	correlation with gross grade 1-5	correlation with normal versus severe degeneration
AF: morphology	46, 50, 69	0.22, 0.35, 0.48	41, 45	0.07, 0.13	n/a	n/a
AF: chondroid metaplasia	75, 89, 100	0.00, 0.42, 1	66, 67	0.00, 0.37	n/a	n/a
AF: tears and cleft formation	61, 63, 100	0.53, 0.74, 1	36, 41	0.21, 0.25	$r = 0.45; p = 0.01^c$	$r = 0.62; p = 0.001^c$
AF: presence of vascular proliferation	97, 100, 100	0.65, 1, 1	100, 100	1, 1	$r = 0.13; p = 0.47$	$r = 0.05; p = 0.81$
NP: chondroid metaplasia	88, 94, 97	0.00, 0.00, 0.06	91, 97	0.00, 0.04	$r = 0.12; p = 0.50$	$r = 0.16; p = 0.43$
NP: chondrocyte-like cell proliferation	53, 59, 77	0.25, 0.51, 0.61	34, 52	0.13, 0.26	n/a	n/a
NP: cellularity	81, 94, 100	n/a ^a , 0.14, 0.64	78, 94	0.00, 0.00	n/a	n/a
NP: presence of notochordal cells	100, 100, 100	n/a ^a	100, 100, 100	n/a ^a	$r = 0; p = 1$	$r = 0; p = 1$
NP: matrix staining	69, 69, 81	0.60, 0.65, 0.70	56, 72	0.44, 0.61	$r = 0.26; p = 0.15$	$r = 0.19; p = 0.35$
NP: tears and cleft formation	38, 59, 66	0.22, 0.63, 0.71	41, 50	0.47, 0.47	$r = 0.32; p = 0.07$	$r = 0.52; p = 0.01^c$
Endplate morphology	58, 77, 88	0.12, 0.16, 0.43	6, 7	0.01, 0.01	n/a	n/a
Subchondral bone sclerosis	67, 72, 80	0.06, 0.18, 0.43	53, 68	0.11, 0.31	n/a	n/a
Total histological score	n/a ^b	n/a ^b	n/a ^b	n/a ^b	$r = 0.45; p = 0.01^c$	$r = 0.56; p = 0.003^c$

n/a: analysis of the correlation with gross degeneration was not applicable because of lack of histological grading reliability

n/a^a: the weighted kappa could not be determined because of the high observer agreement

n/a^b: analyses of the observer agreement or weighted kappa was not applicable

^c: This parameter was significantly correlated with the gross grade of degeneration

AF: annulus fibrosus

NP: nucleus pulposus

r: Pearson correlation coefficient

Table 3. Histological scoring scheme for equine intervertebral disc degeneration using both haematoxylin/eosin and Alcian blue/picrosirius red stains.

A	Tears and cleft formation of the annulus fibrosus <i>(only when scoring cervical intervertebral discs)</i>
0	Absent
1	Rarely present
2	Present in intermediate amounts
3	Abundantly present
4	Scar/tissue defects
B	Presence of vascular proliferation in the annulus fibrosus
0	No vascular proliferation
1	Vascular proliferation
C	Chondroid metaplasia nucleus pulposus
0	No chondrocyte-like cells, only fibroblast-like cells
1	Mixture of chondrocyte-like cells and fibroblast-like cells in the inner 2/3 of the nucleus pulposus
2	Presence of chondrocyte-like cells, with formation of rows within in the inner 2/3 of the nucleus pulposus
3	Presence of chondrocyte-like cells, presence of clusters of chondrocyte-like cells
D	Chondrocyte-like cell proliferation of the nucleus pulposus <i>(only when scoring a combination of cervical, thoracic and lumbar intervertebral discs)</i>
1	Presence of solitary chondrocyte-like cells
2	Connection of two chondrocyte-like cells
3	Formation of small clones of 3-5 chondrocyte-like cells
4	Formation of intermediate clones of 6-10 chondrocyte-like cells
5	Formation of large clones more than 10 chondrocyte-like cells
E	Presence of notochordal cells in the nucleus pulposus
0	Abundantly present (>50%)
1	Present (1-50%)
2	Absent
F	Matrix staining of the nucleus pulposus with Alcian blue/picrosirius red staining
0	Blue (green) stain dominates
1	Mixture of blue and red staining
2	Red stain dominates
G	Tears and cleft formation of the nucleus pulposus
0	Absent
1	Rarely present
2	Present in intermediate amounts
3	Abundantly present
4	Scar/tissue defect

in total collagen in the caudal cervical NPs. In contrast to expectations, the GAG content of the caudal cervical NPs increased very strongly with age.

Association with degeneration.

Detailed information about the biochemical changes associated with gross degeneration can be found in Figures 10 and Supplemental Figures S6–S8. The most important findings were a moderate to strong increase in pentosidine in the AF and the NP, and a moderate (AF) and weak to severe (NP) decrease of hydroxylysine.

In the linear mixed model, the mean pentosidine content in the caudal cervical AFs and NPs of both grade 2 and grade 5 IVDs was higher than those of grade 1 IVDs (AF grade 1 vs 2: mean 1.40, 95% CI 0.68–2.10, $P < .001$; AF grade 1 vs 5: mean 1.40, 95% CI 0.73–2.06, $P < .001$; NP grade 1 vs 2: mean 1.25, $P < .05$; NP grade 1 vs 5: mean 1.49, $P < .01$; Figures. 12, 13).

Furthermore, the collagen type 1 content of the NP increased weakly with degeneration. In contrast to expectations, there was no change in GAG content with degeneration in the NP.

Discussion

The morphology of the equine IVD and its gross changes in degeneration are largely similar to those in dogs and humans.¹⁰ However, the present study demonstrated that aspects of the cellular and biochemical composition, biochemical changes associated with age, and the histological and biochemical changes associated with degeneration differ in horses from those reported in dogs and humans.

Although 6 out of 12 histological variables could be scored reliably, only the total histological score, tearing of the NP, and tearing of the cervical AF correlated with gross degeneration. Thus, these variables can be used to histologically distinguish normal from degenerated discs, especially for the cervical discs. Tearing is an important characteristic in gross grading¹⁰ and can also be seen in degenerated equine discs on magnetic resonance imaging⁶⁰ and therefore it is not surprising that this variable is also of use in histological scoring. Consequently, gross grading is considered to be the leading method for assessment of IVDD in horses.

The histological scoring scheme previously validated for canine disc degeneration⁷ was modified to include vascular proliferation in the outer

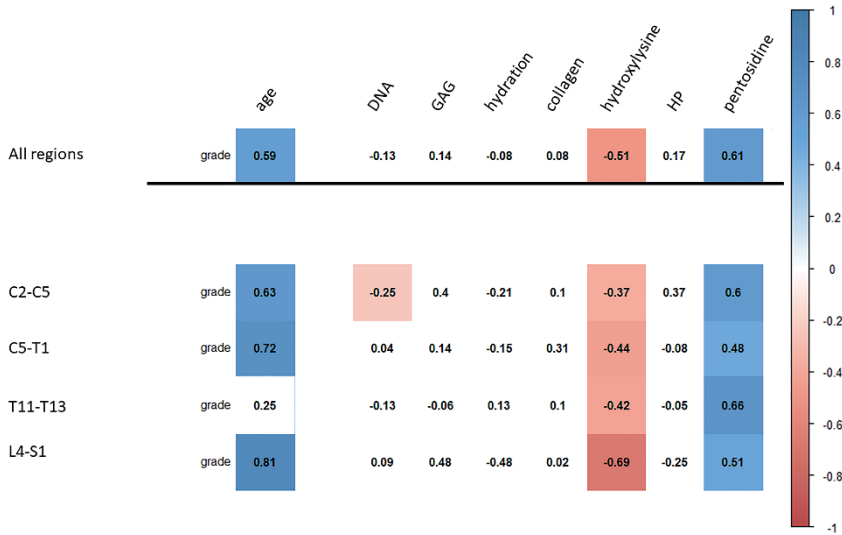
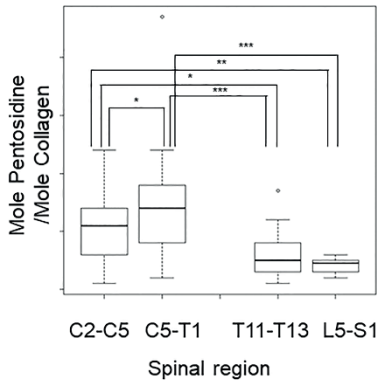
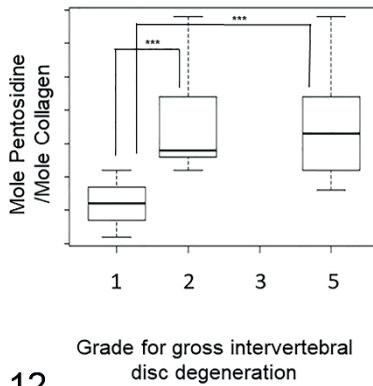


Figure 10. Correlation between degeneration of the nucleus pulposus and biochemical data on equine intervertebral discs. In the heat map, the numbers are Spearman rank correlation coefficients and the red and blue coloured boxes indicate statistically significant ($P \leq .05$), negative and positive correlations, respectively. IVD, intervertebral disc; C, cervical vertebra; T, thoracic vertebra; L, lumbar vertebra; S, sacral vertebra; DNA, DNA per gram (wet weight); GAG, glycosaminoglycans per gram (wet weight); Collagen, total amount of collagen per gram (wet weight); HP, hydroxyllysyl-pyridinoline.

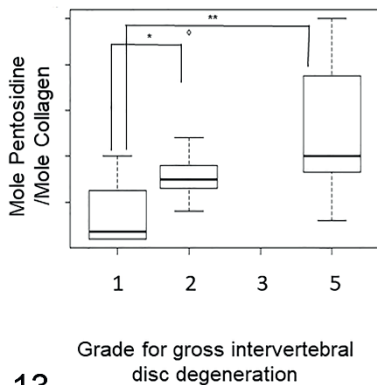
AF because this is a phenomenon that has not been described in dogs and could represent tissue repair induced by microtrauma of the outer AF in horses, although a correlation with gross degenerative changes was not found. It was assumed that degeneration of the IVD starts in the NP, as in dogs and humans; therefore, chondroid metaplasia of the NP was included in the proposed scoring scheme despite the fact that the present study did not show a reliable association of this variable with gross IVD degeneration. Surprisingly, notochordal cells were not seen in any of the IVDs in the current study, although they have an important role in organogenesis of the vertebral column. In children and in the normal discs of adult non-chondrodystrophic dogs, notochordal cells are present in the NP and are replaced by smaller, non-vacuolated chondrocyte-like cells during maturation in humans and during degeneration in the dog.^{12, 26} In mammals, including the horse, the NP is assumed to be formed by the notochord, which



11



12



13

Figures 11-13. Amount of pentosidine within normal intervertebral discs (IVDs) among the different spinal regions (Figure. 11), and among different gross grades for degeneration in the caudal cervical region (Figures. 12, 13). The box shows the median and first and third quartiles; whiskers show the minimum and maximum; o, outliers. * $P < .05$, ** $P < .01$, *** $P < .001$. The amount of pentosidine is expressed as moles of pentosidine per mole of collagen.

Figure 11. The amount of pentosidine in normal nucleus pulposi (NPs) of the caudal cervical region (C5-T1) was higher than in normal NPs of the cranial cervical region (C2-C5). The amount of pentosidine in normal NPs of the cranial and caudal cervical regions was greater than in normal NPs of the thoracic (T11-T13) and lumbosacral (L4-S1) regions.

Figure 12. The amount of pentosidine in the annulus fibrosus (AF) of grade 2 and 5 IVDs is greater than in the AF of grade 1 IVDs.

Figure 13. The amount of pentosidine in the NP of grade 2 and 5 IVDs is greater than in the NP of grade 1 IVDs.

itself disappears during late embryogenesis.^{5, 54} However, the presence of cells with morphological characteristics of notochordal cells could not be confirmed during gestation or postnatally. This finding was substantiated by using immunohistochemistry for cytokeratin 18, a marker expressed by notochordal cells.⁴⁵ According to a previous publication, the formation of the equine NP occurs after gestation day 30, although the exact day of the formation of the NP is not mentioned.⁵ In vitro and in vivo studies in juvenile and adult mice, adult rabbits, and juvenile pigs have shown that notochordal cells can transform into chondrocyte-like cells, implying that these morphologies are not different cell lineages but instead represent different stages of cell activation, differentiation, or metaplasia.^{13, 31, 42, 44, 65} Although unlikely, it can therefore not be ruled out that the equine NP is initially formed from the notochord with transformation of the notochordal cells into chondrocyte-like cells between gestation days 30 and 45, the age of the youngest foetus. Still, it can be concluded that the absence of cells morphologically consistent with physaliferous notochordal cells is not associated with maturation or degeneration of the NP in the horse.

The most important biochemical changes associated with age and degeneration of both the AF and the NP of the equine IVD was a reduction in hydroxylysine and an increase in pentosidine content. Hydroxylysine has 2 important functions in the synthesis of collagen. It plays an important role in collagen crosslinking and in posttranslational enzymatic O-glycosylation. Hydroxylysine is furthermore implicated in the formation of nonenzymatic AGEs.^{14, 53, 56, 63} The decrease of hydroxylysine does not appear to affect crosslinking because the amount of HP, one of the crosslinks formed via hydroxylysine, was not negatively associated with age nor degeneration. It is likely that the reduced hydroxylysine content with age and IVDD is for a large part the result of formation of AGEs, as the decline in hydroxylysine and the increase in AGEs seems to go hand in hand. Hydroxylysine-linked glycosylation is acid-labile and could therefore not be determined after hydrolyzation with hydrochloric acid. However, the decrease in hydroxylysine with age and IVDD may also indicate decreased glycosylation.⁶⁴ Although the exact function of glycosylation of hydroxylysine is yet unknown, it does appear to play a role in collagen crosslink maturation and therefore it likely has an effect on the biological function of collagen.^{14, 53, 56} Hence, the data may suggest that a decrease in glycosylation of hydroxylysine affects the biomechanical properties of affected IVDs. Similar to the equine IVD, an increase in the amount of pentosidine with age

and degeneration has been described in human IVDs.^{1, 40, 61} Pentosidine is the best-characterized AGE crosslink⁴⁸ and is often used as biomarker for non-enzymatic glycation⁴⁷ because it is metabolically stable and correlates well with tissue levels of other AGEs.⁴⁸ An increase in AGEs has been shown to be responsible for yellow discoloration, loss of compliance, increase in tissue stiffness, loss of strength, brittleness, and loss of viscoelasticity of the affected tissues including the IVD.^{1, 3, 20, 22, 61} The increase in pentosidine content and its biomechanical consequences can therefore explain the typical gross changes of tearing and yellow discoloration seen in equine IVDD.

The IVDs with a normal gross morphology in the caudal cervical spine had statistically significantly higher pentosidine levels in the NP compared to the other regions. Considering that also gross degeneration is most prevalent in this region,¹⁰ this indicates accelerated degeneration in the caudal cervical region and in addition suggests that IVDD starts in the NP, as in other species.³⁶ In addition to age,^{3, 14, 20} oxidative stress contributes to the formation of AGEs.^{21, 36} Within an individual, purely age-related degeneration is expected to be the same in all IVDs, and more severe degeneration in a specific region can occur due to increased mechanical loading in that area.^{1, 25} Chronic abnormal loading can cause adverse changes in the composition of the IVD's extracellular matrix,^{15, 25} and it is feasible that increased mechanical loading also leads to microtrauma with resultant production of reactive oxygen species and glycooxidation causing accumulation of AGEs.³⁶ Therefore, increased mechanical loading of the caudal cervical region could be an explanation for the differences in AGE content in this region compared to the other spinal regions.

In vitro studies have shown that accumulation of AGEs in the human NP can cause a decrease in the production of aggrecan and initiate inflammation-related degeneration via binding to the receptor RAGE (receptor for advanced glycation end products), and in this way AGEs can contribute to the initiation and progression of IVDD.^{50, 67} However, in the current study, aggrecan levels were not correlated with degree of degeneration, and thus decrease in production of aggrecan due to AGEs does not seem to be important in the equine disc. Whether or not AGEs initiate inflammation in the equine IVD needs to be further investigated, but a classical inflammatory reaction has not been seen histologically, nor is there substantial neovascularization of the entire IVD.

In contrast to the common NP- and AF-specific biochemical profiles

described in dogs and humans, the equine NP of normal IVDs (of all regions combined) only contained slightly more GAGs than the AF, and there was no statistically significant difference in hydration (both were ~70%). On the contrary, the canine AF contains ~60% and the NP ~81% water and the human AF contains ~66% to 70% and the NP ~80% to 89% water.^{2, 27, 58} This similar water content in NP and AF of horses may explain why the NP in the normal equine IVD cannot be easily distinguished macroscopically from the AF, in contrast to the IVD of dogs and humans.¹⁰

Furthermore, the aggrecan and GAG content in the equine disc, which strongly correlates with the amount of hydration, did not significantly decrease with age or degeneration as is described in dogs and humans.^{1, 2, 7, 8} Loss of GAGs and subsequently of water content are important factors in collapse of severely degenerated discs in dogs and humans^{1, 6} and the constancy of hydration of the equine IVD between the different grades for degeneration could explain why loss in disc height is not seen in equine IVDD.¹⁰ In fact, the GAG content increased in the equine AF and NP with age and in the AF with degeneration.

Furthermore, histologically, GAG-rich mucinous stroma with associated chondrocyte-like cells were commonly seen in the AFs. Proliferation of chondrocyte-like cells and subsequent disorganization of the lamellar structure of the AF are reliable histological indicators of degeneration in dogs and humans.^{7, 46} In the horse, however, disorganization of lamellar architecture and chondroid metaplasia of the AF could not be scored reliably, yet moderate to marked disorganization and rupture of the lamellae and marked chondroid metaplasia were seen in the vast majority of the scored IVDs. Therefore, lamellar disorganization due to chondroid metaplasia is probably a normal feature of the equine IVD. The presence of chondroid material in the AF of the equine IVD has been described before in a study of 255 cervical IVDs from 17 horses.⁶⁸ In that study, chondroid material in the AF was only seen in 5 IVDs and interpreted as a Hansen type 2 herniation. However, only haematoxylin/eosin stains were used to evaluate the histological characteristics of the equine IVD, which could explain why disorganization of the AF by chondroid metaplasia was not clearly visible in the other IVDs examined, since Alcian blue/picrosirius red stain is more suitable to highlight the chondroid intercellular matrix than haematoxylin/eosin.²³

Both aged and degenerated NPs showed a slight fibrotic phenotype of the extracellular matrix in the biochemical assays. Interestingly, the fibrotic

phenotype with age was predominantly seen in the caudal cervical discs, contributing to the suspicion of distinctive biomechanical stress in this specific vertebral region.^{10, 49} Furthermore, the fact that with degeneration an increased fibrotic phenotype is chiefly present in the NP further supports the suggestion that degeneration starts in the NP. However, the fibrotic phenotype of the extracellular matrix in the degenerated equine IVD was mild, and Alcian blue/picrosirius staining of the matrix was not correlated with degeneration even though this variable could be scored reliably. This is in contrast to dogs and humans.^{7, 46} Still, it seems feasible that this weak fibrotic phenotype could impair the physiological function of the NP and contribute to changes in biomechanical properties such as motion stiffness and loss of elasticity of the degenerated equine IVD.³⁴

In conclusion, tearing of the NP and the cervical AF could be reliably scored histologically and were correlated with degeneration. The total histological score included tears and cleft formation and vascular proliferation of the AF, and chondroid metaplasia, proliferation of chondrocyte-like cells, presence of notochordal cells, matrix staining, and tears and cleft formation of the NP, and this total histological score also correlated with degeneration. Therefore, these histological variables can be of use to distinguish normal from degenerated equine IVDs, although it did not offer advantages over gross grading. Biochemically, ageing and degeneration of the equine IVD were characterized by changes in the composition of the NP and less so of the AF, consisting of a significant increase of AGEs and a mild fibrotic biochemical phenotype of the extracellular matrix. These biochemical changes were most prominent in the caudal cervical region. They can explain the typical gross changes of yellow discoloration and cleft formation, and they likely result in altered biomechanical properties that can subsequently cause degenerative changes of spatially close structures such as the articular process joints. As such, we speculate that equine IVDD might contribute to cervical neurological signs as seen in cervical vertebral myelopathy and this should be an area of further study. A decrease in GAGs and subsequent dehydration, the most important biochemical alteration in canine and human IVDD, were not seen in the horse. Furthermore, notochordal cells could not be identified in the equine NP, not even in foetal IVDs.

References

1. Adams MA, Roughley PJ. What is intervertebral disc degeneration, and what causes it?. *Spine*. 2006;31(18):2151-2161.
2. Antoniou J, Steffen T, Nelson F, et al. The human lumbar intervertebral disc: evidence for changes in the biosynthesis and denaturation of the extracellular matrix with growth, maturation, ageing, and degeneration. *J Clin Invest*. 1996;98(4):996-1003.
3. Avery NC, Bailey AJ. Restraining cross-links responsible for the mechanical properties of collagen fibers: natural and artificial. In: Fratzl P, ed. *Collagen: structure and mechanics*. Springer Science+Business Media, LLC; 2008.
4. Bach FC, Tellegen AR, Beukers M, et al. Biologic canine and human intervertebral disc repair by notochordal cell-derived matrix: from bench towards bedside. *Oncotarget*. 2018;9(41):26507-26526.
5. Barreto Rda S, Rodrigues MN, Carvalho RC, et al. Organogenesis of the musculoskeletal system in horse embryos and early fetuses. *Anat Rec (Hoboken)*. 2016;299(6):722-729.
6. Bergknut N, Grinwis G, Pickee E, et al. Reliability of macroscopic grading of intervertebral disk degeneration in dogs by use of the Thompson system and comparison with low-field magnetic resonance imaging findings. *Am J Vet Res*. 2011;72(7):899-904.
7. Bergknut N, Meij BP, Hagman R, et al. Intervertebral disc disease in dogs - part 1: a new histological grading scheme for classification of intervertebral disc degeneration in dogs. *Vet J*. 2013;195(2):156-163.
8. Bergknut N, Rutges JPHJ, Kranenburg H-C, et al. The dog as an animal model for intervertebral disc degeneration?. *Spine*. 2012;37(5):351-358.
9. Bergknut N, Smolders LA, Grinwis GC, et al. Intervertebral disc degeneration in the dog. Part 1: anatomy and physiology of the intervertebral disc and characteristics of intervertebral disc degeneration. *Vet J*. 2013;195(3):282-291.
10. Bergmann W, Bergknut N, Veraa S, et al. Intervertebral disc degeneration in warmblood horses: morphology, grading, and distribution of lesions. *Vet Pathol*. 2018;55(3):442-452
11. Bollwein A, Hänichen T. Age-related changes in the intervertebral disks of the cervical vertebrae of the horse. *Tierarztl Prax*. 1989;17(1):73-76.
12. Boos N, Weissbach S, Rohrbach H, et al. Classification of age-related changes in lumbar intervertebral discs: 2002. *Spine*. 2002;27(23):2631-2644.
13. Choi KS, Cohn MJ, Harfe BD. Identification of nucleus pulposus precursor cells and notochordal remnants in the mouse: implications for disk degeneration and chordoma formation. *Dev Dyn*. 2008;237(12):3953-3958.
14. Chow WY, Li R, Goldberga I, et al. Essential but sparse collagen hydroxylysyl post-translational modifications detected by DNP NMR. *Chem Commun (Camb)*. 2018;54(89):12570-12573.
15. Colombini A, Lombardi G, Corsi MM, et al. Pathophysiology of the human intervertebral disc. *Int J Biochem Cell Biol*. 2008;40(5):837-842.

16. Dyson SJ. Lesions of the equine neck resulting in lameness or poor performance. *Vet Clin North Am Equine Pract.* 2011;27(3):417-437.
17. Erwin WM, DeSouza L, Funabashi M, et al. The biological basis of degenerative disc disease: proteomic and biomechanical analysis of the canine intervertebral disc. *Arthritis Res Ther.* 2015;17:240-015-0733-z.
18. Evans JD. *Straightforward statistics for the behavioral sciences.* Brooks/Cole Publishing Company; 1996.
19. Farndale RW, Buttle DJ, Barrett AJ. Improved quantitation and discrimination of sulphated glycosaminoglycans by use of dimethylmethylene blue. *Biochim Biophys Acta.* 1986;883(2):173-177.
20. Fratzl P. Collagen: structure and mechanics, an introduction. In: Fratzl P, ed. *Collagen: structure and mechanics.* Springer Science+Business Media, LLC; 2008.
21. Fu MX, Knecht KJ, Thorpe SR, et al. Role of oxygen in cross-linking and chemical modification of collagen by glucose. *Diabetes.* 1992;41(Suppl 2):42-48.
22. Gautieri A, Passini FS, Silvan U, et al. Advanced glycation end-products: mechanics of aged collagen from molecule to tissue. *Matrix Biol.* 2017;59:95-108.
23. Gruber HE, Ingram J, Hanley Jr. EN. An improved staining method for intervertebral disc tissue. *Biotech Histochem.* 2002;77(2):81-83.
24. Hadjipavlou AG, Tzermiadianos MN, Bogduk N, et al. The pathophysiology of disc degeneration: a critical review. *J Bone Joint Surg Br.* 2008;90(10):1261-1270.
25. Habermehl K-H. 2nd ed. *Die Altersbestimmung bei Haus- und Labortieren.* Paul Parey; 1975.
26. Hansen T, Smolders LA, Tryfonidou MA, et al. The myth of fibroid degeneration in the canine intervertebral disc: a histopathological comparison of intervertebral disc degeneration in chondrodystrophic and nonchondrodystrophic dogs. *Vet Pathol.* 2017;54(6):945-952.
27. Holm S, Nachemson A. Nutritional changes in the canine intervertebral disc after spinal fusion. *Clin Orthop Relat Res.* 1982;(169)(169):243-258.
28. Hsueh MF, Khabut A, Kjellstrom S, et al. Elucidating the molecular composition of cartilage by proteomics. *J Proteome Res.* 2016;15(2):374-388.
29. Hulmes DJS. Collagen diversity, synthesis and assembly. In: Fratzl P, ed. *d Mechanics.* New York, USA: Springer Science+Business Media, LLC; 2008:15-41.
30. Ikegawa S. The genetics of common degenerative skeletal disorders: osteoarthritis and degenerative disc disease. *Annu Rev Genomics Hum Genet.* 2013;14:245-256.
31. Kim JH, Deasy BM, Seo HY, et al. Differentiation of intervertebral notochordal cells through live automated cell imaging system in vitro. *Spine.* 2009;34(23):2486-2493.
32. Landis JR, Koch GG. The measurement of observer agreement for categorical data. *Biometrics.* 1977;33(1):159-174.
33. Laugier C, Tapprest J, Foucher N, et al. A necropsy survey of neurologic diseases in 4,319 horses examined in Normandy (France) from 1986 to 2006. *J Equine Vet Sci.* 2009;29(7):561-568.

34. Leung VY, Aladin DM, Lv F, et al. Mesenchymal stem cells reduce intervertebral disc fibrosis and facilitate repair. *Stem Cells*. 2014;32(8):2164-2177.
35. Levine JM, Adam E, MacKay RJ, et al. Confirmed and presumptive cervical vertebral compressive myelopathy in older horses: A retrospective study (1992-2004). *J Vet Intern Med*. 2007;21(4):812-819.
36. Nerlich AG, Schleicher ED, Boos N.. Immunohistologic markers for age-related changes of human lumbar intervertebral discs. *Spine*. 1997;22(24):2781-2795.
37. Nout YS, Reed SM. Cervical vertebral stenotic myelopathy. *Equine Vet Educ*. 2003;15(4):212-223.
38. Oegema TR,Jr, Johnson SL, Aguiar DJ, et al. Fibronectin and its fragments increase with degeneration in the human intervertebral disc. *Spine*. 2000;25(21):2742-2747.
39. Pinheiro J, Bates D, DebRoy S, Sarkar D, R Core Team (2019). nlme: Linear and nonlinear mixed effects models. R package version 3.1-140. <https://CRAN.R-project.org/package=nlme>.
40. Pokharna HK, Phillips FM. Collagen crosslinks in human lumbar intervertebral disc aging. *Spine*. 1998;23(15):1645-1648.
41. Powers BE, Stashak TS, Nixon AJ, et al. Pathology of the vertebral column of horses with cervical static stenosis. *Vet Pathol*. 1986;23(4):392-399.
42. Purmessur D, Guterl CC, Cho SK, et al. Dynamic pressurization induces transition of notochordal cells to a mature phenotype while retaining production of important patterning ligands from development. *Arthritis Res Ther*. 2013;15(5):R122.
43. Rhind SM KJ. Polycystic kidney disease in a mature horse: report and review of previously reported cases . *Equine Vet .Educ*. 2010;16(4):178-183.
44. Risbud MV, Schoepflin ZR, Mwale F, et al. Defining the phenotype of young healthy nucleus pulposus cells: recommendations of the Spine Research Interest Group at the 2014 annual ORS meeting. *J Orthop Res*. 2015;33(3):283-293.
45. Rodrigues-Pinto R, Richardson SM, Hoyland JA. Identification of novel nucleus pulposus markers: interspecies variations and implications for cell-based therapies for intervertebral disc degeneration. *Bone Joint Res*. 2013;2(8):169-178.
46. Rutges JPHJ, Duit RA, Kummer JA, et al. A validated new histological classification for intervertebral disc degeneration. *Osteoarthr Cartil*. 2013;21(12):2039-2047.
47. Sell DR, Lane MA, Johnson WA, et al. Longevity and the genetic determination of collagen glycoxidation kinetics in mammalian senescence. *Proc Natl Acad Sci U S A*. 1996;93(1):485-490.
48. Sell DR, Monnier VM. Structure elucidation of a senescence cross-link from human extracellular matrix. Implication of pentoses in the aging process. *J Biol Chem*. 1989;264(36):21597-21602.
49. Sleutjens J, Voorhout G, Van Der Kolk JH, et al. The effect of ex vivo flexion and extension on intervertebral foramina dimensions in the equine cervical spine. *Equine Vet J*. 2010;42(Suppl. 38):425-430.

50. Song Y, Wang Y, Zhang Y, et al. Advanced glycation end products regulate anabolic and catabolic activities via NLRP3-inflammasome activation in human nucleus pulposus cells. *J Cell Mol Med.* 2017;21(7):1373-1387.
51. Souza MV, van Weeren PR, van Schie HT, et al. Regional differences in biochemical, biomechanical and histomorphological characteristics of the equine suspensory ligament. *Equine Vet J.* 2010;42(7):611-620.
52. Speltz MC, Olson EJ, Hunt LM, et al. Equine intervertebral disk disease: a case report. *J Equine Vet Sci.* 2006;26(9):413-419.
53. Sricholpech M, Perdivara I, Yokoyama M, et al. Lysyl hydroxylase 3-mediated glucosylation in type I collagen: molecular loci and biological significance. *J Biol Chem.* 2012;287(27):22998-23009.
54. Stemple DL. Structure and function of the notochord: an essential organ for chordate development. *Development.* 2005;132(11):2503-2512.
55. Taiyun W, Viliam S. R package "corrplot": Visualization of a correlation matrix (Version 0.84). <https://github.com/taiyun/corrplot>.
56. Terajima M, Perdivara I, Sricholpech M, et al. Glycosylation and cross-linking in bone type I collagen. *J Biol Chem.* 2014;289(33):22636-22647.
57. To WS, Midwood KS. Plasma and cellular fibronectin: distinct and independent functions during tissue repair. *Fibrogenesis Tissue Repair.* 2011;4:21-1536-4-21.
58. Urban JPG, Roberts S. Degeneration of the intervertebral disc. *Arthritis Res Ther.* 2003;5(3):120-130.
59. van der Harst MR, DeGroot J, Kiers GH, et al. Biochemical analysis of the articular cartilage and subchondral and trabecular bone of the metacarpophalangeal joint of horses with early osteoarthritis. *Am J Vet Res.* 2005;66(7):1238-1246.
60. Veraa S, Bergmann W, Wijnberg ID, et al. Equine cervical intervertebral disc degeneration is associated with location and MRI features. *Vet Radiol Ultrasound.* 2019;60(6):696-706.
61. Wagner DR, Reiser KM, Lotz JC. Glycation increases human annulus fibrosus stiffness in both experimental measurements and theoretical predictions. *J Biomech.* 2006;39(6):1021-1029.
62. Wijnberg D, Bergmann W, Veraa S. Neurological neck problems, diagnostics and prognosis in the horse. *Prakt Tierarzt.* 2015;96(2):150-158.
63. Yamauchi M, Sricholpech M. Lysine post-translational modifications of collagen. *Essays Biochem.* 2012;52:113-133.
64. Yamauchi M, Sricholpech M, Terajima M, et al. Glycosylation of type I collagen. *Methods Mol Biol.* 2019;1934:127-144.
65. Yang F, Leung VY, Luk KD, et al. Injury-induced sequential transformation of notochordal nucleus pulposus to chondrogenic and fibrocartilaginous phenotype in the mouse. *J Pathol.* 2009;218(1):113-121.
66. Yee A, Lam MP, Tam V, et al. Fibrotic-like changes in degenerate human intervertebral discs revealed by quantitative proteomic analysis. *Osteoarthr Cartil.* 2016;24(3):503-513.

67. Yokosuka K, Park JS, Jimbo K, et al. Advanced glycation end-products downregulating intervertebral disc cell production of proteoglycans in vitro. *J Neurosurg Spine*. 2006;5(4):324-329.
68. Yovich JV, Powers BE, Stashak TS. Morphologic features of the cervical intervertebral disks and adjacent vertebral bodies of horses. *Am J Vet Res*. 1985;46(11):2372-2377.

Supplemental table S1. Signalment and experimental usage of the intervertebral discs of the warmblood horses in this study

The sampled area and the amount of discs used is noted in brackets.

case number	breed	sex	cause of death	age	gross scoring	histological evaluation	biochemical evaluation
1	RDSH	mare	death dam	45 days gestation	no	yes (whole vertebral column, 29)	no
2	RDSH	unknown	aborted as part of a study	61 days gestation	no	yes (whole vertebral column, 29)	no
3	RDSH	mare	torsio umbilicalis	9 months gestation	no	yes (C3-T2, 6)	no
4	RDSH	mare	necrotizing placentitis	9 months gestation	no	yes (T11-T12, 2; L5-S1, 2)	no
5	RDSH	unknown	interstitial pneumonia and necrotizing hepatitis	10 months gestation	no	yes (C3-C4, 1; C6-C7, 1)	no
6	RDSH	mare	herpes viral hepatitis	0 day	no	yes (C3-C4, 1; C6-C7, 1)	no
7	RDSH	mare	herpes viral pneumonia and hepatitis	1 day	no	yes (C3-C4, 1; C6-C7, 1)	no
8	RDSH	unknown	interstitial pneumonia	4 days	no	yes (C3-C4, 1; C6-C7, 1)	no
9	RDSH	stallion	clostridial enterocolitis	5 days	no	yes (C3-C4, 1; C6-C7, 1)	no
10	RDSH	mare	clostridial enteritis	5 days	no	yes (C3-C4, 1; C6-C7, 1)	no
11	RDSH	mare	fibrinosuppurative typhlocolitis and purulent hepatitis	7 days	no	yes (C3-C4, 1; C6-C7, 1)	no
12	RDSH	stallion	herpes viral pneumonia	8 days	no	yes (C3-C4, 1; C6-C7, 1)	no
13	RDSH	stallion	interstitial pneumonia	10 days	no	yes (C3-C4, 1; C6-C7, 1)	no
14	Zangesheide	stallion	hydrocephalus	6 weeks	no	yes (C4-T2, 5)	no
15	RDSH	stallion	necrotizing colitis	13 weeks	no	yes (C3-C4, 1; C6-C7, 1)	no
16	RDSH	stallion	anesthesia death after dental surgery	8 months	yes	Yes (C2-C3, 1; C7-T2, 2; T11-T12, 2; L5-S1, 2).	yes (C2-C3, 1; C6-C7, 1; T11-T13, 2; L5-S1, 2)
17	RDSH	mare	fungal eustachitis	11 months	yes	Yes (C2-T2, 7; T12-T12, 1)	yes (C2-C3, 1; C6-C7, 1; T11-T13, 2)
18	Zangesheide	stallion	invagination caecum	1 year	yes	no	yes (C3-C4, 1; C6-C7, 1; T11-T13, 2)

19	RDSH	stallion	cervical ataxia	2 years	yes	yes (C5-C7, 2; T11-T12, 1; L6-S1, 1)	no
20	Holsteiner	gelding	cervical and back pain	4 years	yes	yes (C2-C3, 1; C7-T1, 1; L6S1, 1)	yes (C2-C3, 1; C6-C7, 1; T11-T13, 2)
21	RDSH	mare	cervical ataxia	5 years	yes	yes (C2-C3, 1; C6-T1, 2; L6-S1, 1)	no
22	RDSH	gelding	kissing spines	6 years	yes	yes (C2-C3, 1; T11-T12, 1; L5-S1, 2)	yes (C2-C3, 1; L5-S1, 2)
23	RDSH	mare	suspensory desmitis	7 years	yes	no	yes (C2-C3, 1; C6-C7, 1; T11-T13, 2; L5-L6, 1)
24	RDSH	gelding	myopathy	7 years	yes	yes (C2-T1, 6)	no
25	RDSH	mare	dislocation cervical vertebra	10 years	yes	yes (C3-T1, 5; T11-T12, 1; L5-S1, 2))	no
26	RDSH	gelding	cervical ataxia	11 years	yes	yes (C2-T2, 7)	no
27	RDSH	gelding	cervical ataxia	11 years	yes	yes (C3-C5, 2; C7-T1, 1; L5-S1, 2)	yes (C2-C3, 1; C6-T1, 2; T11-T13, 2; L5-S1,2)
28	RDSH	gelding	equine multinodular pulmonary fibrosis	12 years	yes	yes (C3-C4, 1; T12-T13, 1; L6-S1, 1)	no
29	RDSH	gelding	cervical ataxia	12 years	yes	yes (C3-T1, 5; T11-T12, 2; L5-S1, 2)	no
30	RDSH	mare	colic	13 years	yes	no	yes (C2-T1, 6)
31	RDSH	mare	displacement colon	13 years	yes	no	yes (C2-T2, 7)
32	RDSH	mare	fibrinous peritonitis	15 years	yes	yes (C6-C7, 1; T11-T12, 2)	no
33	RDSH	mare	gallstones	15 years	yes	yes (C3-C4, 1; C6-C7, 1; L5-S1, 2)	no
34	RDSH	gelding	cervical ataxia	16 years	yes	yes (T11-T12, 2)	no
35	RDSH	mare	torsion colon	16 years	yes	yes (C4-T1, 4; T12-T13, 1; L5-S1, 2)	yes (C6-C7,1; T11-T13, 2)
36	RDSH	mare	colic	17 years	yes	no	yes (C2-C5, 3; C6-T1, 2; T11-T13, 2; L5-S1, 2)
37	RDSH	gelding	foramen epiploicum strangulation	18 years	yes	yes (C2-C7, 5; T12-T13, 1; L6-S1, 1)	yes (C6C7, 1; T11-T13, 2; L5L6, 1)

38	RDSH	mare	neuroma	18 years	yes	yes (C2-C7 , 5; T11-T13, 2)	no
39	RDSH	mare	arthrosis	18 years	yes	yes (C2-C6, 4; C7-T1,1)	no
40	RDSH	gelding	haemothorax	21 years	yes	yes (C3-C4, 1)	no
41	RDSH	gelding	maxillary carcinoid	21 years	yes	no	yes (C2-T2, 7; T11-T13, 2; L5-S1, 2)

RDSH = Royal Dutch Sport Horse

C= cervical vertebra, T= thoracic vertebra, L= lumbar vertebra, S= sacral vertebra

Table S2. Histological scoring scheme for equine intervertebral disc degeneration using both hematoxylin/eosin and Alcian blue/picrosirius red stains

A.Morphology of the lamellae of the annulus fibrosus (best viewed in the Alcian blue/picrosirius red stain; area with the highest score)

- 0 Well-organized, half ring-shaped, collagen lamellae
- 1 Mild disorganized; some loss of half ring-shaped structure, most lamellar layer, still distinguishable (<25%)
- 2 Moderately disorganized; partly ruptured annulus fibrosus, loss of half ring-shaped structure (25-75%)
- 3 Completely ruptured annulus fibrosus; no or few distinguishable half ring-shaped collagen lamellae (>75%)

B.Chondroid metaplasia of the annulus fibrosus

- 0 No chondrocyte morphology, just spindle-shaped cells
- 1 Mild chondrocyte-like cell proliferation (i.e. limited to inner most annulus fibrosus layers)
- 2 Moderate chondrocyte-like cell proliferation (i.e. chondrocyte-like cells up to half of the annulus fibrosus)
- 3 Marked chondrocyte-like cell proliferation (i.e. chondrocyte-like cells up to outer layers of the annulus fibrosus)

C.Tears and cleft formation of the annulus fibrosus

- 0 Absent
- 1 Rarely present
- 2 Present in intermediate amounts
- 3 Abundantly present
- 4 Scar/tissue defects

D.Presence of vascular proliferation in the annulus fibrosus

- 0.No vascular proliferation
- 1.Vascular proliferation

E.Chondroid metaplasia nucleus pulposus

- 0 No chondrocyte-like cells, only spindle cells
- 1 Mixture of chondrocyte-like cells and spindle cells in the inner 2/3 of the nucleus pulposus
- 2 Presence of chondrocyte-like cells, with formation of rows within in the inner 2/3 of the nucleus pulposus
- 3.Presence of chondrocyte-like cells, presence of clusters of chondrocyte-like cells

F.Chondrocyte-like cell proliferation of the nucleus pulposus

- 1 Presence of solitary chondrocyte-like cells
- 2 Connection of two chondrocyte-like cells
- 3 Formation of small clones of 3-5 chondrocyte-like cells
- 4 Formation of intermediate clones of 6-10 chondrocyte-like cells
- 5 Formation of large clones more than 10 chondrocyte-like cells

G.Cellularity of the nucleus pulposus taken from the most cell poor area

- 0 No areas without viable cells present per high power field (400 x)
- 1 More than 75 % of space of a high power field (400 x) is occupied by cells
- 2 Between 50-75 % of space of a high power field (400x) is occupied by cells
- 3 Between 25-50 % of space of a high power field (400x) is occupied by cells
- 4 Less than 25 % of space of a high power field (400x) is occupied by cells

H.Presence of notochordal cells in the nucleus pulposus

- 0 Abundantly present (>50%)
- 1 Present (1-50%)
- 2 Absent

I.Matrix staining of the nucleus pulposus with Alcian blue/Picrosirius red staining

- 0 Blue (green) stain dominates
- 1 Mixture of blue and red staining
- 2 Red stain dominates

J.Tears and cleft formation of the nucleus pulposus

- 0 Absent
- 1 Rarely present
- 2 Present in intermediate amounts
- 3 Abundantly present
- 4 Scar/tissue defects

K.Endplate morphology

- 0 Regular thickness; homogeneous structure
- 1 Slightly irregular thickness
- 2 Moderately irregular thickness
- 3 Severely irregular thickness with interruption of the endplate

L.Subchondral bone sclerosis

- 0 No sclerosis
- 1 Cranial formation of compact bone
- 2. Cranial and caudal formation of compact bone

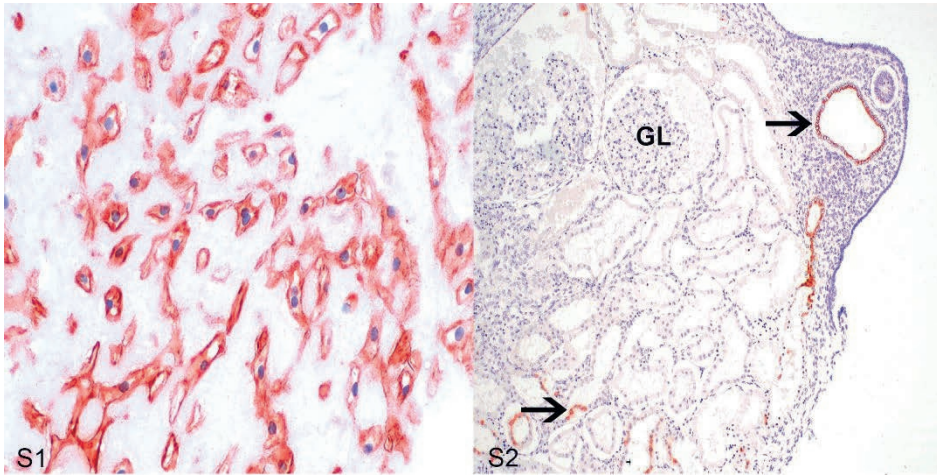
Supplemental Table S3. Grades for intervertebral disc degeneration used for biochemical analysis distributed among the different spinal regions. ^a

Region	Total	Grade 1	Grade 2	Grade 3	Grade 4-5
Cranial cervical	19	4	13	2	0
Caudal cervical	19	5	5	0	9
Cranial thoracic	2	1	0	0	1
Thoracic	20	7	8	5	0
Lumbo-sacral	13	5	4	4	0

^aNumber of discs used for biochemical analysis.

Supplemental Table S4. Histological variables with limited variation

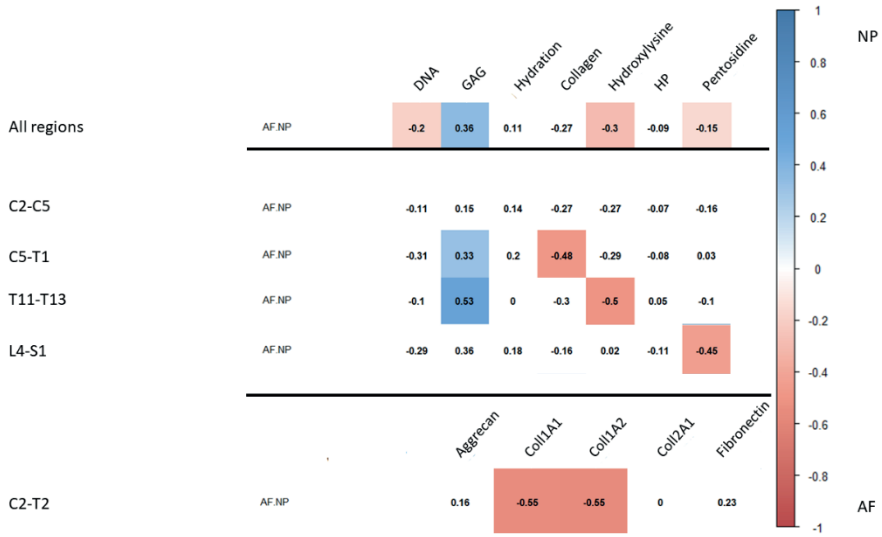
Histological variable	Most common scores given	
	All regions	Cervical
AF: Morphology of the lamellae	35 % moderate, 55% complete	37 % moderate, 53 % complete
AF: Chondroid metaplasia	80 % marked	82 % marked
AF Presence of vascular proliferation	95 % positive presence	96 % positive presence
NP: Chondroid metaplasia	presence of clusters in 82 %	presence of clusters in 92 %
NP: Cellularity	most cell poor in 82 %	most cell poor in 95 %
NP: Presence of notochordal cells	100 % no notochordal cells	100 % no notochordal cells
Subchondral bone sclerosis	cranial and caudal compact bone in 76 %	cranial and caudal compact bone in 73 %



Supplemental Figures S1 and S2. Cytokeratin 18 stain

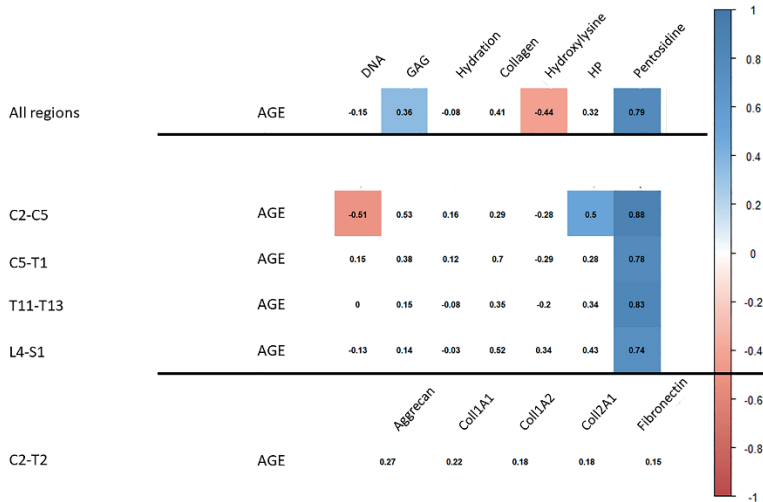
Figure S1 Nucleus pulposus of a herniated intervertebral disc, non-chondrodystrophic dog. In the nucleus pulposus are cytotubular cells. IHC for Cytokeratin 18.

Figure S2. Normal kidney, horse, foetus of 45 days gestation. The distal and collecting tubules are cytotubular cells (arrows). GL= glomerulus. IHC for Cytokeratin 18.

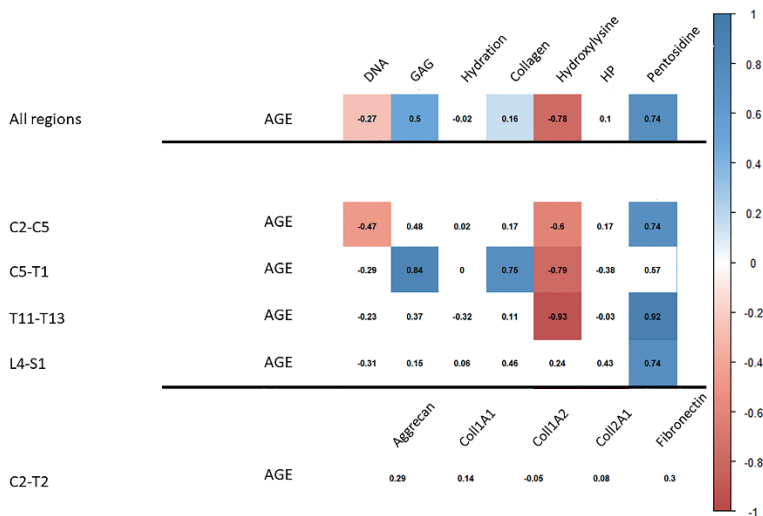


S3

Supplemental Figure S3. Heat maps of Spearman rank correlation coefficients of the composition of the intervertebral disc (IVD). A red colour is given when the amount of the variable is statistically significantly higher in the annulus fibrosus compared to the nucleus pulposus. A blue colour is given when the amount of the variable is statistically significantly higher in the nucleus pulposus compared to the annulus fibrosus. $P \leq 0.05$. C= cervical vertebra. T= thoracic vertebra. L=lumbar vertebra. S=sacral vertebra. DNA= DNA per gram wet weight. GAG= glycosaminoglycans per gram wet weight. collagen= total amount of collagen per gram wet weight. HP= hydroxyl-lysyl-pyridinoline.

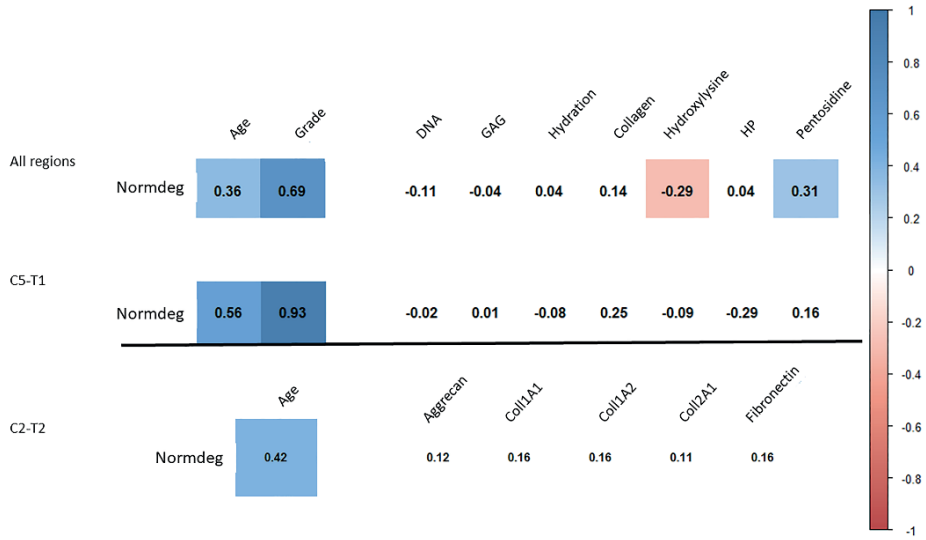


S4

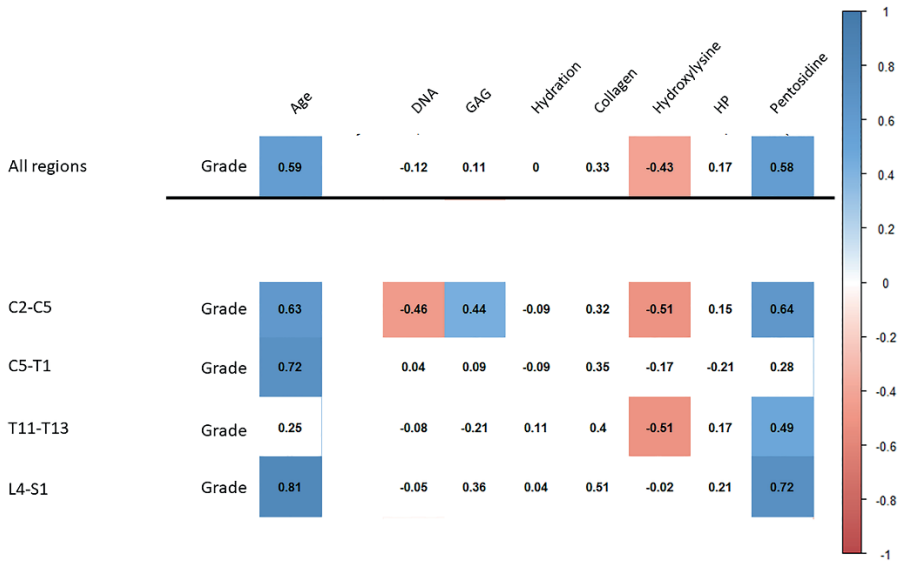


S5

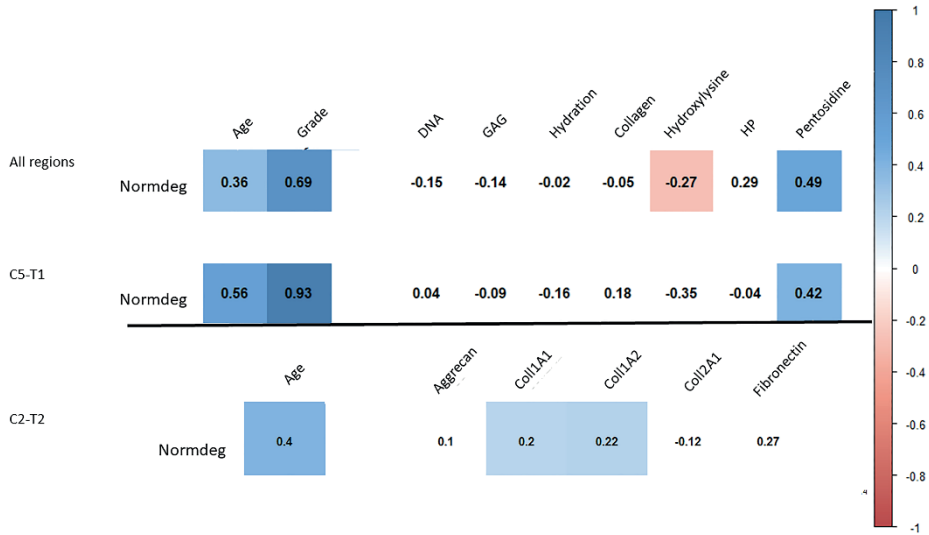
Supplemental Figures S4 and S5. Heat maps of Spearman rank correlation coefficients of age related changes of the intervertebral disc (IVD). A red colour is given when there is a negative statistically significant correlation and a blue colour is given when there is a positive statistically significant correlation. $P \leq 0.05$. C= cervical vertebra. T= thoracic vertebra. L=lumbar vertebra. S=sacral vertebra. Normdeg= normal versus severely degenerated. DNA= DNA per gram wet weight. GAG= glycosaminoglycans per gram wet weight. collagen= total amount of collagen per gram wet weight. HP= hydroxyl-lysyl-pyridinoline. Figure S4. Age related changes of the annulus fibrosus. Figure S5. Age related changes of the nucleus pulposus.



S6

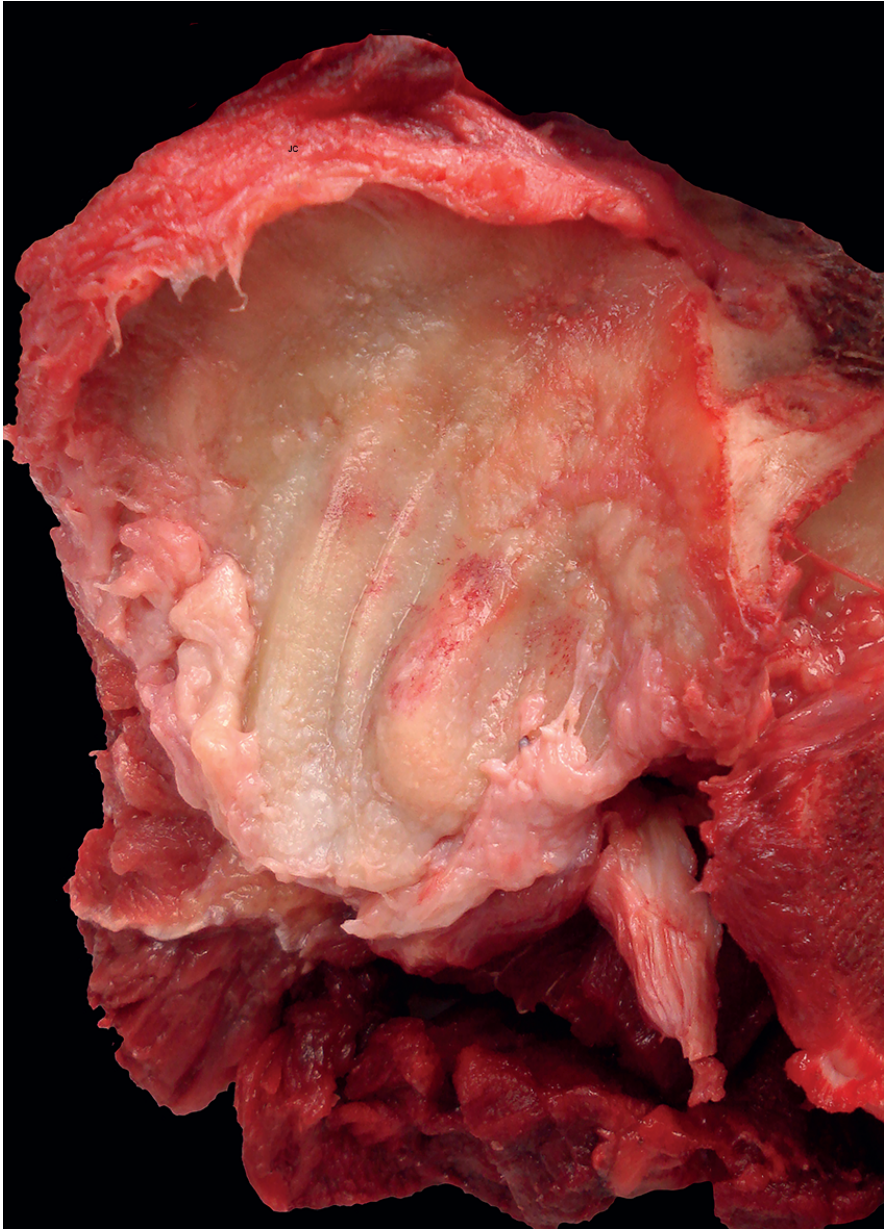


S7



S8

Supplemental Figures S6-S8. Heat maps of Spearman rank correlation coefficients of degeneration related changes of the intervertebral disc (IVD). A red colour is given when there is a negative statistically significant correlation and a blue colour is given when there is a positive statistically significant correlation. $P \leq 0.05$. C= cervical vertebra. T= thoracic vertebra. L=lumbar vertebra. S=sacral vertebra. Normdeg= normal versus severely degenerated DNA= DNA per gram wet weight. GAG= glycosaminoglycans per gram wet weight. collagen= total amount of collagen per gram wet weight. HP= hydroxyl-lysyl-pyridinoline. Figure S6. Degeneration related changes of the annulus fibrosus of the normal versus the severely degenerated intervertebral disc. Figure S7. Degeneration related changes of the annulus fibrosus, all grades. Figure S8. Degeneration related changes of the nucleus pulposus of the normal versus the severely degenerated intervertebral disc.



General discussion

6

The aim of the research described in this thesis was to gain more knowledge of the contribution of osteochondrosis (OC) and intervertebral disc degeneration (IVDD) to cervical vertebral compressive myelopathy (CVM) in warmblood horses. CVM is the most common non-macro traumatic, non-infectious neurological syndrome in horses, affecting 15.3% of all neurological cases (n=4.319) in a French study.⁴⁴ Nervous signs are the result of compression of the cervical spinal cord and spinal nerves and include spastic paresis, hypermetria, ataxia and cervical hyperaesthesia. Compression can be the result of various pathological changes such as congenital malformation and mal-articulation of the vertebrae and the articular process joints (APJs), osteochondrosis (OC) and osteoarthritis (OA) of the APJs, ligamentum flavum hypertrophy and osteosclerosis and thickening of the cervical vertebral lamellae.^{46, 50, 58, 67, 74} In horses of 4 years and older, especially warmblood horses, OA of the APJs in the caudal part of the neck is the most common cause for CVM^{45, 50, 74}, and OC has been suggested as the main cause for APJ OA.^{50, 58} In **chapter 2 and 3** this theory has been explored.

OC results from necrosis of the blood vessels within the epiphyseal cartilage canals and is manifested initially as chondronecrosis. The cause of the necrosis of these blood vessels is at this moment not known.^{4, 5, 53, 55} OC occurs at certain predilection sites.⁸⁴ Differences in joint shape/conformation are associated with differences in biomechanical forces/loading and therefore microtrauma was previously thought to be the cause of the necrosis of these blood vessels and the reason for these predilection sites.^{5, 78, 84} However, this theory could not be confirmed⁵¹ and currently it is suggested that these predilection sites are the result of anatomical differences in the number of blood vessels in the epiphyseal cartilage and the thickness of the cartilage.³⁴ Yet, progression of non-clinical OC into osteochondrosis dissecans (OCD) is still assumed to be the result of biomechanical overload.^{52, 77}

In **chapter 2** APJ OC was investigated in relation to the biological factors age, sex, side (left, right), and position (cranial, caudal) of the APJ on the vertebrae and the region of the APJs within the cervical spinal column. In this chapter it was hypothesized that the caudal cervical column is a predilection site for

the presence of OC, corresponding with the predilection site for APJ OA.⁴⁵
⁵⁰ Although APJ OC in warmblood foals was shown to be common, no predilection site for the occurrence of non-clinical OC (OC latens and OC manifesta) could be identified, suggesting that other factors for the development of APJ OA should be considered too. However, it was found that OC was significantly more common in cranial facets of the cervical (C2-C7) and the cervical- thoracic (C7T1) APJs and in the caudal APJs within the cranial thoracic region (T1T2).

In **chapter 3**, the occurrence of OC in relation to the shape of the facet/articular surface of the APJs was explored. According to literature, the normal shape of an APJ facet is oval (top view) and flat (side view).^{18,33} In the study described in **chapter 3**, 2 additional top view shapes and 6 extra side view shapes were commonly encountered. APJ facets with certain “aberrant” shapes did have an increased likelihood to have OC compared to the assumed normal shape and also between the different aberrant shapes significant differences in likelihood to have OC was found. None of these more OC-affected shapes had a predilection site, consistent with the lack of a predilection site found in **chapter 2**.

Whether variations in the number of cartilage canals and cartilage thickness between the different APJ locations, and differences in APJ shape are indeed the cause for these differences in likelihood to have OC needs to be explored further. During histological evaluation of these facets for OC, no obvious differences in number of cartilage canals nor thickness of the cartilage were noticed. Measurements of the cartilage thickness and the amount of blood vessels in the histological slides of the foals described in **chapter 2 and 3**, while blinded for the spinal origin and shape of the APJ in question, would be highly informative, especially as the hypothesis of blood vessel density and cartilage thickness as explanation for predilection sites is based on a study comparing epiphyseal cartilage of the OC-prone horse and the OC-resistant pony.³⁴ In that study it was found that Fjord ponies had fewer cartilage canals and thinner cartilage in the talus than standardbred horses and it was suggested that these differences explain the variance in prevalence of OC between these horse types. By examining the density of the cartilage canals in the same breed/type of horse (Royal Dutch Sport Horses) breed/type-related differences can be eliminated.

Still, biomechanical differences as factor for the increased likelihood to develop OC in APJs at different positions on the vertebrae and with a certain shape still seems compelling, especially because vascular failure occurs at the ossification front which advances rapidly over time. Therefore, structural changes such as trabecular bone micro-fractures, which could cause damage to the epiphysial vasculature, could easily become obscured soon after they occur.^{52, 55}

A limitation of the studies described in **chapter 2 and 3** is the fact that two thirds of the foals used were less than 1 month old. This overrepresentation is because foals at this age are more likely to be submitted for necropsy and therefore more foals of this age group were available during the time of animal collection. In this age range of 1 month and less, OC can still develop and regress.⁷⁶ Also, in none of the foals studied in **chapter 2 and 3** OCD was found, probably due to limited biomechanical stress at this age.⁸⁴ Although these studies resulted in new information about the initial occurrence of subclinical OC, these studies should be repeated in older horses to gain more knowledge about the evolution and regression of OC. As it has been suggested that the majority of OC lesions in the equine APJ will develop before the age of 5 months and that regression after the age of 11 months is no longer likely, resulting in persistent OC lesions⁷⁶, the horses in these follow-up studies would preferably be between 4 up to 18 months of age. If OCD is indeed more commonly found in the caudal neck in these older horses, this would be suggestive for OC to be a major contributor to OA in this spinal region. If the caudal neck still does not appear to be a predilection site for OC(D) in these follow-up studies, other factors contributing to the development of OA should probably be considered to be more important.

Another reason why follow-up studies in older foals and yearlings are important, is possible remodelling of the APJ facets during maturation. The assumption that oval and flat is the normal shape of the APJ was based on studies in horses of 1 year and older^{18, 33}, no literature on the normal APJ shape in foals was found. The most common facet shape combinations in the foals studied in **chapter 2 and 3** was oval and bevelled (24%), whereas the assumed normal oval and flat form was encountered in only 10% of

facets. In **chapter 3** it was found that 2 shape combinations, oval and concave (associated with an increased likelihood to have OC) and oval and bevelled (overall the most common shape combination found) were significantly less present in older foals than in younger foals compared to the assumed normal shape combination. This indicates that remodelling during maturation very likely occurs, and these findings also suggest that the main, and therefore likely normal, facet shape will eventually indeed become oval and flat in older horses. Moreover, it also indicates that APJ shapes with an increased likelihood to develop OC can become less prevalent with age and therefore also the occurrence of OC. A follow up study with older foals and yearlings would give more information about changes in prevalence of the different APJ shapes, which if present, would suggest remodelling of the facet. Also, such a study would give information on the likelihood of certain shapes to have OCD, as it is to be expected that this late phase of OC occurs more often in this age range because of expected higher (physiological) biomechanical forces.⁸⁴ If a certain facet shape is found to have an increased likelihood to have OCD and this shape has also a significant prevalence, an useful next step would be to study if these shapes of interest are hereditary and if so, if they can be visualised in vivo. Preferably this would be done by radiographs that can be made without sedation or anaesthesia and are commonly made as part of pre-purchase examinations, therefore also limiting extra exposure to X-rays. In this way, APJ facet shapes with increased likelihood to develop OCD can be phased out by selective breeding, and as such CVM and its related signs might be reduced in the population.

Evaluation of facet shapes would also be valuable in adult and aged horses as this would give the opportunity to gain information about the likelihood of APJ facets with specific shapes to have OA. If OC(D) and OA are more prevalent in APJ with the same specific shape, this would support the hypothesis that APJ OC is likely a significant contributor to APJ OA. Evaluation of facet shapes in this group of older horses would also be of interest for OA that develops without preceding OC. It is known in equines, but also in other species such as pigs, that differences in joint anatomy are correlated with different biomechanical loading of the joint.^{5, 21, 29, 78} OA can also develop as a result of aberrant biomechanical forces in pigs^{22, 29}, humans²⁷ and in

horses⁴², and it is likely that repeated microtrauma due to biomechanical overload can also lead to OA of the APJs. Therefore, it would be likely that anatomical variation in APJs results in differences in biomechanical loading and therefore in the likelihood to develop OA.

Finally, it would also be very interesting to examine the role of specific facet shape combinations within one APJ regarding mal-articulation, one of the causes for compression of nervous tissue in CVM. Although this form of CVM is most commonly seen in the cranial part of the neck of young thoroughbreds, it can also occur in other spinal regions and in other types of horses.^{46, 74} Next to its direct role in CVM, mal-articulation can also be a initiating factor for OA due to instability and therefore the development of aberrant biomechanical forces within the joint. To investigate the presence of (in)stability of certain combinations of facet shapes, dynamic three-dimensional computed tomographic imaging could be used, a technique that recently proved to be very promising for evaluation of the equine neck.⁶¹ Application of this technique in living (*in vivo*) and non-anesthetized patients as done in human medicine seems as of yet unfortunately not feasible.⁶¹ A possible alternative would be the use of fluoroscopy (a continuous X-ray imaging method), however no literature about its usage for evaluation of cervical spinal kinetics in the horse could be found. The next step would be to see if shape combinations associated with instability are more likely to develop OA using repeated diagnostic imaging and final pathomorphological follow up.

In both dogs (cervical spondylomyelopathy) and in humans (degenerative cervical myelopathy), syndromes comparable to CVM are known.^{13, 14, 43, 56} In both syndromes, intervertebral disc degeneration (IVDD) is an important factor in the pathogenesis by its contribution to the development of OA of the APJs.^{14, 43, 56} Moreover, it is widely accepted that lumbar IVDD leads to OA of the APJs of the same spinal unit and adjacent spinal units.^{17, 36} Also in other species, such as sheep and dogs^{28, 48}, this correlation has been established experimentally. Therefore, it was decided to investigate the potential role of IVDD in horses to the pathogenesis of CVM in **chapter 4 and 5**.

At the start of this thesis, not much was published on the equine intervertebral disc (IVD). Only a few case reports concerning protrusion/herniation and development of fibrocartilaginous emboli were available.^{23, 25, 38, 62, 63} Systematic studies on IVD related disease in the horse were however lacking. Moreover, in literature there was not even consensus about the anatomical characteristics of the equine IVD. Especially the existence and composition of a nucleus pulposus (NP) was under debate.^{12, 50, 59, 71, 72, 83}

Therefore, in **chapter 4 and 5**, the gross, histological, and biochemical composition of the non-degenerated equine IVD was described. Although its anatomical composition appeared generally comparable to that of dogs and humans, there were differences, mainly in the NP. In contrast to dogs and humans, no notochordal cells were seen, not even in embryos. Yet according to literature, the equine NP does originate from the notochord.^{6, 65} A possible explanation for the lack of cells with the typical morphology of notochordal cells as seen in other species, is that these cells transformed between day 30 of gestation (after which the NP is formed) and day 42 of gestation (the age of the youngest embryo investigated) into chondrocyte-like cells, the cells that were seen in the NP of all IVDs examined (including the embryos) and corresponds to fibrocartilage. Because of the fibrocartilaginous composition, the equine NP proved to be far less hydrated than the non-degenerated canine and human NPs.^{2, 35, 73} This results in a more opaque appearance and this likely explains the previously assumed lack of an equine NP.

To objectively and reliably investigate the clinical relevance of equine IVDD, a standardized, reproducible, and biological credible grading scheme is necessary.⁶⁸ Therefore, in **chapter 4** a gross grading scheme for equine IVDD was developed and validated. This grading scheme was subsequently used for the assessment of a predilection site for IVDD in **chapter 4**, and histological and biochemical changes that occur during degeneration in **chapter 5**.

In both dogs and humans, IVDD is characterized by replacement of a glycosaminoglycan-rich, hydrated NP with notochordal cells by a dehydrated NP composed of fibrocartilage with chondrocyte-like cells.^{1, 2, 4, 8, 9, 10, 15, 32, 82} Grossly this results in a change of a gel-like, translucent NP into

a consolidated white, “fibrous” NP with clefts. In more severe stages of degeneration, even collapse (without herniation) can occur as result of the dehydration. In dogs and humans, these changes in cellular and biochemical composition can eventually lead to biomechanical changes and the formation of vertebral osteophytes.^{7, 68}

In **chapter 4** it is reported that gross IVDD is characterized by a NP changing from gelatinous, semi-translucent and white to fibrillar and yellow with cleft formation in the horse. The AF changes from white and shiny with distinct lamellae to yellow with cleft formation. This is comparable to the gross changes seen in dogs and humans.^{7, 68} The histological and biochemical changes seen in equine IVDDs are however markedly different from those seen in dogs and humans. As described in **chapter 5**, the most important histological change in the equine IVD is cleft formation. In contrast to dogs and humans, no significant cellular changes are seen.^{8, 15} Biochemically, loss of glycosaminoglycans and therefore dehydration are not present in the horse and this likely explains why collapse was not seen in any of the equine IVDs analysed in **chapter 4 and 5**, nor is collapse described in literature, this in contrast to dogs and humans.¹⁰ The most important biochemical changes associated with gross degeneration in the horse are an increase in advanced glycation end-products (AGE's) and a decrease in hydroxylysine in both the NP and the AF, and an increase in collagen type 1 in the NP. These biochemical changes have been linked to yellow discoloration, loss of compliance, increase in tissue stiffness, loss of strength and brittleness in human and rat tissue including human IVDs^{1, 3, 24, 26, 80, 81}, and can therefore also likely explain the gross changes seen in equine IVDD and may, also in horses, eventually lead to degenerative changes in adjacent structures such as the APJs. Yet, in contrast to dogs and humans, equine IVDD is not correlated with the formation of vertebral osteophytes or spondylosis as demonstrated in **chapter 4**. A probable explanation for this might be that degeneration of the equine IVD leads to less biomechanical instability than in dogs and humans. Another possibility might be potential differences between these species in loading redistribution between the structures of the spinal unit after degeneration. Differences in the change of biomechanical properties due to IVDD in dogs, humans and horses are even

to be expected. Although in dogs, humans and horses, the severely degenerated discs are fissured, and are likely more stiff because of the biochemical changes, the biomechanical starting point of a gel-like NP in dogs and humans¹ is quite different from the fibrocartilaginous equine NP. Therefore, the biomechanical impact of IVDD and its subsequent effect on structures in the vicinity of the degenerated disc are also likely different between these species.

Yet, many space-occupying lesions such as osteosclerosis and thickening of the dorsal lamina, hypertrophy of the ligamentum flavum, hypertrophy of the APJ capsule, formation of synovial cysts and of osteophytes of the APJs and OCD are thought to result from aberrant biomechanical forces.^{52, 58, 84} As the predilection site for degenerative joint disease of the APJs and equine IVDD are both the caudal neck^{45, 50, 74}, a correlation seems very likely. In humans it is known that increased biomechanical forces on the IVD play a major role in the pathogenesis of its degeneration.^{1, 19, 30} It is to be expected that increased biomechanical loading is also an important factor in equine IVDD. Therefore, it cannot be ruled out that greater biomechanical forces are the common initiator of equine IVDD and APJ OA in the caudal neck instead of one preceding the other. **Chapter 5** reports that grossly normal IVDs of the caudal neck have a significantly higher AGEs content than the grossly normal discs of the other examined spinal regions. The presence of greater biomechanical forces in the caudal neck compared to the cranial neck, thoracic and lumbosacral spine could indeed be a possible explanation for this difference. These expected regional differences could be physiological/ anatomy related, but usage-related differences cannot be excluded. To obtain more information about the possible role of IVDD in the pathogenesis of APJ OA in the horse more research is necessary. A logical first step would be to investigate whether there is a correlation between IVDD and APJ OA within the same spinal units and the units within the same cervical spinal region. To do this, a validated grading scheme for equine APJ OA is essential, preferably composed of both changes of the articular cartilage and the presence of osteophytes, two hallmarks of OA.^{39, 41, 47, 69, 75} Of these, osteophytes are considered to be more a sign of mechanical stimulation than of established joint degeneration⁷⁵ and therefore it would be highly informative to study these hallmarks. If a correlation between

equine IVDD and APJ OA is found, further investigation into causality would be the next stage. For example, differences in biomechanical loading of the APJs within the same spinal units as either normal IVDs or discs with experimentally simulated degeneration could be evaluated with the use of a Tensile Testing Machine.³¹ Experimentally inducing IVDD by use of chymopapain or annular incision as previously done in dogs and sheep^{28, 48} with subsequent *in vivo* longitudinal evaluation of secondary morphological changes in the spinal column by the use of MRI and CT with eventually pathomorphological evaluation would be highly informative but unethical. Advanced equine IVDD can be demonstrated by MRI⁷⁹, and both early stages as advanced stages of APJ OA can be demonstrated by use of MRI and CT.^{16, 49, 60} Therefore, it would be useful to alternatively evaluate horses with established IVDD *in vivo* over a longer period of time by use of the above mentioned diagnostic imaging with eventually pathological evaluation to investigate the possible clinical relevant effects of IVDD in the horse. Unfortunately, *in vivo* evaluation by MRI is presently only possible for the cranial part of the neck due to size restrictions.

As mentioned before, clinical signs caused by changes of the IVD alone are considered to be rare in horses. Yet, two recent articles do touch on this subject. In a MRI study of 11 warmblood horses with ataxia and neck pain, mild to severe cervical IVD protrusion appeared to be correlated with gross degeneration. However, in that study only one herniated disc caused compression of the spinal cord, and protrusion was never severe enough in these examined horses to cause compression.⁷⁹ Yet, protrusions that were severe enough to cause compression have been described in literature.^{38, 64} Whether this is because of even more severe protrusion than seen in the MRI study, or because of a smaller diameter of the spinal canal of these horses is unclear. The diameters of the spinal canal of the horses of the MRI study were not reported. The diameter of the spinal canal is indeed of importance in relation to development of cervical spinal signs. In dogs, humans and horses, cervical spinal signs are more likely to develop in individuals with a narrow spinal canal whereas the same lesions can be clinically irrelevant in individuals with a wider spinal canal.^{18, 20, 37, 43, 57, 66, 70,}

74

Furthermore, a recent ultrasound study on the lumbosacral symphysis (intervertebral articulations, IVD and ventral and dorsal longitudinal ligaments) in a mixed breed horse population suggested that IVDD and disc protrusion are associated with regional pain although it was proposed that the IVD changes were part of a complex of lesions in closely related anatomical structures.¹¹

In conclusion, the information obtained in this thesis provide a base for further research into both the pathogenesis and the role of OC, IVDD and also the shape of the APJ in CVM.

References

1. Adams MA, Roughley PJ. What is intervertebral disc degeneration, and what causes it? *Spine*. 2006;31(18):2151-2161.
2. Antoniou J, Steffen T, Nelson F, et al. The human lumbar intervertebral disc: evidence for changes in the biosynthesis and denaturation of the extracellular matrix with growth, maturation, ageing, and degeneration. *J Clin Invest*. 1996;98(4):996-1003.
3. Avery NC, Bailey AJ. Restraining cross-links responsible for the mechanical properties of collagen fibers: natural and artificial. In: Fratzl P, ed. *Collagen: Structure and mechanics*. Springer; 2008.
4. Bach FC, Tellegen AR, Beukers M, et al. Biologic canine and human intervertebral disc repair by notochordal cell-derived matrix: from bench towards bedside. *Oncotarget*. 2018;9(41):26507-26526.
5. Back W, Remmen JL, Knaap J, et al. Effect of lateral heel wedges on sagittal and transverse plane kinematics of trotting Shetland ponies and the influence of feeding and training regimes. *Equine Vet J*. 2003;35(6):606-612.
6. Barreto Rda S, Rodrigues MN, Carvalho RC, et al. Organogenesis of the musculoskeletal system in horse embryos and early fetuses. *Anat Rec (Hoboken)*. 2016;299(6):722-729.
7. Bergknut N, Grinwis G, Pickee E, et al. Reliability of macroscopic grading of intervertebral disk degeneration in dogs by use of the Thompson system and comparison with low-field magnetic resonance imaging findings. *Am J Vet Res*. 2011;72(7):899-904.
8. Bergknut N, Meij BP, Hagman R, et al. Intervertebral disc disease in dogs - part 1: a new histological grading scheme for classification of intervertebral disc degeneration in dogs. *Vet J*. 2013;195(2):156-163.
9. Bergknut N, Rutges JPHJ, Kranenburg H-C, et al. The dog as an animal model for intervertebral disc degeneration? *Spine*. 2012;37(5):351-358.
10. Bergknut N, Smolders LA, Grinwis GC, et al. Intervertebral disc degeneration in the dog. Part 1: anatomy and physiology of the intervertebral disc and characteristics of intervertebral disc degeneration. *Vet J*. 2013;195(3):282-291.
11. Boado A, Nagy A, Dyson S. Ultrasonographic features associated with the lumbosacral or lumbar 5–6 symphyses in 64 horses with lumbosacral-sacroiliac joint region pain (2012–2018). *Equine Vet Educ*. 2020;32(S10):136-143.
12. Bollwein A, Hänichen T. Age-related changes in the intervertebral disks of the cervical vertebrae of the horse. *Tierärztl Prax*. 1989;17(1):73-76.
13. Bonelli MA, da Costa L. B. S. B. C., da Costa RC. Association of neurologic signs with high-field MRI findings in 100 dogs with osseous-associated cervical spondylomyelopathy. *Vet Radiol Ultrasound*. 2021;62(6):678-686.
14. Bonelli MA, da Costa L. B. S. B. C., da Costa RC. Magnetic resonance imaging and neurological findings in dogs with disc-associated cervical spondylomyelopathy: a case series. *BMC Vet Res*. 2021;17(1):145-5.
15. Boos N, Weissbach S, Rohrbach H, et al. Classification of age-related changes in lumbar intervertebral discs: 2002 Volvo award in basic science. *Spine*. 2002;27(23):2631-2644.

16. Brown KA, Davidson EJ, Johnson AL, et al. Inflammatory cytokines in horses with cervical articular process joint osteoarthritis on standing cone beam computed tomography. *Equine Vet J.* 2021;53(5):944-954.
17. Butler D, Trafimow JH, Andersson GB, et al. Discs degenerate before facets. *Spine.* 1990;15(2):111-113.
18. Claridge HAH, Piercy RJ, Parry A, et al. The 3D anatomy of the cervical articular process joints in the horse and their topographical relationship to the spinal cord. *Equine Vet J.* 2010;42(8):726-731.
19. Colombini A, Lombardi G, Corsi MM, et al. Pathophysiology of the human intervertebral disc. *Int J Biochem Cell Biol.* 2008;40(5):837-842.
20. de Decker S, Gielen IMVL, Duchateau L, et al. Magnetic resonance imaging vertebral canal and body ratios in dobermann pinschers with and without disk-associated cervical spondylomyelopathy and clinically normal English foxhounds. *Am J Vet Res.* 2011;72(11):1496-1504.
21. de Koning DB, van Grevenhof EM, Laurensen BF, et al. Associations of conformation and locomotive characteristics in growing gilts with osteochondrosis at slaughter. *J Anim Sci.* 2015;93(1):93-106.
22. Della Salda L, Borghetti P, Maltarello MC, et al. Superficial and deep defects in dyschondroplastic and degenerated pig articular cartilage. *J Submicrosc Cytol Pathol.* 1997;29(1):51-58.
23. Foss RR, Genetzky RM, Riedesel EA, et al. Cervical intervertebral disc protrusion in two horses. *Can Vet J.* 1983;24:188-191.
24. Fratzl P. Collagen: structure and mechanics, an introduction. In: Fratzl P, ed. *Collagen: Structure and mechanics.* Springer; 2008.
25. Fuentealba IC, Weeks BR, Martin MT, et al. Spinal cord ischemic necrosis due to fibrocartilaginous embolism in a horse. *J Vet Diagn Invest.* 1991;3(2):176-179.
26. Gautieri A, Passini FS, Silvan U, et al. Advanced glycation end-products: mechanics of aged collagen from molecule to tissue. *Matrix Biol.* 2017;59:95-108.
27. Goldring MB, Goldring SR. Articular cartilage and subchondral bone in the pathogenesis of osteoarthritis. *Ann New York Acad Sci.* 2010;1192:8.
28. Gotfried Y, Bradford DS, Oegema TR, Jr. Facet joint changes after chemonucleolysis-induced disc space narrowing. *Spine (Phila Pa 1976).* 1986;11(9):944-950.
29. Grondalen T. Osteochondrosis and arthrosis in pigs. VII. Relationship to joint shape and exterior conformation. *Acta Vet Scand Suppl.* 1974;46(0):1-32.
30. Hadjipavlou AG, Tzermiadianos MN, Bogduk N, et al. The pathophysiology of disc degeneration: a critical review. *J Bone Joint Surg. Br.* 2008;90(10):1261-1270.
31. Hafer TR, O'Brien M, Dryer JW, et al. The role of the lumbar facet joints in spinal stability: Identification of alternative paths of loading. *Spine.* 1994;19(23):2667-2671.
32. Hansen T, Smolders LA, Tryfonidou MA, et al. The Myth of Fibroid Degeneration in the Canine Intervertebral Disc: A histopathological comparison of intervertebral disc degeneration in chondrodystrophic and nonchondrodystrophic Dogs. *Vet Pathol.* 2017;54(6):945-952.

33. Haussler KK, Pool RR, Clayton HM. Characterization of bony changes localized to the cervical articular processes in a mixed population of horses. *PLoS One*. 2019;14(9):e0222989.
34. Hendrickson EHS, Olstad K, Nødtvedt A, et al. Comparison of the blood supply to the articular-epiphyseal growth complex in horse vs. pony foals. *Equine Vet J*. 2015;47(3):326-332.
35. Holm S, Nachemson A. Nutritional changes in the canine intervertebral disc after spinal fusion. *Clin Orthop Relat Res*. 1982;(169)(169):243-258.
36. Iorio JA, Jakoi AM, Singla A. Biomechanics of degenerative spinal disorders. *Asian Spine J*. 2016;10(2):377-384.
37. Janes JG, Garrett KS, McQuerry KJ, et al. Cervical vertebral lesions in equine stenotic Myelopathy. *Vet Pathol*. 2015;52(5):919-927.
38. Jansson N. What is your diagnosis? Multiple cervical intervertebral disk prolapses. *J Am Vet Med Assoc*. 2001;219(12):1681-1682.
39. Jaumard NV, Welch WC, Winkelstein BA. Spinal facet joint biomechanics and mechanotransduction in normal, injury and degenerative conditions. *J Biomech Eng*. 2011;133(7):071010.
40. Jeffcott LB, Dalin G. Natural rigidity of the horse's backbone. *Equine Vet J*. 1980;12(3):101-108.
41. Kettler A, Werner K, Wilke HJ. Morphological changes of cervical facet joints in elderly individuals. *Eur Spine J*. 2007;16(7):987-992.
42. Lacourt M, Gao C, Li A, et al. Relationship between cartilage and subchondral bone lesions in repetitive impact trauma-induced equine osteoarthritis. *Osteoarthr Cartil*. 2012;20(6):572-583.
43. Lannon M, Kachur E. Degenerative cervical myelopathy: clinical presentation, assessment, and natural history. *J Clin Med*. 2021;10(16):10.3390/jcm10163626.
44. Laugier C, Tapprest J, Foucher N, et al. A necropsy survey of neurologic diseases in 4,319 horses examined in Normandy (France) from 1986 to 2006. *J Equine Vet Sci*. 2009;29(7):561-568.
45. Levine JM, Adam E, MacKay RJ, et al. Confirmed and presumptive cervical vertebral compressive myelopathy in older horses: a retrospective study (1992-2004). *J Vet Intern Med* 2007;21(4):812-819.
46. Levine JM, Scrivani PV, Divers TJ, et al. Multicenter case-control study of signalment, diagnostic features, and outcome associated with cervical vertebral malformation-malarticulation in horses. *J Am Vet Med Assoc*. 2010;237(7):812-822.
47. Li J, Muehleman C, Abe Y, et al. Prevalence of facet joint degeneration in association with intervertebral joint degeneration in a sample of organ donors. *J Orthop Res*. 2011;29(8):1267-1274.
48. Moore RJ, Crotti TN, Osti OL, et al. Osteoarthrosis of the facet joints resulting from anular rim lesions in sheep lumbar discs. *Spine*. 1999;24(6):519-525.
49. Nelson BB, Kawcak CE, Barrett MF, et al. Recent advances in articular cartilage evaluation using computed tomography and magnetic resonance imaging. *Equine Vet J*. 2018;50(5):564-579.

50. Nout YS, Reed SM. Cervical vertebral stenotic myelopathy. *Equine Vet Educ.* 2003;15(4):212-223.
51. Olstad K, Cnudde V, Masschaele B, et al. Micro-computed tomography of early lesions of osteochondrosis in the tarsus of foals. *Bone.* 2008;43(3):574-583.
52. Olstad K, Ekman S, Carlson CS. An update on the pathogenesis of osteochondrosis. *Vet Pathol.* 2015;52(5):785-802.
53. Olstad K, Hendrickson EH, Carlson CS, et al. Transection of vessels in epiphyseal cartilage canals leads to osteochondrosis and osteochondrosis dissecans in the femoro-patellar joint of foals; a potential model of juvenile osteochondritis dissecans. *Osteoarthr Cartil.* 2013;21(5):730-738.
54. Olstad K, Ytrehus B, Ekman S, et al. Early lesions of articular osteochondrosis in the distal femur of foals. *Vet Pathol.* 2011;48(6):1165-1175.
55. Olstad K, Ytrehus B, Ekman S, et al. Epiphyseal cartilage canal blood supply to the tarsus of foals and relationship to osteochondrosis. *Equine Vet J.* 2008;40(1):30-39.
56. Onofrei LV, Henrie AM. Cervical and thoracic spondylotic myelopathies. *Semin Neurol.* 2021;41(3):239-246.
57. Panjabi MM, Krag MH, Chung TQ. Effects of disc injury on mechanical behavior of the human spine. *Spine.* 1984;9(7):707-713.
58. Powers BE, Stashak TS, Nixon AJ, et al. Pathology of the vertebral column of horses with cervical static stenosis. *Vet Pathol.* 1986;23(4):392-399.
59. Rooney JR. The horse's back: biomechanics of lameness. *Vet. Clin North Am Equine Pract.* 1982;4(2):17-27.
60. Rovel T, Zimmerman M, Duchateau L, et al. Computed tomographic examination of the articular process joints of the cervical spine in warmblood horses: 86 cases (2015-2017). *J Am Vet Med Assoc.* 2021;259(10):1178-1187.
61. Schulze N, Werpy N, Gernhardt J, et al. Dynamic three-dimensional computed tomographic imaging facilitates evaluation of the equine cervical articular process joint in motion. *Equine Vet J.* 2023;55(1):83-91.
62. Sebastian MM, Giles RC. Fibrocartilaginous embolic myelopathy in a horse. *J Vet Med A Physiol Pathol Clin Med.* 2004;51(7-8):341-343.
63. Speltz MC, Olson EJ, Hunt LM, et al. Equine intervertebral disk disease: a case report. *J Equine Vet Sci.* 2006;26(9):413-419.
64. Stadler P, van den Berg SS, Tustin RC. Cervical intervertebral disk prolapse in a horse. *J S Afr Vet Assoc.* 1988;59(1):31-32.
65. Stemple DL. Structure and function of the notochord: an essential organ for chordate development. *Development.* 2005;132(11):2503-2512.
66. Stewart RH, Reed SM, Weisbrode SE. Frequency and severity of osteochondrosis in horses with cervical stenotic myelopathy. *Am J Vet Res.* 1991;52(6):873-879.
67. Summers BA, Cummings JF, de Lahunta A. *Veterinary Neuropathology.* Mosby; 1995.

68. Thompson JP, Pearce RH, Schechter MT, et al. Preliminary evaluation of a scheme for grading the gross morphology of the human intervertebral disc. *Spine*. 1990;15(5):411-415.
69. Tischer T, Aktas T, Milz S, et al. Detailed pathological changes of human lumbar facet joints L1-L5 in elderly individuals. *Eur Spine J*. 2006;15(3):308-315.
70. Tomizawa N, Nishimura R, Sasaki N, et al. Morphological analysis of cervical vertebrae in ataxic foals. *J Vet Med Sci*. 1994;56(6):1081-1085.
71. Townsend HG, Leach DH. Relationship between intervertebral joint morphology and mobility in the equine thoracolumbar spine. *Equine Vet J*. 1984;16(5):461-465.
72. Townsend HG, Leach DH, Doige CE, et al. Relationship between spinal biomechanics and pathological changes in the equine thoracolumbar spine. *Equine Vet J*. 1986;18(2):107-112.
73. Urban JPG, Roberts S. Degeneration of the intervertebral disc. *Arthritis Res Ther*. 2003;5(3):120-130.
74. van Biervliet J, Mayhew J, de Lahunta A. Cervical vertebral compressive myelopathy: diagnosis. *Clin Tech Equine Pract*. 2006;5(1):54-59.
75. van der Kraan PM, van den Berg WB. Osteophytes: relevance and biology. *Osteoarthr Cartil*. 2007;15(3):237-244.
76. van Weeren PR, Barneveld A. The effect of exercise on the distribution and manifestation of osteochondrotic lesions in the warmblood foal. *Equine Vet J Suppl*. 1999(31):16-25.
77. van Weeren PR, Denoix JM. The Normandy field study on juvenile osteochondral conditions: conclusions regarding the influence of genetics, environmental conditions and management, and the effect on performance. *Vet J*. 2013;197(1):90-95.
78. van Weeren RP, Olstad K. Pathogenesis of osteochondrosis dissecans: how does this translate to management of the clinical case?. *Equine Vet Educ*. 2016;28(3):155-166.
79. Veraa S, Bergmann W, Wijnberg ID, et al. Equine cervical intervertebral disc degeneration is associated with location and MRI features. *Vet Radiol Ultrasound*. 2019;60(6):696-706.
80. Wagner DR, Reiser KM, Lotz JC. Glycation increases human annulus fibrosus stiffness in both experimental measurements and theoretical predictions. *J Biomech*. 2006;39(6):1021-1029.
81. Yamauchi M, Sricholpech M. Lysine post-translational modifications of collagen. *Essays Biochem*. 2012;52:113-133.
82. Yee A, Lam MP, Tam V, et al. Fibrotic-like changes in degenerate human intervertebral discs revealed by quantitative proteomic analysis. *Osteoarthr Cartil*. 2016;24(3):503-513.
83. Yovich JV, Powers BE, Stashak TS. Morphologic features of the cervical intervertebral disks and adjacent vertebral bodies of horses. *Am J Vet Res*. 1985;46(11):2372-2377.
84. Ytrehus B, Carlson CS, Ekman S. Etiology and pathogenesis of osteochondrosis. *Vet Pathol*. 2007;44(4):429-448.



Addendum

Nederlandse samenvatting
Dankwoord
Curriculum vitae

A

Nederlandse samenvatting

Bij het paard is cervicale vertebrale compressie myelopathie (CVM) een veel voorkomende oorzaak voor neurologische problemen uitgaande van de nek. De neurologische symptomen zijn het gevolg van ruimte innemende processen welke op het ruggenmerg en de spinale zenuwen drukken. Compressie kan alleen tijdens het bewegen van de nek optreden (dynamische CVM) of constant aanwezig zijn (statische CVM).

Dynamische CVM komt voornamelijk voor bij jonge (8-18 maanden), mannelijke volbloedpaarden en de compressie bevindt zich meestal ter hoogte van het voorste deel van de nek tussen de derde en vierde halswervels. Deze vorm van CVM is meestal het gevolg van misvormingen of slechte gewrichtsaansluiting (malarticulatie) van de wervelkolom. Ook osteochondrose, een verstoringen in de groei van het botweefsel van de wervelgewrichten kan tot dynamische CVM leiden.

De statische vorm van CVM komt vooral voor bij paarden vanaf 1 jaar oud. Hierbij bevindt de compressie zich voornamelijk in het achterste deel van de nek ter hoogte van de vijfde tot en met de zevende halswervels. Vooral bij mannelijke warmbloedpaarden van 4 jaar en ouder is statische CVM het gevolg van artrose van de wervelgewrichten. Er wordt aangenomen dat deze artrose het gevolg is van osteochondrose. Osteochondrose zelf, kan ook tot statische CVM leiden.

Artrose en osteochondrose van de wervelgewrichten komen echter ook voor bij paarden zonder neurologische klachten. Paarden met CVM hebben echter vaak een nauw wervelkanaal, waardoor ruimte innemende processen sneller tot compressie van het zenuwweefsel kunnen leiden.

Bij honden en mensen zijn tussenwervelschijfdegeneratie en de daaruit voortvloeiende hernia ook een bekende oorzaak voor neurologische symptomen uitgaande van de nek. Daarnaast is zowel bij de hond als de mens bekend, dat tussenwervelschijfdegeneratie tot secundaire wervelgewrichtsartrose kan leiden met pijn en neurologische klachten/symptomen tot gevolg.

Bij het paard is een tussenwervelschijfhernia echter zeer zeldzaam en om deze reden is tussenwervelschijfdegeneratie heel lang als niet klinisch relevant beschouwd bij het paard. Hierdoor is bijna geen (systematisch) onderzoek gedaan naar de anatomie en degeneratie van de paarden tussenwervelschijf en de daaruit voortvloeiende secundaire veranderingen aan de wervelkolom.

Het doel van dit proefschrift is om de rol van wervelgewrichtsosteochondrose en tussenwervelschijfdegeneratie bij het ontstaan van wervelgewrichtsartrose te onderzoeken en daarmee de potentiële rol hiervan in de pathogenese van CVM.

In **hoofdstuk 1** wordt een overzicht van de pathogenese, klinische symptomen en pathologische veranderingen van CVM gegeven. Vervolgens worden analoge syndromen bij de hond en de mens besproken. Daarbij wordt het belang van tussenwervelschijfdegeneratie in de pathogenese van het ontstaan van wervelgewrichtsartrose bij de hond en de mens duidelijk gemaakt. Hierbij wordt de basis gelegd voor de probleemstelling van dit proefschrift. Namelijk, als tussenwervelschijfdegeneratie van essentieel belang is in de pathogenese van wervelgewrichtsartrose en de daarmee samenhangende zenuwweefselcompressie in de hals van de hond en de mens, is er dan ook niet een belangrijke rol voor tussenwervelschijfdegeneratie in het ontstaan van CVM bij het paard? Bij het paard wordt echter aangenomen dat osteochondrose de basis is voor wervelgewrichtsartrose, hoewel onderzoek hiernaar niet aanwezig is.

Om het belang van osteochondrose in het ontstaan van wervelgewrichtsartrose te onderzoeken wordt in **hoofdstuk 2** de voorkeursregio in de nek voor het ontstaan van wervelgewrichtsosteochondrose onderzocht. Als osteochondrose inderdaad van belang is voor het ontstaan van artrose zal de voorkeursregio overlappen met die van wervelgewrichtsartrose, namelijk het achterste deel van de nek. Uit de resultaten blijkt er geen voorkeursregio te zijn, ondanks dat bijna 21 % van de onderzochte wervelgewrichten osteochondrose heeft. Ook is er geen voorkeurslocatie voor ernstige osteochondrose. Osteochondrose kan alleen tijdens een bepaalde periode in het leven van

een veulen ontstaan. Bij de wervelgewrichten is dit tot ongeveer een leeftijd van 5 maanden. Dit komt omdat in de pathogenese van osteochondrose het falen van bloedvaten binnen het groeikraakbeen van het gewricht van essentieel belang is. Na een bepaalde leeftijd zijn deze bloedvaten niet meer aanwezig, waardoor osteochondrose zich niet meer kan ontwikkelen. Osteochondrose kan genezen maar ook in ernst toenemen. Genezing kan ook alleen binnen een bepaalde periode, namelijk in wervelgewrichten tot ongeveer 11 maanden leeftijd. Daarna zullen de osteochondrose veranderingen blijven bestaan. Ongeveer twee-derde van de veulens die onderzocht zijn voor de studie van hoofdstuk 2 zijn jonger dan 1 maand en slechts 2 veulens zijn ouder dan 5 maanden. Daarom kunnen bij deze studie alleen uitspraken gedaan worden over het ontstaan van osteochondrose in jonge veulens. Er kunnen geen conclusies getrokken worden over voorkeurslocaties voor het persisteren of voor progressie van osteochondrose. Dus hoewel er vooralsnog geen voorkeursregio in de hals lijkt te zijn voor het ontstaan van osteochondrose is verder onderzoek bij oudere veulens/jaarlingen nodig om de vraag van de rol van osteochondrose in het ontstaan van wervelgewrichtsartrose verder te beantwoorden.

Tijdens de sectie van de veulens ten behoeve van de studie van hoofdstuk 2 viel op dat er een grote variatie is in de vorm van de gewrichtsoppervlakken van de wervelgewrichten. Binnen het ontstaan van (klinisch relevante) osteochondrose zijn biomechanische krachten op een gewricht van groot belang. De mate van deze krachten hangen samen met de anatomie en daarmee ook de vorm van een gewricht. Illustratief hiervoor is dat bij varkens, welke dezelfde pathogenese hebben voor het ontwikkelen van osteochondrose als paarden, bepaalde gewrichts- en pootvormen gecorreleerd zijn met het ontstaan van klinisch relevante osteochondrose. Uitselecteren van dieren met deze anatomie heeft het aantal varkens met klinische relevante osteochondrose daarom sterk laten afnemen. In **hoofdstuk 3** is daarom onderzocht of bij veulens het ontstaan van osteochondrose ook samenhangt met bepaalde gewrichtsvormen en of deze vormen dan voornamelijk in het achterste deel van de nek te vinden zijn. Hierbij wordt aangenomen, zoals beschreven in de literatuur, dat een normaal gewrichtsoppervlak van een wervelgewricht ovaal en plat is. Uit de resultaten van dit onderzoek blijkt dat er inderdaad een grote variatie is in

gewrichtsvlakvorm waarbij er 3 regelmatig voorkomende bovenaanzicht - en 7 regelmatig voorkomende zijaanzichtvormen zijn vastgesteld. Daarnaast is het mogelijk dat een en hetzelfde gewrichtsvlak meerdere zijaanzicht vormen kan hebben. De normale gewrichtsvlakvorm (ovaal en plat) is niet de meest voorkomende vorm bij jonge warmbloed veulens. Tevens is er geen voorkeurslocatie voor een van de gewrichtsvlakvormen. Wel is vastgesteld dat 3 afwijkende gewrichtsvlakvormcombinaties (ovaal en gevouwen, ovaal en hol, ovaal en plat met een tweede zijaanzichtvorm) een hogere kans hebben tot het ontwikkelen van osteochondrose. Daarmee kan geconcludeerd worden dat de vorm van een gewrichtsvlak een, weliswaar bescheiden, rol kan hebben in het ontstaan van CVM.

Omdat er over de tussenwervelschijf van het paard weinig bekend is en er zelfs geen consensus is over de anatomie zijn in **hoofdstuk 4** de macroscopische en histologische anatomie van de normale tussenwervelschijf onderzocht. Hieruit blijkt dat, net als bij ander zoogdieren, de paarden tussenwervelschijf bestaat uit een centrale nucleus pulposus, een perifere annulus fibrosus en een kraakbenige eindplaat. Uit dit onderzoek blijkt ook dat tussenwervelschijfdegeneratie bij het paard veel voorkomt, het voorkomen toeneemt met de leeftijd, de degeneratie morfologisch grotendeels lijkt op tussenwervelschijfdegeneratie bij de hond en mens en dat er een voorkeurslocatie is voor het achterste deel van de nek. De voorkeurslocatie komt dus overeen met die van wervelgewrichtsartrose van het paard. In tegenstelling tot de hond en de mens worden er bij het paard geen botveranderingen van de wervel gezien als onderdeel van tussenwervelschijfdegeneratie.

De secundaire veranderingen die in de wervelkolom van honden en mensen gezien worden als gevolg van tussenwervelschijfdegeneratie, ontstaan door afwijkende biomechanische krachten. Door degeneratie van de tussenwervelschijf vinden er cellulaire en biochemische veranderingen plaats in de tussenwervelschijf waardoor deze droger van structuur en stijver wordt. Hierdoor kan de tussenwervelschijf niet meer goed functioneren en komen biomechanische krachten, die bij normale bewegingen in het wervelkanaal ontstaan, onevenredig veel op de andere

structuren van de wervelkolom terecht, waaronder de wervelgewrichten. Door deze toename van krachten op deze gewrichten ontstaat artrose.

Om in te schatten of ook bij het paard degeneratie van de tussenwervelschijf waarschijnlijk tot functieverlies leidt, worden in **hoofdstuk 5** de histologische en biochemische veranderingen die bij degeneratie optreden onderzocht. Omdat bij de hond en de mens histologische scoring als gouden standaard wordt gezien bij het vaststellen van degeneratie van de tussenwervelschijf wordt in dit hoofdstuk ook de ontwikkeling en validatie van een scoringsprotocol specifiek voor het paard beschreven.

Uit de resultaten blijkt dat de histologische beoordeling van de tussenwervelschijf van het paard geen significant toegevoegde waarde heeft ten opzichte van macroscopische gradering.

Uit het biochemisch onderzoek blijkt dat bij het paard degeneratie van de tussenwervelschijf niet gepaard gaat met dehydratie en daarom wordt het weefsel niet droger. Wel vindt er een toename van collageen, een verandering in de verhouding tussen de verschillende types collageen en een toename van abnormale dwarsverbindingen tussen de collageenmoleculen in de gedegenererde paarden tussenwervelschijf plaats. Deze biochemische veranderingen suggereren dat de gedegenererde paarden tussenwervelschijf stijver en brozer wordt. Daarom lijkt het waarschijnlijk dat ook bij het paard de gedegenererde tussenwervelschijf minder goed kan functioneren waardoor de aangrenzende structuren in de wervelkolom grotere krachten moeten doorstaan. Dit suggereert dat ook bij het paard tussenwervelschijfdegeneratie tot wervelgewrichtsartrose kan leiden.

In **hoofdstuk 6** worden uiteindelijk alle bevindingen bediscussieerd en worden suggesties gegeven voor toekomstig onderzoek.

Dankwoord

En dan volgt nu het meest gelezen deel van menig proefschrift: het dankwoord.

Bij deze wil ik mijn dank uitspreken aan de volgende mensen die een belangrijke bijdrage hebben geleverd aan het tot stand komen van dit proefschrift:

Andrea Gröne. Ik wil je bedanken voor alle mogelijkheden die je mij gegeven hebt. Je hebt mij ruim 13 jaar geleden, zonder elkaar ooit echt gesproken te hebben, aangenomen om het VPDC team te komen versterken, waarbij ik vermoed dat ons beider (hoewel niet gedurende dezelfde tijdsperiode) Bernese achtergrond een belangrijke rol heeft gespeeld.

Gelukkig beviel de samenwerking en al snel heb je mij gestimuleerd om opzoek te gaan naar een onderwerp voor een PhD onderzoek. Natuurlijk wil ik je niet alleen bedanken voor de werk gerelateerde mogelijkheden die je me geboden hebt maar ook voor de gezellige uitjes naar plantenkwekers en het Bomenmuseum in Doorn waarbij we ook nog mijn Duits geoefend hebben.

Guy Grinwis. Ik wil je bedanken dat je altijd tijd had om mij met raad en daad bij te staan. Ik kon altijd zowel met vragen over de diagnostiek, het onderzoek als ook logistiek bij je terecht. Ook heb ik bij dit onderzoek kunnen meeliften op jouw uitgebreide kennis van tussenwervelschijfdegeneratie bij de hond en kan ik dankzij jou zowel macroscopisch als histologisch degelijke foto's produceren. En daarnaast wil ik je natuurlijk ook bedanken voor de tussendoor praatjes in de insprekruimte.

Wim Back. Ik wil je bedanken voor je aanstekelijke enthousiasme en gedrevenheid en natuurlijk voor het actief verzamelen van paarden. Dankzij jou heb ik een mooi aantal aan paarden kunnen onderzoeken!

Inge Wijnberg. Dit onderzoek had nooit plaatsgevonden zonder jouw initiële onderzoek naar de correlatie van EMG afwijkingen en veranderingen

die te zien zijn op beeldvorming en bij de pathologie. Het was tijdens het onderzoek van de paarden die jij hebt opgestuurd voor pathologisch onderzoek dat de gedegeneerde tussenwervelschijven bij het paard opvielen en zo ons onderzoek startte.

Louis van den Boom. Niet alleen heb jij mij geholpen met de secties van de paarden en het vele zagen, ook ben jij degene die de gedegeneerde tussenwervelschijven het eerst opvielen en die je nieuwsgierigheid naar het ontstaan en de mogelijke klinische impact uitte waarmee je een belangrijke drijfveer bent geweest voor de start van dit onderzoek. Verder wil ik je bedanken dat je altijd bereid was mij te helpen ook al zou het dan weer een latertje worden, voor de mogelijkheid tot sparren over hoe we het best een sectie zouden kunnen uitvoeren, ook binnen de diagnostiek, en natuurlijk ook de Brabantse gezelligheid!

Hans Vernooij. Ik wil je bedanken voor de uitgebreide, gedetailleerde besprekingen van de statistiek die is toegepast in ons onderzoek en ook voor de uitleg over het gebruik van R. Ik heb heel veel van je geleerd! Dat we nog lang samen mogen forensen op de fiets.

Manon en **Darryl**. Louis is natuurlijk niet de enige sectiezaalmedewerker die mij geholpen heeft met de secties van de velen paarden (en natuurlijk alle andere dieren in de diagnostiek). Ook aan jullie ben ik hiervoor dank verschuldigd!

Charlotte, Lotte, Hennie, Ronald, Tim, Liesbeth en **Deepak**. Ik wil jullie bedanken voor het ontkalken (soms tot 9 maanden lang voor een en het zelfde stuk botweefsel) en het kleuren van de grote hoeveelheid van het door mij verzamelde weefsel. Verder wil ik jullie bedanken voor het overleg dat altijd mogelijk is zodat we een optimaal resultaat kunnen behalen. Liesbeth en Deepak wil ik nog speciaal bedanken voor het mij stimuleren om een lunchpauze te houden (gezelligheid!).

Ruby, Joke en **Ilonne**. Bedankt voor de fijne samenwerking en het inschrijven van de paarden die gebruikt zijn voor dit onderzoek. Ook Ruby

wil ik extra bedanken voor het stimuleren tot het nemen van een lunchpauze.

Mijn co-auteurs **Stefanie, Marjolijn, Jan, Niklas, Chris, Saskia, Mark, Nermin en Marianna**. Bedankt voor de fijne samenwerking en het kritisch doorlezen van de manuscripten. Verder wil ik Chris ook nog bedanken voor het uitgebreide uitzoekwerk over hoe we de tussenwervelschijven het beste konden verwerken en de uitleg over de voor mij toch wel onbekende biochemie. Saskia wil ik nog apart bedanken voor je vriendelijkheid en geduld die je met mij had in het lab. De oefjes die je mij geleerd hebt om zo gestructureerd mogelijk te werken om zo zoveel mogelijk fouten te vermijden pas ik nog steeds toe! Niklas, toen ik je vertelde dat ik onderzoek zou gaan doen naar tussenwervelschijfdegeneratie bij het paard gaf je mij meteen jouw proefschrift en zij met een brede lach: "copy and paste". Dat is niet helemaal gelukt maar ik heb wel geput uit je uitgebreide kennis en connecties waarbij je me in contact hebt gebrachte met Marianna en Saskia. Ik kijk er naar uit samen weer neuroseminars te geven!

Mijn paranimfen **Theresia** en **Irene**. Theresia, wij delen al ons hele leven lief en leed. Ik ben blij dat je mijn zus bent! Irene, ik heb met je mogen sparren over de mogelijkheden van diagnostische beeldvorming, zodat de discussie geen science fiction verhaal werd. En natuurlijk heb je de mooie foto's gemaakt die gebruikt zijn voor de kaft en de uitnodiging, mijn dank daarvoor!. We hebben veel dezelfde interesses en wat is het fijn om samen uitstapjes te maken en op vakantie te gaan. Waar gaan we nog meer samen heen? Italië, Zweden, Japan?

Hoewel niet direct betrokken bij het onderzoek beschreven in dit boekje wil ik natuurlijk ook mijn mede pathologen **Erik, Joeske, Marja, Judith** en **Nynke** bedanken voor de interesse en steun met betrekking tot mijn PhD onderzoek, de gezellige tussendoor-gesprekjes, het ventileren en de bereidheid die er altijd is tot overleg.

Tenslotte wil ik ook al mijn andere **(ex) collega's van de divisie pathologie** bedanken voor de fijne samenwerking de afgelopen jaren. We doen het allemaal maar wel samen!

Curriculum Vitae

Willie (Wilhelmina) is geboren en getogen in Utrecht op 22 maart 1978. Na de middelbare school doorgelopen te hebben op het Sint Gregorius College te Utrecht is zij in 1996 aan de studie diergeneeskunde in Utrecht begonnen. In 2003 studeerde zij af met als differentiatie gezelschapsdieren. Al vroeg in de studie had zij behoefte aan verdieping en ontwikkelde ze een sterke affiniteit voor pathologie. Na 2 jaar als waarnemend dierenarts gewerkt te hebben vertrok zij naar Bern, Zwitserland om daar haar wens om veterinaire patholoog te worden te vervullen. In 2011 werd zij diplomaat van het European Collage of Veterinary Pathologists. Na haar residency begon zij haar werkzaamheden bij het Veterinair Pathologisch Diagnostisch Centrum (VPDC) aan de Universiteit van Utrecht waar zij al snel aan haar PhD onderzoek begon. Momenteel werkt zij nog altijd bij het VPDC waar zij betrokken is bij diagnostiek, onderzoek en onderwijs.

